UNIVERSITY OF LATVIA

Faculty of Biology

ARNIS STRODS

HEPATITIS B CORE PROTEIN AND BACTERIOPHAGE AP205 AND GA COAT PROTEIN FORMED VIRUS-LIKE PARTICLES FOR PACKAGING AND ADDRESSING

DOCTORAL THESIS

Submitted for the degree of Doctor of Biology

Subfield: Molecular Biology

Rīga, 2015

The doctoral thesis was carried out:

at the Chair of department of Molecular Biolgy, Faculty of Biology, University of Latvia, Latvian Biomedical Research and Study Centre and Latvian Institute of Organic Synthesis from Year 2008 to 2015.

This research was supported by the European Social Fund (ESF) project Nr. 2013/0002/1DP/1.1.1.2.0/13/APIA/VIAA/005, by a European Regional Development Fund grant 2DP/2.1.1.1.0/10/APIA/VIAA/052 and European Social Fund (ESF) project Nr. 2009/0138/1DP/1.1.2.1.2/09/IPIA/VIAA/004.

The thesis contains the annotation, aim and tasks, three chapters, publication list, reference list, and one appendix.

Form of the thesis: collection of research papers in biology, subfield – molecular biology.

Supervisor: Dr. chem. Regīna Renhofa

Reviewers:
1) Prof. Dr. Wolfram H. Gerlich, University of Giessen;
2) Dr. habil. biol. Indriķis Muižnieks, University of Latvia;
3) Dr. biol. Andris Dišlers, Latvian Biomedical Research and Study Centre

The thesis will be defended at the public session of the Doctoral Committee of biology, University of Latvia, at November 5th on 14:00, 2015, at Latvian Biomedical Research and Study Centre, Ratsupites Str. 1 k-1.

The thesis is available at the Library of the University of Latvia, Kalpaka blvd. 4.

Chairman of the Doctoral Committee _____/ *Kaspars Tārs* /

Secretary of the Doctoral Committee _____/ *Daina Eze* /

Annotation

Virus-like particles (VLPs) are protein structures formed from one or few types of protein capable to self-assemble in complex and highly organised structures. Due to the symmetrical fashion and multimeric structure pattern, VLPs can be used in two ways – as perspective carriers for exposition of foreign sequences and as a delivery vehicles containing packaged cargo inside them. One of the most promising area of VLPs utilization is vaccine development. Bacteriophages GA and AP205 are among one of the smallest and simplest viruses, extensively used as a study model for molecular biology. Coat protein expressed in bacteria or yeast forms VLPs. Another object – hepatitis B virus (HBV) core protein produced as recombinant protein also self-assemble into VLPs.

The aim of the work was to test various virus-like particle usage possibilities, therefore different test objects were used. First, West-Nile virus protein E domain III (WNV-DIII) protein sequence attachment to AP205 coat protein leaded to mosaic particle formation when expressed in *E.coli* cells. Mosaic particle formation was also achieved when HIV-Tat or WNV-DIII protein sequences were genetically attached to phage GA coat protein and expressed in yeast. Both WNV envelope protein equipped carriers showed specific immune response. Second, *in vivo* packaging of IL-2 and GFP mRNA into GA coat protein particles synthesized in *S.cerevisiae* was achieved. The packaging was improved by supplementing MS2 operator sequence to mRNA and using GA VLP mutants that mimicks MS2 operator binding site. Third, the methodology to obtain empty full-length HBV core VLPs was elaborated and successfully used for both bacteria- and yeast-produced particles. Four novel HBV core proteins (HBc-K75, HBc-K77, HBc-K79, HBc-K80) with lysine point-mutations on the protruding structure elements of particles, reveal perspective for addressing through chemical coupling. We proved, that elaborated alkali treatment method is effective for obtaining empty particles for all six cases – yeast-source, bacteria-source, as well for four lysine mutants. Fourth, *in vitro* packaging of nucleic acid fragments into alkali-treated empty HBc VLPs was studied. Packaging of DNA fragments was achieved through scarification of particles in urea and subsequent reconstruction, whereas RNA and short oligodeoxynucleotides were included in VLPs by simple mixing. Individual double-stranded DNA fragments of maximum length in range between 1289 to 1737 base pairs were found as packaged in equimolar ratio, whereas longer DNA fragments / plasmids were embraced by empty particles in large molar excess of them. Packaged DNA was protected from DNAse, whereas RNA, despite its capability to bind and package into VLPs, after extraction showed strong degradation, possibly explainable with ribonuclease activity of empty HBc VLPs.

Our novel and perspective technologies in field of small RNA phage and HBv core based virus-like particles can be used for vaccine development or utilized for generation of delivery cargo with abilities te be chemically addressed for specifical targeting and interaction with cells of interest.

Keywords: VLP, core, packaging

Anotācija

Vīrusiem līdzīgās daļiņas (VLD) ir proteīnu struktūras, kas veidotas no viena vai vairāku veidu proteīniem, kas spējīgi pašsavākties kompleksās un augsti organizētās struktūrās. Simetriskās un multimērās struktūras dēļ VLD var tikt izmantotas divos veidos – kā perspektīvi svešu sekvenču nesēji un eksponētāji, un kā piegādes vektori ar iepakotu kravu tajos. Viena no daudzsološākajām VLD pielietojuma jomām ir vakcīnu izstrāde. Bakteriofāgi GA un AP205 ir vieni no mazākajiem un vienkāršākajiem vīrusiem, plaši izmantoti kā modeļobjekts molekulārajā bioloģijā. Apvalka proteīnu ekspresējot baktērijās vai raugos, veidojas VLD. Cita objekta – hepatīta B vīrusa (HBV) core proteīna gadījumā, tas kā rekombinants proteīns spēj pašsavākties vīrusiem-līdzīgās daļiņās.

Darba mērķis bija pārbaudīt dažādas vīrusiem līdzīgo daļiņu pielietojuma iespējas, tāpēc tika izmantoti dažādi testa objekti. Pirmkārt, West-Nīlas vīrusa E proteīna DIII domēna (WNV-DIII) proteīna sekvences piesaistīšana pie AP205 apvalka proteīna un ekspresija *E.coli* šūnās nodrošināja mozaīkveida daļiņu veidošanos. Mozaīkveida daļiņas veidojās arī ģenētiski pievienojot HIV-Tat un WNV-DIII proteīnu sekvences pie GA apvalka proteīna un ekspresējot tās raugos. Abi WNV apvalka proteīnu saturošie nesēji parādīja specifisku imūno atbildi. Otrkārt, tika novērota IL-2 un GFP mRNS *in vivo* iepakošana GA apvalka proteīna veidotajās VLD, sintezējot tās *S.cerevisiae*. Iepakošanās tika uzlabota, papildinot mRNS ar MS2 operatora sekvenci un izmantojot GA VLD mutantus ar MS2 operatoram līdzīgu operatora saitu. Treškārt, metodika tukšu pilna garuma HBV core daļiņu iegūšanai tika izstrādāta un veiksmīgi pielietota daļiņām, kas ekspresētas baktērijās un raugos. Četri jauni HBV *core* proteīni (HBc-K75, HBc-K77, HBc-K79, HBc-K80) ar lizīna punktveida mutācijām uz daļiņu ārējās virsmas var tikt izmantoti perspektīvai adresēšanai, izmantojot ķīmisko piešūšanu. Mēs pārbaudījām, ka izstrādātā sārmainās apstrādes metode ir efektīva visu sešu veidu – bakteriālās izcelsmes, rauga izcelsmes un četru lizīna mutantu – tukšo daļiņu iegūšanai. Ceturtkārt, tika pētīta nukleīnskābju fragmentu *in vitro* iepakošana ar sārmu apstrādātajās tukšajās HBc VLD. DNS fragmentu iepakošanai tika izmantota daļiņu uzirdināšana urīnvielā un tai sekojoša rekonstrukcija, savukārt RNS un īsi oligodezoksinukleotīdi tika iekļauti VLD sastāvā tos vienkārši pievienojot. Tika parādīts, ka individuālie divpavediena DNS fragmenti ar maksimālo garumu starp 1289 bp un 1737 bp ir spējīgi iepakoties daļiņās vienādās molārās attiecībās, savukārt garāki DNS fragmenti un plazmīdas tika ieskautas ar tukšajām daļiņās to lielā molārā pārākumā. Iepakotās DNS bija pasargātas no DNāzes, turpretim RNS gadījumā, neskatoties uz tā spēju piesaistīties un iepakoties tukšās VLD, tik novērota spēcīga izekstraģētā materiāla degradācija, ko varētu skaidrot ar iespējamu tukšo HBV *core* VLD ribonukleāžu aktivitāti.

Mūsu jaunās un pespektīvās tehnoloģijas mazo RNS fāgu un HBV core pētījumu jomā var tikt izmantotas vakcīnu izstrādei vai arī pielietotas piegādes vektoru izveidei ar spēju tikt ķīmiski adresētām specifiskai mijiedarbībai ar šūnām.

Atslēgvārdi: VLD, *core*, iepakošana

Table of contents

The aim and tasks of research

The aim of the work was to test various modification and usage possibilities of bacteriophage GA and AP205 and hepatitis B virus (HBV) core protein assembled virus-like particles (VLPs).

Therefore following tasks were established:

- genetical introduction of HIV-Tat and WNV envelope protein sequences into phage GA and / or phage AP205 coat protein formed particles;
- characterization of WNV protein sequence bearing VLPs immunogenicity in mice;
- approbation and improvement of two-promoter yeast expression system for phage GA coat protein expression and particle assembly;
- *in vivo* packaging of IL-2 and GFP mRNA into phage GA VLPs;
- creation of technology for repackaging of full-length HBV core particles and testing this system with various nucleic acid based substances;
- introduction of lysine in the core protein in the outer region of particle's surface to enlarge chemical coupling features of HBV *core* formed VLPs

1. Literature overview

1.1. Virus-like particles

Virus-like particles or VLPs are multimeric nano-size particles, formed from self-assembly competent proteins of viruses of different origin and lacking infectious nucleic content. VLPs come from broad spectra of viruses, including them different in shape, genome type, infecting species and complexity. Highly complex VLPs are so-called enveloped VLPs consist from nucleocapsid that is surrounded with lipid bilayer (comprised from cell membrane), containing lipoproteins within outer layer. Simpler are protein-only VLPs, formed from structural proteins capable to self-assembly into highly oriented symmetric structures, morphologically similar to virus source structures. According shape, non-enveloped particles are divided into two groups – either spherical (icosahedral) or filamentous (rod-shaped) ones. Development of genetical methods provided not only synthesis of such recombinant structures; in many cases VLPs were capable to include foreign sequences – epitopes, addresses and markers – without loss of self-assembly. Such amino acid sequences – epitopes – can be used not only as a functional motifs (such as DNA/RNA binding sites, receptor/receptor binding sequences, etc.), but also as antigenic determinants (for detailed review see (Pumpens and Grens, 2002; Roldão et al., 2010; Zeltins, 2013)). VLPs structure forming proteins can be synthesized and VLPs can be obtained in various expression systems, specifically, in bacteria and yeast cells, baculovirus / insect system, in mammalian cells and also in plant-based systems (for review see (Pushko et al., 2013). Despite advanced functions of other expression systems, expression in *E.coli* as a producer leads to good VLPs yields and approved purification procedures.

From a vast majority of virus-like particle candidates, in our work we used recombinant self-assembled structures from hepatitis B virus and from one kind of the simplest viruses – RNA bacteriophages AP205 and GA. In case of bacteriophage GA and AP205 particles are formed from coat protein, in case of Hepatitis B virus the core protein serve as a base of VLPs. All those three objects share common property – they are protein-only VLPs. These VLPs are highly structured particles mimicking conformation of native viruses, but lacking genome and therefore also infectivity. Safety provided by VLPs is main thing of importance when potential vaccine candidates are developed.

To rise the potential of VLPs, foreign sequences from organisms of the different origin can be added, generating so called chimeric VLPs. Chimeric particles reveal additional functions of the VLPs, main of them are targeted delivery of particles and induction of specific immune response. One of the possible usage of the protein-only VLPs is addressing that can be done generally in two ways – through chemical coupling or genetic attachment. The chemical attachment of foreign sequences is more universal and somehow reliable method, leaving VLPs intact. On other hand – genetic attachment of foreign sequences to the VLPs forming protein provide clearly defined amount and also spatial orientation of attached amino acid sequence. Such a particles can carry more than one type of attached sequence, however different strategy of VLPs formation should be used – either multiepitope peptide-loaded VLPs (Ding et al., 2009) or mosaic VLPs need to be expressed. Mosaic VLPs are particles, consisting from different types of VLP forming protein monomers, and mostly they consist from unmodified structural protein and from this protein supplemented with desired sequence. This method is widely used when it is not possible to obtain the particles due to the negative impact on VLPs formation, caused by genetically added foreign protein sequence. At the same time such approach in

process of VLPs modelling allows dosing of the foreign protein in the particle, thereby admitting to vary with binding specificity or immune response. Latter one statement can be extended by constructing mosaic virus like particles, consisting from more than two different proteins. These are so called hybrid VLPs, displaying (at least) two different peptides on a single virus-like particle (Tyler et al., 2014).

Virus like particles can be used in different approaches – as a delivery vessels by packaging some useful preps into themselves or as an exposition vectors by containing sequences on the outer surface of VLPs possible to interact with specific receptors or elicit certain response from cells. These two properties can be unified to obtain packaged particles equipped with specific addresses, possible to serve as a cell directed delivery vectors (for review see (Garcea and Gissmann, 2004; Pokorski and Steinmetz, 2011)).

1.1.1. Immunology

Although targeted delivery is a perspective way for the VLPs to be used, main interest of the VLPs could be related with its role as a tools for immunisation. The use of VLPs in the past decade in vaccine development has been increased considerably, leading to development of so-called "nanovaccinology" (Mamo and Poland, 2012). Nano-particles are used in both prophylactic and therapeutic approaches, it also includes them either as delivery systems for enhanced antigen processing and/or as immunostimulant adjuvant for activation or enhancement of the immunity. From immune system point of view VLPs are the right-sized particles (between 10nm to 100nm in diameter) to be taken up in lymph nodes to elicit strong immune response even without adjuvants. Due to the highly symmetrical structure and possibility to add various immunological epitopes or their fragments, recombinant VLPs could be used as a safe alternative for the vaccination in place of attenuated viruses. One of such example is commercial preparation Engerix® (GlaxoSmithKline) that is VLPs-derived vaccine made from HBsAg protein and is used globally for effective immunisation against Hepatitis B virus infection. However, worldwide licensed vaccines Cervarix® (GlaxoSmithKline) and Gardasil® (Merc & Co., Inc.) against cervical cancer can be considered as a more true VLPs because resembling structure identical to intact virions (for review see (Zhao et al., 2014)).Vaccines are a mixture of VLPs formed by human papilloma virus (HPV) L1 protein, bearing L1 protein sequence variants from either type 16, 18 or type 6, 11, 16, 18 HPVs for Cervarix and Gardasil vaccines, respectively (Monie et al., 2008).

The broad spectrum of VLPs sources provides material for the different types and sizes of VLPs, giving therefore possibility to choose for appropriate and best suitable type of VLPs, and also permitting us to change carrier if immune response is developed against it.

1.1.2. Addressing

Addressing of the VLPs with epitopes on their surfaces is one way how VLPs can be utilised. There can be mentioned numerous epitopes, added to the surface of the VLPs by using diverse ways of attachment. As one of the example can be mentioned addition of the HIV-Tat protein derived peptide, possessing strong internalisation properties (Vivès et al., 1997). Chemical attachment of the HIV-Tat (47-57) to the MS2 surface allowed internalization of VLPs into cells and release of functional *in vivo* packaged antisense RNA (Wei et al., 2009), using sulfosuccinimidyl-4-(p-maleimidophenyl)-butyrate reagent for binding of N-terminal cysteine in HIV-tat sequence. For protein chemical attachment there are actually four targets in protein structure – primary amines ($-NH_2$), carboxyls (-COOH), sulfhydryls (-SH) and

carbonyls (-CHO). One approach is based on a fact, that particles contain bifunctional amino acids on the surface able to bind proteins by using crosslinking reagents as shown in abovementioned examples. If the VLPs surface does not contain such bifunctional amino acids, then other variant is chemical functionalization of the surface of virus-like particles, for example, using azide-alkyne click chemistry (Patel and Swartz, 2011).

Chemical attachment can be used for binding of non-protein origin substances, for example, the company Cytos Biotechnology AG bound nicotine to Qb VLPs and induced strong immune responses in preclinical studies (Maurer et al., 2005). Another perspective substances (addresses) for targeted drug delivery and use in clinical applications are aptamers – short oligonucleotides for specific binding to target molecules (for review see (Pei et al., 2014; Ray and White, 2010), however they are jet not coupled to VLPs.

For the specific ligand to work, appropriate receptor on the cell surface should be overexpressed, as was shown in example with one of the most commonly used ligand – transferrin (Daniels et al., 2012). The cellular binding and uptake of Qb virus like particles conjugated with transferrin was higher in case with transferrin receptor overexpressed cells, and the same study revealed positive correlation between ligand density on the particle surface and internalisation capacity into the cells (Banerjee et al., 2010).

An interesting approach was tried by Gleiter and Lillie, where antibody-binding domain Z was fused to polyomavirus VP1 protein and was able to specifically bind and functionally present antibody trastuzumab. Such VLP / antibody complex provided delivery of packaged reported plasmid DNA to the ErbB2-positive tumour cell lines using receptor-specific endocytosis (Gleiter and Lilie, 2003).

1.1.3. Packaging

The other application is to use internal space of the particles – the inner content of the particles can be filled or exchanged with substances of interest, including not only nucleic acid sequences, but also organic structures – proteins (Kaczmarczyk et al., 2011), antibiotics (Brown et al., 2002), etc. and even inorganic material – nanogold (Freivalds et al., 2014; Sun et al., 2007), magnetic nanoparticles (Huang et al., 2011), etc. Jason Clark with group used bacteriophage lambda as a base for packaging of DNA into particles, and after incubation with them observed specific immunoresponse against appropriate protein expressed from packaged DNA sequence (Clark and March, 2004). Further experiments showed that bacteriophage packaged with HBsAg coding DNA sequence elicited stronger immuneresponse in comparison with commercial vaccine Engerix B, what is based on a recombinant HBsAg protein (Clark et al., 2011). Also between the promising substances to be packed are so called CpG oligonucleotides, known as immune stimulatory sequences (Krieg, 2012). On the other side, RNA sequences can be also packaged. As a successful example can be mentioned JC virus VLPs packaged with short hairpin RNA (shRNA) and acting as an inhibitor against synthesis of IL-10 (Chou et al., 2010).

All those abovementioned approaches shows high versatility of VLPs usage purposes and areas, and many of them can be attributed to our used objects.

1.2. Bacteriophage GA

Bacteriophage GA belongs to the single stranded positive-sense RNA viruses – largest group of the VLPs candidates. One large and widely used class of them are RNA bacteriophages

capable to infect bacteria. They were among the first objects used to discover molecular biology processes. Bacteriophage MS2 was the first organism with fully sequenced genome (Fiers et al., 1976). RNA phages are divided into four serologic groups – I and II are members of *Levivirus* genus and III and IV belong to *Allolevivirus* genus. Main disparity between groups is presence of the A1 protein – read-through variant of the coat protein for the latter one group phages, necessary for production of viable phage particles (Hofstetter et al., 1974). Bacteriophage GA belongs to group II (*Levivirus* genus), and similarly as other RNA bacteriophages, consist from 180 coat protein monomers forming spherical particles. Coat protein forms dimers, which subsequently are arranged in icosahedral structure with triangulation number T=3.

Bacteriophage GA genome consists from 4 genes, coding coat protein, maturation protein, replicase subunit and lysis protein (Inokuchi et al., 1986). Of main interest is coat protein, which expressed as recombinant protein can freely form virus-like particles. Coat protein monomers are 129 amino acids long and fold into three parts: five stranded anti-parallel β-sheets and to the capsids outer surface oriented N-terminal hairpin and C-terminal α-helice (see Figure 1) (Ni et al., 1996).

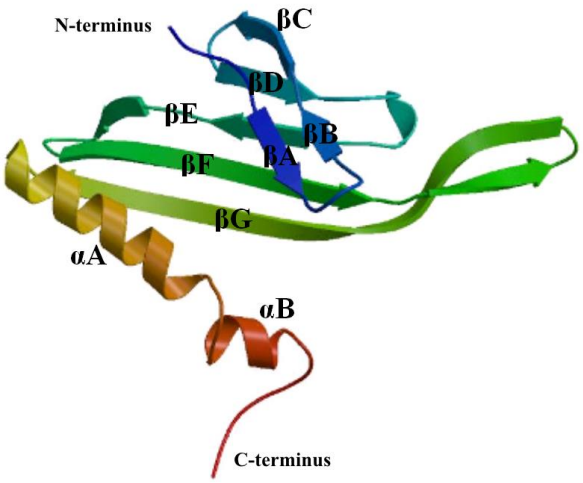

Figure 1 Three-dimensional structure of bacteriophage GA coat protein monomer (adaptation from (Tars et al., 1997)).

The C-terminal α-helice of one monomer fits in the groove between N-terminal hairpin and C-terminal α-helice of the second monomer, extending β-sheets into ten-stranded lattice and providing strong interaction between monomers. Therefore dimer structure can be considered as "building block", forming capsid with approximate diameter 27 nm as for the other RNA phages (Fiers, 1979).

Native formation of phage GA particles in cells involves also synthesis of maturation protein and packaging of phage specific genomic RNA. The studies on more explored phage MS2 showed, that originally, during phage maturation, genomic RNA is specifically packaged using small RNA hairpin – translational operator at the beginning of replicase gene (Hohn, 1969). RNA hairpin structure for specific binding with coat protein is known also for phage GA (Gott et al., 1991). VLP formation from RNA bacteriophage coat protein is sufficient with expression of only coat protein in *E.coli* cells; for GA phage it was shown by (Lim et al., 1994).

In case when recombinant protein was expressed, it was shown packaging of unspecific nucleic material encapsidated during VLPs assembly (Pickett and Peabody, 1993).

RNA bacteriophage inner content can be changed through *in vitro* repackaging (Wu et al., 1995). However, the binding of operator sequence can be used for directed packaging of foreign RNA *in vivo*, i.e., by simultaneously expressing MS2 bacteriophage coat protein and *lac*Z-operator RNA in *E.coli* cells (Pickett and Peabody, 1993). The *in vivo* packaging system for RNA phages on a basis of eukaryotic cells – yeasts *S.cerevisiae* – was firstly developed by Fastrez and Legendre on basis of phage MS2 (Legendre and Fastrez, 2005). Based on those authors work, MS2 VLPs with *in vivo* packaged HIV-1 *gag* mRNS were successfully tested for functionality of extracted RNA and VLPs were used for mice immunisation, inducing strong antibody response against HIV-1 p24 antigen (Sun et al., 2011).

Despite the fact that originally maturation of coliphage GA occurs in presence of native phage genome in *E.coli*, self-assembly of the particles can be also achieved when bacteriophage GA coat protein is expressed in other organisms – in yeasts *S.cerevisiae* and *P.pastoris* (Freivalds et al., 2008). Based on other authors work, we tried to alter phage GA surface properties and inner content through different methods.

1.3. Bacteriophage AP205

Acinetobacter phage AP205 belongs to positive single-stranded RNA bacteriophage family *Leviviridae*, but infects *Acinetobacter* instead of *Escherichia coli*. It genome consists from three "main" genes, encoding maturation (A), coat and replicase subunit protein (Klovins et al., 2002). Unlike all other members of *Leviviridae*, phage AP205 genome bears two additional small open reading frames (ORF's), one of which contains lysis protein expressing gene, but the function of second is unclear (Klovins et al., 2002). Although all proteins are necessary for proper virus maturation, in our case of main importance is the ability of the coat protein to self-assemble into VLPs (without help of other virus proteins). Cryo-EM analysis reveled the same icosahedral structure as for other small RNA bacteriophages, differing with slightly larger capsid size in 29 nm diameter (van den Worm et al., 2006). There are little of publications describing this phage, however present experiments show promising tendencies regarding of its possible use.

Although virus-like particles are supposed to be as a drug delivery system (for review see (Georgens et al., 2005)) and different methods to receive immune response for specific peptides are described, the numerous amounts of publications proofs that virus-like particles can be successfully used as a basement for vaccine production (for reviews see (Gregory et al., 2013; Kushnir et al., 2012; Roldão et al., 2010; Zhao et al., 2013)). Specifically, one of our object - coat protein from *Acinetobacter* phage AP205 - can also be used as a carrier for foreign antigens to determine them to immune system (Bachmann et al., 2010), either conjugating protein sequences chemically (Bachmann et al., 2012) or using gene engineering methods (Bachmann et al., 2008). Latter one statement is possible also due to the ability of AP205 coat protein to carry large protein fragments at both C- and N-terminus, at the same time maintaining ability to self-assemble into capsids (Tissot et al., 2010). Attached sequences include variety of proteins – hormones (angiotensin II, gonadotropin releasing hormone), cell receptor fragments (CXCR4) etc., tolerating up to 55 amino acids insertions (Tissot et al., 2010). VLPs containing peptide p33 (CTL epitope) chemically coupled to coat protein and loaded with CpG to enhance their immunogenicity (Storni et al., 2004) induce not only strong primary CTL response, but also can be efficiently boosted with the same modified/packaged VLPs (Schwarz et al., 2005).

One of the latest advantage is obtained by using phage AP205 equipped with alpha-helical regions of HIV gp41 on the surface of VLPs, where after mice immunization strong specific humoral response and inhibition of native HIV virus infection was observed (Pastori et al., 2012).

1.3.1. Acinetobacter phage AP205 and WNV protein E domain III

One of the perspective target for vaccination can be pathogenic arboviruses, specifically, member of *Flaviviridae* – West Nile virus (Ishikawa et al., 2014). Despite the fact that West-Nile virus infection are mainly asymptomatic, symptomatic cases cause mild febrile illness (so called West Nile fever) an in rear cases neuroinvasive diseases (meningitis, encephalitis, etc.), yielding overall fatality rate near 4% (Lindsey et al., 2010). A lot of succesfull vaccine or vaccine candidates are developed for arboviruses, nevertheless for many of them (including West Nile virus) viable vaccines should be produced. In parallel to attenuated virus vaccines, novel approach in vaccine development is the use of enveloped VLPs (Pijlman, 2015).

West Nile virus consists from nucleocapsid, formed from nucleocapsid protein (C) and genome RNA, and from envelope, formed from lipid membrane protein (M) and large envelope protein (E) together with host's membrane (Murphy, 1980). As can be seen from crystal structure of WNV protein E (Figure 2), domain III are localized toward the outer surface of West Nile virus (Kanai et al., 2006).

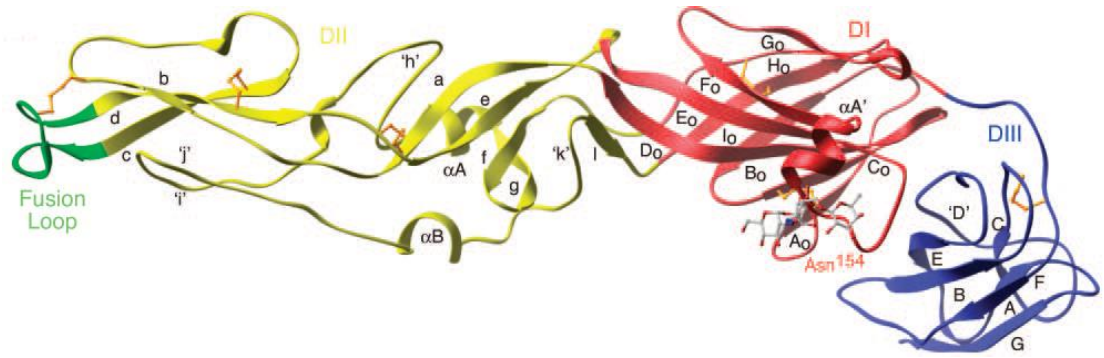

Figure 2 Crystal structure of the WNV protein E (adaptation from (Nybakken et al., 2006)).

To proof the concept if outside located protein E domains can be used for immunological purposes, a recombinant protein from protein E domain III was expressed in *E.coli*, purified as insoluble protein, refolded and finally used for polyclonal antibody production. Although the expressed protein was not glycosylated (apart from the glycosylated protein in native virus) and VLPs cannot be considered as enveloped, obtained antibodies showed inhibition of WNV entry into Vero cells and C6/68 mosquito cells, and what is the most important - murine polyclonal serum inhibited infection with WNV (Chu et al., 2005). The same is proofed also in case where protein E domain III (EDIII) specific monoclonal antibodies were used (Liu et al., 2008). The sequence region most probably responsible for infection is so called DIII lateral ridge (DIII-lr) (Figure 3), where full inhibition of infection *in vitro* are observed after treatment with DIII-lr specific monoclonal antibodies (Nelson et al., 2008).

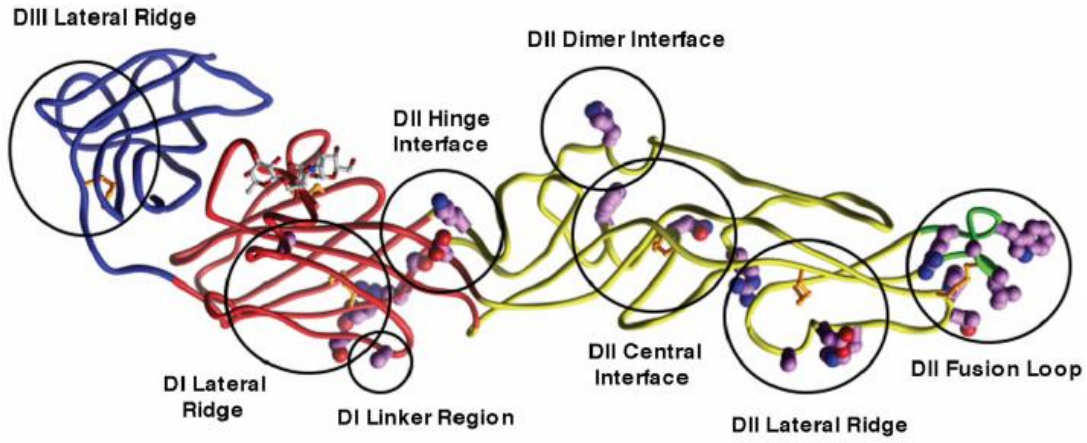

Figure 3 West-Nile virus protein E, circled regions shows epitopes specific for interaction with WNV neutralizing mAbs (adaptation from (Diamond et al., 2008)).

Previous successful experiments, showing no need for post-translational modifications of protein E fragments, promoted the usage of this protein as an easy attachable epitope on the surface of VLPs. After chemical coupling of unmodified AP205 coat protein and purified fusion protein, consisting from fragment of domain III of the WNV E protein, a hexahistidine tag and cysteine containing linker, mice were immunized in order to obtain WNV specific antibodies. After immunisation with mixture of coat protein and abovementioned WNV protein fragment, similarly as in case when immunising with WNV protein alone, no specific WNV immunoresponse was detected. After isotyping, WNV specific antibodies obtained after immunisation with chemically coupled VLP-WNV complex, were IgG2a specific (Spohn et al., 2010). This is opposite to the antibodies obtained after immunisation with WNV protein alone, where mainly IgG1 class antibodies are represented (Liu et al., 2008; Spohn et al., 2010). Together with the fact that with VLP-WNV complex immunised mice were able to survive admission of virulent WNV in lethal concentration, such complex of AP205-WNV can be used as attractive vaccine candidate for WNV prophylaxis (Spohn et al., 2010).

1.4. Hepatitis B

Hepatitis B virus genome encodes two viral genes S and C, forming two antigens – HBsAg and HBcAg, respectively. S gene codes three surface proteins – large (L), middle (M) and small (S), the last one is known to form particles with 22 nm diameter (Gerin et al., 1971). M and L proteins are prolonged variants of S protein, N-terminally containing prolongations with preS2 and preS1 sequences, respectively (for review see (Paul Pumpens, 2008)). Expression of surface antigen in *E.coli* cells have not lead to assembly of particles, but expression in yeast was successful (Hitzeman et al., 1983; Valenzuela et al., 1982), serving as a basis for vaccine development against Hepatitis B virus. Both vaccine products Engerix-B (GlaxoSmithCline) and Recombivax (Merck) are yeast-expressed non-glycosylated protein S-derived particles. In order to acquire better immunological responses against Hepatis B virus, preS2 epitope and especially preS1 epitope for binding with hepatocyte receptors were attached to the S protein, yielding either full-length non-reconstructed M (GenHevac B, Pasteur) or M and L (Bio-Hep-B, BioTechnology General Ltd.) vaccines or Hepacare vaccine containing complete sequences of S and preS2 region and preS1 sequence 20-47. Many other attempts to improve current Hepatitis B vaccine on a basis of HBsAg are tried, involving DNA vaccines

and plant-expressed edible vaccines. Despite a complex and irregular lipoprotein structure of HBsAg formed VLPs, they are tried to be used as a vaccine candidates for other diseases (for review see (Paul Pumpens, 2008; Roose et al., 2013)).

1.4.1. Structure of HBc

Hepatitis B virus C gene codes at least four different polypeptides: p25, p22, p21, and p17 (Scaglioni et al., 1997), however only p21 (HBc monomer as such) codes for self-assembly capable protein and therefore is widely used as a target for VLP engineering. This so-called core protein monomer is 183(185) amino acids long and composed as two α-helical hairpins forming dimer with a four-helix bundle (Figure 4A). Dimers assemble in to two types of particles – T=4 particles from 240 molecules with diameter 34 nm (Figure 4B) and T=3 particles from 180 molecules with diameter 30 nm – observed as mixture of both size particles in electron micrographs (Cohen and Richmond, 1982). Core protein contains four Cys residues – Cys107 is free thiol, Cys61 fully and Cys48 partly forms interchain disulphide bonds with another monomer and Cys183 forms disulphide bonds with monomer of another dimer (Nassal et al., 1992; Zheng et al., 1992). However, replacement of all Cys to Ser showed no requirement of cysteine residues for assembly of replication-competent particles nor for envelopment of them (Nassal, 1992a). Fine structure of HBc particles was ascertained using X-ray crystallography (Wynne et al., 1999) and cryo electron microscopy (Yu et al., 2013).

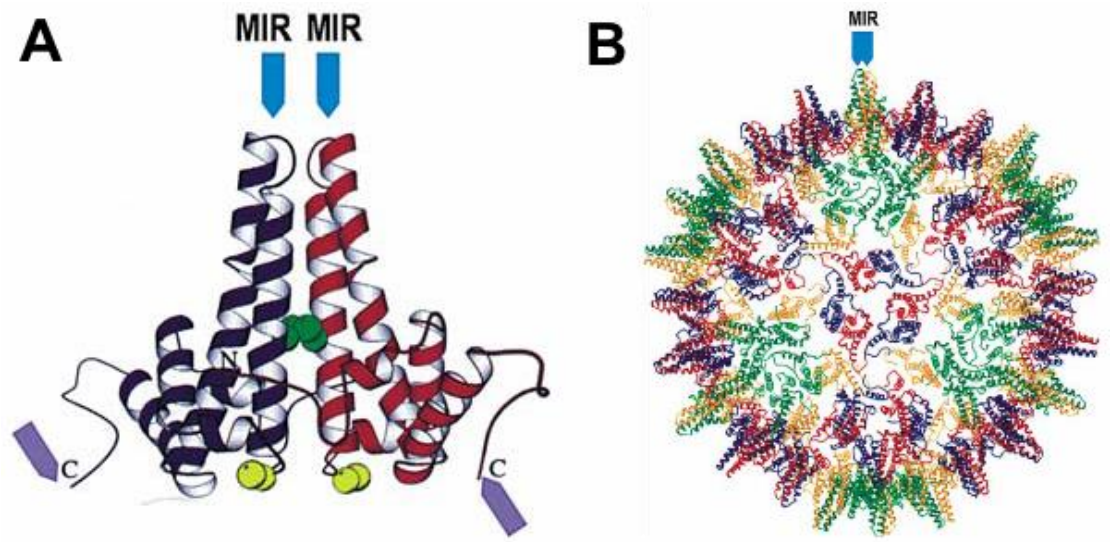

Figure 4 Three dimensional structure of hepatitis B core protein dimes (**A**) and core protein formed capsid (**B**) (adaptation from (Pumpens and Grens, 2001)).

One of the intriguing part of the core protein is major immunodominant region (MIR) with central positions around 78-82 in the α-helical hairpin, forming tip of the spike on the capsid surface. The other interesting part of core protein is C-terminus, specifically, its property to withstand truncation of last C-terminal amino acids but at the same time retaining the self-assemble capability of capsids (Birnbaum and Nassal, 1990). These C-terminal protamine-like arginine-rich domain lacking particles (so-called HBcΔ particles) were microscopically almost indistinguishable from full-length core protein formed particles, however they failed to accumulate nucleic material and therefore assembled as empty particles with impaired stability

(Crowther et al., 1994; Gallina et al., 1989). Therefore also efficient pregenomic RNA encapsidation was observed only in HBc VLPs truncated from C-terminus not more than till amino acid 164 (Nassal, 1992b). Also ratio between T=4 and T=3 particles in electron microscopy changed – full length core protein formed almost only T=4 symmetry particles whereas C-terminally reduced core protein generated T=3 symmetry particles (Wingfield et al., 1995; Zlotnick et al., 1996). Initially Birnbaum and Nassal showed that C-terminal deletions till approximately 139-143 amino acids can be tolerated (Birnbaum and Nassal, 1990), and only later after creation and purification of a set of C-terminus absent mutants it was precised that 140 amino acids are minimal length for particle assembly (Sominskaya et al., 2013). C-terminally truncated variants HBcAg1-149 and HBcAg1-140 were more like "thin-walled" particles with much larger inner space when compared to "thick-walled" full-length particles (Newman et al., 2003).

HBc protein is somehow different among other VLP carriers because of its high-level expression and effective particle formation in almost all known expression systems, including *E.coli*. This fact in combination with non-traditional three-dimensional structure of core protein in comparison to other viral capsid protein possibly leaded to extensive investigation of HBV core VLPs.

1.4.2. HBc as exposition vectors

The closer searches for the appropriate sites for insertions of foreign epitopes pointed toward MIR region and N- and C-terminus of core protein, not involving critical region for capsid assembly and being in good agreement with capsids three-dimensional structure (Wynne et al., 1999).

N-terminal end of core protein was capable to withstand deletion of 4 amino acids or insertions of up to 50 amino acids. Among the numerous attachments some of the promising are chimeric particles carrying 23 amino acid fragment of extracellular domain of influenza A minor protein M2 (Neirynck et al., 1999) and fusion of 45 amino acids of the Puumala hantavirus nuclecapsid protein to the HBcΔ (Koletzki et al., 2000).

Opposite to the N-terminal insertions where only full-length core protein VLPs can be used to achieve self-assembly, C-terminal attachments were to both the full-length and C-terminally truncated HBc. Full-length HBc were capable to carry C-terminal fusions of up to 55 amino acids from the HBV preS (Borisova et al., 1989) and SIV Env (Yon et al., 1992). As example for HBcΔ was shown C terminal fusions at positions 144, 149 and 156, by introduced sequences that exceeded even 100 amino acids (Pumpens et al., 1995). HBcΔ were appended C-terminally with HBV preS (Schödel et al., 1990) and S (Murray and Shiau, 1999), HIV-1 gp120 and Gag (Grene et al., 1997), cytomegalovirus gp58 (Tarar et al., 1996), two epitopes from FMDV VP1 (Nekrasova et al., 1997). On the basis of HBcΔ even extremely long sequences from HCV core protein in length of up to 540 amino acids (and to some extent up to 720) were successfully added without disrupting self-assembly capability of VLPs (Yoshikawa et al., 1993). Despite the good self-assembly of HBcΔ VLPs, after immunisation only moderate specific immune response against inserted epitopes are acquired.

Of the main interest, however, are insertions into the MIR region, i.e., in the tip of the spike of the HBc molecule. Due to the capability to include long amino acid sequences without loss of self-assembly of VLPs and ability to guarantee high B and T cell immunogenicity, MIR region is favourite site of choice for foreign epitope insertions. Insertions of hantavirus nucleoprotein 120 amino acid (Koletzki et al., 1999) and 45 amino acid (Ulrich et al., 1999)

long fragments in MIR region of HBc generated not only strong immune response, but also ensured protection against virus challenge after immunisation, whereas N- and C-terminally fused analogues showed poorer responses. MIR insertions cover the same fragments of interest as with N- and C-terminal attachments, namely, 27 amino acid epitope of the preS (Schödel et al., 1992), 18 amino acids of VP2 protein form the human rhinovirus type 2 (Brown et al., 1991), 30 amino acids of the SIV Env (Yon et al., 1992) and 25 amino acid (Brunn et al., 1993) and 43 amino acid (Borisova et al., 1996) sequences from V3 loop of the HIV-1 gp120 were inserted. Also recent finding showed successful construction of VLPs, bearing major rubella virus E1 protein (Skrastina et al., 2013), *Mycobacterium tuberculosis* CFP-10 protein (Dhanasooraj et al., 2013), etc., all capable to induce antibodies and protect against appropriate virus challenge.

preS epitopes were used to construct first multivalent particles, simultaneously containing different foreign sequences from preS1 and preS2 regions (Makeeva et al., 1995). Some special interest may be devoted to MIR deletion, where from numerous amount of data is deduced that region between glycines G73 and G94 can be used as a target for deletion, rearrangement and substitution (Borisova et al., 1996, 1997, 1999). Green fluorescent protein (GFP) and HBc chimeras retained both VLP self-assembly and GFP fluorescent capability, hence showing at least partially correct folding of 238 amino acid long protein inserted in MIR region and guided onto the surface of particles (Kratz et al., 1999). Similarly, fluorescent chimeric viral nanoparticles were obtained after addition of full length sequences of eGFP and DsRed proteins through glycine-rich flexible linker. This way attached fluorescent proteins showed higher fluorescence intensity than cognate fluorescent monomer proteins and also particles were more stable against photobleaching *in vitro* and *in vivo* inside mouse (Yoo et al., 2012).

Also mosaic particle production was adopted in HBc by introducing linker containing translational stop codons (UGA, or UAG) between C-terminally truncated HBcΔ and a foreign sequence (Koletzki et al., 1997). Elsewhere full-length preS-containing and native (helper) core vectors were co-transfected in *E.coli* cells, yielding mosaic VLPs (Kazaks et al., 2004). Chemical coupling as the attachment method was also tried on HBc particles using influenza virus M2e protein as a bound moiety, however induced antibodies after vaccination have not promoted virus-neutralizing effect (Jegerlehner et al., 2004). Another approach to overwhelm structural disorder of epitopes after chemical binding was tried by using non-covalent interaction between HBc spike and it specific peptide ("binding tag") supplemented with multiple copies of the extracellular domain of the M2 protein of influenza virus (Blokhina et al., 2013).

It can be concluded that robust structure and convincing assembly of the HBc VLPs allows successful self-assembly even after insertion of long sequences in various places of coat protein monomer.

1.4.3. HBc mediated immunogenicity

The matter of fact that HBV patients develop strong and long-lasting humoral anti-HBc response (Hoofnagle et al., 1973) demonstrate extremely high immunogenicity of the HBc protein. HBV core protein in native virus is as an internal antigen, however strong B-cell, T-cell and cytotoxic T lymphocyte (CTL) response (especially for epitope 18-27) promotes therapeutic vaccine searches also in this field (Livingston et al., 1999). Therefore it is not surprisingly that combination of HBV preS and S epitopes on the HBc carrier are tried to be

used for further HBV vaccine development (as examples see (Chen et al., 2004; Kazaks et al., 2004; Yang et al., 2005; Zhao and Zhan, 2002)). As another immune system affecting agents can be mentioned CpGs – DNA sequences rich in non-methylated CpG motifs greatly facilitating immune responses and inducing through strong T-helper and CTL response, and therefore can be considered among most promising adjuvants today. The packaging of CpG sequence in VLPs allows to overcome some drawbacks – unfavourable pharmacokinetics and vulnerability to DNase I digestion, at the same time ensuring strong response against CTL epitopes attached onto VLPs.

1.4.4. HBc as delivery vectors

HBc inner content deprivation

The inner space of full length HBc protein VLPs is filled with RNA that mainly corresponds to core protein mRNA (Birnbaum and Nassal, 1990). Up to the 156 amino acid long core protein formed particles can be characterized as almost empty (Sominskaya et al., 2013), however, packaging of desirable (required) nucleic acid material is difficult. Therefore another way is to seek for methods to empty full-length HBc particles needed (necessary) for repackaging of their inner content. Today two methods are known – osmotic shock based and through dissociation / reassociation of HBc. The first one method is more like "budding" of VLPs by in low ionic strength buffer solution, supplemented with RNAse A treatment (Kann and Gerlich, 1994). This method for obtaining empty HBc particles was later improved and characterized in details (Broos et al., 2007). However, logical limitation of this method is due to the RNAse A that permits the packaging of nucleic acid sequences of RNA origin. However, this method with slight variations was successfully used to package short CpG oligodeoxynocleotides in chimeric HBc VLPs harbouring tumour-associated MAGE-3 epitope (Kazaks et al., 2008). When micrococcal nuclease was used instead of RNAse A, beside the foreseen eating out the inner content of particles the significant degradation of HBc VLPs was observed (Newman et al., 2009). Another approach to obtain empty particles with help of nucleases was construction of chimeras from HBc core and enzymatically active region of 17kDa *Staphylococcus aureus* nuclease, that was able to produce empty particles upon protein synthesis in cell (Beterams et al., 2000).

The re-association was promoted after addition of oligodeoxynucleotides, poly-glutamic acid and polyacryl acid, nevertheless polylisine, polyethyleneimine and inositol triphosphate induced no capsid assembly. C-terminally truncated variants after treatment according to this method was not affected (Newman et al., 2009).

Fairly different method to get empty particles without nucleases was elaborated through core particle chemical disassembly. Guanidine HCl or urea treatment was used to disrupt truncated (3-148 amino acids) HBc particles, followed by packaging of GFP protein into VLPs by subsequent removing of denaturant by dialysis (Lee and Tan, 2008). Guanidine HCl and LiCl buffer was used to produce core dimers, that were either assembled as empty particles at higher ionic strength buffer or packed with various RNA samples (Porterfield et al., 2010).

In studies with bacteriophage MS2 viral capsids alkaline treatment of VLPs was used in order to remove genomic material (Hooker et al., 2004). Based on data about extreme chemical stability of HBc capsids in pH range 2 - 14 (Newman et al., 2003) we worked out our method for production of empty HBc VLPs through alkaline treatment of purified particles.

Binding and internalization of HBc VLPs

The possibility of HBc VLPs to interact with cells and to be internalized into cells were studied by several authors. In Kann and Gerlich group were used digitonin permeabilized cells to assess that *E.coli* expressed and *in vitro* phosphorylated HBc VLPs go into cells, reach the nucleus of the cells and bind to nuclear pore complexes (Kann et al., 1999). The detailed investigations regarding HBc VLP binding to cells and internalization were carried out by Vanlandschoot group (Vanlandschoot et al., 2005), who showed no binding of C-terminus deficient (lacking 145-183 amino acids) and strong binding of full-length HBc VLPs to various cells that was completely blocked by using heparin, heparin sulfate or chondroitin sulfate B.

These observations shows crucial role of arginine-rich protamine-like domain for binding of capsids to glucosaminoglycans expressed on cell surface. The RNAse treatment of particles enhanced binding of full-length HBc even more and, on the base of previous statement, authors hypothesize that after removal of packaged RNA, protamine-like domains are easier accessible by long sugar (glycosaminoglycan) chains on surface of cells (Vanlandschoot et al., 2005). Cooper and Shaul showed internalisation of full-length HBc VLPs into broad spectrum of cells, that was determined using fluorescently labelled oligonucleotide packaged in to the particle (Cooper and Shaul, 2005). Following experiments showed heparin and chlorpromazine but not nystatin inhibition of binding, thereby specifying that type of internalization for unmodified HBc particles are energy-dependent clathrin-mediated endocytosis. Additionally, confocal microscopy pointed that endocytosed HBc particles are targeted to lysosomes (Cooper and Shaul, 2006).

Meanwhile intact cell membrane trespassing of whole HBc VLPs was achieved after N-terminal fusion with protein transduction domains (PTDs), specifically, 12 amino acid long translocation motif from HBV surface protein. Such particles were capable to cross the cell membrane and move toward nucleus, bearing HBsAg or eGFP sequence. Clear ability of PTD-driven internalization was seen in ultra-thin sections in electron microscopy and in confocal microscopy (Brandenburg et al., 2005). One of recent findings shows cellular uptake of HBc VLPs when using fibronectin-binding fragment of *B.burgdorferi* BBK32 protein sequence inserted in MIR region (Ranka et al., 2013).

Last advances in HBV core protein modification leads to development of so-called Split Core technology. The native core monomer was genetically split in MIR tip between P79 and A80 via introduction of stop and start codons. Both coreN and coreC proteins expressed in cells formed capsid-like particles, capable to fuse heterologous sequences in sterically unrestrained fashion (Walker et al., 2011). This perspective system was recently used to successfully attach hepatitis C virus hypervariable region 1, capable to induce cross-neutralizing antibodies against hepatitis C after immunization of mice (Lange et al., 2014).

Also, another one ingenious approach is tandem fusion where both HBc dimer-forming monomers are joined together as single polypeptide. Therefore, insertion of large heterologous sequences in only one of the MIR spikes can be better tolerated in terms of VLP formation, because foreign sequences on particle surface are “diluted” two-fold if compared with full-epitope VLPs where each core protein monomer contains additive. This technological solution was used to express tandem HBc protein either in bacteria (*E.coli*) or plants (*N. bethamiana*) unmodified and also supplemented with full sequence of GFP or camelid single-domain antibody fragments by inserting them in second MIR site of tandem polypeptide (Peyret et al., 2015).

2. Materials and methods

2.1. Plasmid construction and protein expression

For *E.coli* cells, plasmids containing trp promoter were used for AP205 phage derived coat protein and hepatitis B core protein expression. AP205 coat protein containing plasmids were constructed on the basis of plasmid pAP283-58 (Tissot et al., 2010). Bacteriophage GA coat protein containing plasmid, as well as HBV core protein containing plasmids were constructed on the base of pGEM-1 based plasmid (Freivalds et al., 2008). All construction procedures were performed according standard cloning procedures described elsewhere, specifically – fragments were either cut out by using restriction endonucleases or cloned out using PCR, whereas point-mutants in case of HBV core protein was obtained by standard mutagenesis procedures.

All plasmids were replicated in *E.coli* strain RR1; for expression of GA and AP205 coat protein were used strain JM109 and for expression of HBV core protein were used strains K802 or BL21. Therefore that AP205 constructions contained either amber or opal suppression stop codons, they were expressed in modified JM109 strains containing helper-plasmids pISM579 and pISM3001. In case of WNV protein, it gene sequence was inserted in pET28+ plasmid under T7 promoter and grown in *E.coli* cells in strain C2566, applying IPTG as promoter inducer. For other *E.coli* transformed plasmids, growth medium was supplemented with tryptophan as a protein synthesis inducer.

In case of yeast-expressed constructions, shuttle-vector plasmids pESC-URA and pFX were used. For construction purposes, both type of plasmids were transformed in *E.coli* cells in strain RR1. Plasmid pFX was transformed in yeast *S.cerevisiae* in strain AH22 according (Freivalds et al., 2008) methodology. Plasmid pESC-URA contains two opposite-direction promoters GAL1 and GAL10, suitable for both expression of two types of proteins for mosaic particle production and for *in vivo* packaging. All constructions procedures are the same, as in case with *E.coli* expression meant constructions. pESC-URA based plasmids were transformed in yeast *S.cerevisiae* strain YPH499 competent cells using Yeast Transformation Kit (provided by and according Sigma-Aldrich protocol), then positive clones were selected in uracil-free agarised synthetic dextrose minimal medium and grown for expression in uracil-free synthetic galactose minimal medium. Yeast *P.pastoris* was used for expression of HBV core protein and obtaining of VLPs (Freivalds et al., 2011).

2.2. Purification of VLPs or protein

VLPs from *E.coli* cells were purified by suspending cells in lysis buffer and sonicated by using 22kHz ultrasound, whereas yeast cells were additionally disrupted by subjecting through French press and vortexing with glass beads. Further purification procedures varied between each type of VLPs, however, for AP205- and GA- based VLPs, lysate was centrifuged to sediment debris and supernatant was then chromatographed through gelfitration chromatography (using Sepharose CL-2B and/or Sepharose CL-4B), ion-exchange chromatography (using Sephadex A50) un sucrose density gradient ultracentrifugation. All concentrations between purification steps were done by using Amicon ultrafiltration devices or in dialysis tubes against dry Sephadex G-100 for AP205 or GA VLPs, respectively. AP205 working buffer was TEN, but GA VLPs as well as core VLPs needs addition of NaCl (i.e., TEN+0.5M NaCl was used). As one of the methods to distinguish VLPs and nucleic acids or

complexes of them was based on CsCl density gradient, relying on different densities of proteins and nucleic acids.

Fairly different is purification procedure for core VLPs, where cell lysate after ultrasonication was supplemented with urea till 0.45M, then centrifuged and supernatant was precipitated with ammonia sulphate in two steps, collecting the part that sediments in saturation range from 10% till 60%. Then subsequently Sepharose CL-2B and Sepharose CL-4B chromatography columns were used, concentrating appropriate fractions with ammonia sulphate (at 60% saturation). Next, material was dialysed against water and subjected through Sephacryl S-300 gelfiltration column using 0.1 M Na_2CO_3, 2 mM DTT as the eluent. Last step is essential for emptying of HBV VLPs.

WNV protein was extracted from cell lysate debris using 7M urea. To get rid of nucleic acid contaminants, either DEAE-cellulose ion-exchange chromatography or ammonia sulphate precipitation was used. Then refolding in presence of 2M urea + 0.5M arginine-HCl (pH8.0) and gelfiltration through Sepharose CL-4B column was done.

2.3. Detection of protein / VLPs and nucleic acids

During VLP and protein purification, detection of protein was done mainly using polyacrylamide gel electrophoresis (PAGE) and quantity was assessed by spectrophotometric methods (according (Ehresmann et al., 1973)). Western blot and Ouchterlony double-radial immune diffusion were used to immunologically approve presence of right one protein and electron microscopy was used to show VLPs morphology. For VLPs or their aggregate detection as one of the methods was used dynamic light scattering (DLS).

Native agarose gel electrophoresis (NAGE) was used to assess movement of VLPs and also if nucleic acids are alone or in complexes with VLPs. The inner content of VLPs were extracted using phenol/chloroform (1:1), then diethyl ether washed and finally precipitated with ethanol. Extracted content was tested on NAGE for DNA fragments or formaldehyde agarose gel electrophoresis (FAGE) for RNA fragments integrity. As a better alternative to FAGE was used also capillary electrophoresis system 2100 Bioanalyser (Agilent Technologies). Extracted RNA samples were analysed using reverse transcription PCR reaction to prove the presence of gene, and if necessary, qPCR was used to precise the relative amount of packaged gene inside particles. For PCR reaction, reverse transcription with random hexamer, oligo(dT) and gene-specific primers were used to produce cDNA, that used for PCR as a template with gene specific-primers.

2.4. Deprivation of HBc particles and re-packaging

To obtain empty particles, alkali treatment of HBc VLPs was used. Purified fractions after Sephacryl S-300 column were intensively dialysed against “alkaline” solution (0.1 M Na_2HPO_4 / Na_3PO_4, 0.65 M NaCl, pH 12 (NaOH)) at +37°C for 18 h. Then dialysis medium was exchanged to a restoration buffer (0.1 M Na_2HPO_4, 0.65 M NaCl, pH 7.8 (H_3PO_4)) at room temperature and at +4°C. Additional separation of aggregates and empty particles was done onto a Sepharose CL-4B column. Change of absorbance ratio A260/A280 and lack of EtBr fluorescence and presence of Coomassie blue staining in NAGE analysis demonstrated formation of empty particles.

Packaging of empty VLPs were conducted by mixing empty HBc particles with RNA or short DNA fragments. Reconstruction procedure included subsequent dialysis against 7 M urea

+ 1 M NaCl at +4°C for one hour followed by dialysis against multiple portions of fresh restoration buffer and was used particularly for long DNA fragments and plasmids.

2.5. Immunization with VLPs and proteins

Female BALB/c mices were immunised with both WNV-DIII fragment bearing VLPs and also with WNV protein. Immunisation was done on days 0, 14 and 28 with 25μg of protein per injection, and at the day 42 serum was taken. In parallel, immunisation experiment was expanded with samples, supplemented with adjuvants Alum and SiO_2. Direct ELISA was done according standard protocols, first, by coating plates with DIII protein, then, second, incubating them with immunised mice serum followed by incubation with horseradish peroxidase conjugated anti-mouse antibody, and, finally, determining the titre.

IgM and IgG subtypes were detected with direct ELISA, except that in goat/sheep produced monoclonal antibodies against different mouse antibody subclasses were sorbed on a plate and then incubated with immunised mice serum followed by peroxidase conjugated anti-goat/sheep IgG antibody.

3. Results and discussion

3.1. Bacteriophage GA VLPs

The abovementioned possibilities to use phage GA as a delivery and exposition vector were used in our experiments (Strods et al., 2013).

Previous possibilities to use RNA bacteriophages as a delivery and exposition vectors were used also in case with phage GA recombinant particles (Strods et al., 2013). First, we improved coat protein expression and therefore also overall VLP yields in *S.cerevisiae* cells by rewriting phage GA coat protein nucleotide sequence to the yeast cell more optimised codons. Nucleotide sequence was substituted according built-in yeast *S.cerevisiae* codon table in software package Vector NTI 10.0.1 (Invitrogen). Amino acid sequence was not changed and remained the same as described in (Tars et al., 1997). Albeit the previous research (Freivalds et al., 2008) suggests to take more productive yeast types, our experiment design demanded two-promoter system for simultaneous processing of two genes. Therefore we used expression vector pESC-URA and created workaround through codon optimisation. The strategy was advantageous and VLPs yield level was comparable to those obtained by using formaldehyde inducible promoters (vector pFX using *S.cerevisiae*) or vector pPIC3.5K using *P.pastoris* (Freivalds et al., 2008).

Second, we used previous experience (Rūmnieks et al., 2008) and produced *in vivo* packaged particles containing GFP and interleukin-2 mRNA. After thorough purification of particles, inner content was extracted and tested for presence of either GFP or IL-2 gene via reverse transcription PCR. This method does not allow to estimate specificity of packaging of our gene of interest, however, from our and previous (Rūmnieks et al., 2008) study we can deduce that large proportion of non-specific RNA are present in the particles. Therefore, as a continuation of (Strods et al., 2013) work, we set a task for us to improve the encapsidation rate through using the replication origin of MS2. Previously, MS2 and GA phage coat protein and translational operator interaction experiments revealed that of main importance are amino acids at positions 43, 55, 59, 83, 87, 89 (Lim et al., 1994) and 29, 66 (Lim and Peabody, 1994), and on the base of them single-point (S87N, K55N, R43K) and double-point (S87N+K55N and S87N+R43K) mutations were introduced in GA coat protein (Strods et al., 2015, manuscript submitted, see appendix). Parallel, advantage of two promoter system was used and in all constructions under second promoter was inserted GFP gene coding sequence. Additionally to those abovementioned variants was synthesized construction where GFP sequence are complemented with MS2 operator sequence. The idea to use MS2 tagging (Chubb et al., 2006) and tethering (Keryer-Bibens et al., 2008) techniques is based upon strong and highly-specific MS2 protein – MS2 operator interaction. Analysis of inner content from thoroughly cleaned VLPs revealed that all VLPs packed GFP mRNA. With MS2 operator supplement, quantity of packaged GFP mRNA was relatively higher, showing expected specificity. Despite the considerable specificity of gene packaging directed by MS2 operator, VLPs still continue to package its own GA coat protein mRNA and possibly some unspecific sequences (Strods et al., 2015, manuscript submitted, see appendix).

And the third, we used genetic engineering methods to covalently attach HIV-Tat (48-60) and WNV-DIII amino acid sequences to the GA coat protein. The third task was accomplished by simultaneous expression of native coat protein and prolonged coat protein through usage of dual promoter system, therefore producing mosaic virus-like particles. Foreign sequence was attached either at N-terminus or C-terminus of coat protein for HIV-Tat or WNV-DIII proteins,

respectively. Purified protein from phage AP205 coat protein genetically fused with WNV-DIII was used for production of polyclonal antibodies in mice, and then with the help of these antibodies proper exposition of WNV-DIII sequence onto the surface of mosaic particles was shown (Strods et al., 2013).

PROCEEDINGS OF THE LATVIAN ACADEMY OF SCIENCES. Section B, Vol. 66 (2012), No. 6 (681), pp. 234–241.
DOI: 10.2478/v10046-012-0015-y

EXPRESSION OF GA COAT PROTEIN-DERIVED MOSAIC VIRUS-LIKE PARTICLES IN *Saccharomyces cerevisiae* AND PACKAGING *in vivo* OF mRNAs INTO PARTICLES

Arnis Strods, Dagnija Ārgule, Indulis Cielēns, Ludmila Jackeviča, and Regīna Renhofa

Biomedical Research and Study Centre, Rātsupītes ielā 1, Rīgā, LV-1067, LATVIA;
a.strods@biomed.lu.lv

Communicated by Pauls Pumpēns

Our previous research showed that the best yield of virus-like particles (VLPs) formed by RNA bacteriophage GA coat protein was obtained by expression in yeast Pichia pastoris*, while other used expression systems in* Saccharomyces cerevisiae *gave much lower amounts of capsids. The main reasons to attempt further studies in* Saccharomyces cerevisiae *were to improve the yield of GA-based VLPs using constructs with optimised nucleotide triplets in coding sequences, and to exploit the possibilities of the two-promoter Gal1/Gal10 system of expression vector pESC-URA for production of the desired mosaic VLPs and for packaging of mRNAs into VLPs* in vivo.

INTRODUCTION

Yeast expression systems are successfully used for production of heterologous proteins and for generation of virus-like particles (VLPs) of several sources (Strausberg and Strausberg, 2001; Sasnauskas *et al*., 2002; Tsunetsugu-Yokota *et al*., 2002; Chen *et al*., 2004; Juozapaitis *et al*., 2005; Mach *et al*., 2006; Freivalds *et al*, 2011). Our particular interest is the potential of yeast cells as a host for producing properly folded bacteriophage MS2, Qβ and GA coat protein-derived VLPs (Legendre and Fastrez, 2005; Freivalds *et al*., 2006; Freivalds *et al*., 2008; Rūmnieks *et al*., 2008; Sun *et al*., 2011), also with simultaneously packaged mRNAs *in vivo* (Legendre and Fastrez, 2005; Rūmnieks *et al*., 2008; Sun *et al*., 2011). Here we continue our previous investigations (Freivalds *et al*., 2008; Rūmnieks *et al*., 2008) in several aspects: 1) to improve the yield of VLPs formed by GA coat protein in *Saccharomyces cerevisiae* by use of optimised, yeast-characteristic codons, 2) to produce nanoparticles with *in vivo* packaged mRNAs coding „reporter" protein GFP or interleukin-2, 3) to exploit the two-promoter expression system pESC-URA for production of mosaic particles formed from two proteins — GA coat protein and this protein fused with the desired eukaryotic sequence, this time with fragment of HIV Tat sequence and with West Nile Virus E protein DIII chain. Such an approach to form mosaic particles often is the only possibility to involve foreign protein sequences into soluble structures and to utilise them in further investigations.

In our previous papers (Freivalds *et al*., 2008; Rūmnieks *et al*., 2008), the GA coat protein (CP) encoding gene was amplified from *Escherichia coli* expression plasmid pGA-355-24. The CP aminoacid sequence encoded by this plasmid is identical to that published by Tars *et al*., 1997. The coding sequence for this plasmid was obtained by RT of full-length bacteriophage GA RNA, and therefore, it could be designated as original (*Escherichia coli* specific). Previously it was shown (Freivalds *et al*., 2008) that the highest yield of GA CP VLPs was obtained in the case of yeast *Pichia pastoris*. In *Saccharomyces cerevisiae*, the yield of GA CP-formed particles was lower — up to two times for AH22/pFX-GA and remarkably low for YPH499/pESCURA. Both *Saccharomyces cerevisiae* vectors exist in cells as episomes. Our particular interest was vector pESC-URA from Stratagene, which has two regulated promoters Gal1 and Gal10 that are very powerfully induced by galactose (up to 1000-fold). The Gal1 and Gal10 promoters share a common upstream activating sequence, which transcribe in opposite orientations and can be used to express two products simultaneously and in approximately equivalent amounts. To attempt to improve yield of GA CP-derived particles, we decided to switch from original *Escherichia coli* preferred codons to optimised ones for yeast. It is considered that optimal codons can aid to achieve faster translation rates and higher accuracy of those processes. Optimal codons in fast-growing microorganisms, like *Escherichia coli* or *Saccharomyces cerevisiae*, reflect the composition of their respective genomic tRNA pool. Preferred codon usage in *E. coli* and yeast is quite different (Klump and Maeder, 1991). To convert the *E. coli* original GA CP sequence into an optimal one for yeast, a built-in *Saccharomyces cerevisiae* codon table from the Invitrogen software package Vector NTI 10 was used. Additional corrections were made by us to eliminate blocks with more than four identical nucleotides. The resulting GA CP coding sequence used in further work is displayed in Figure 1.

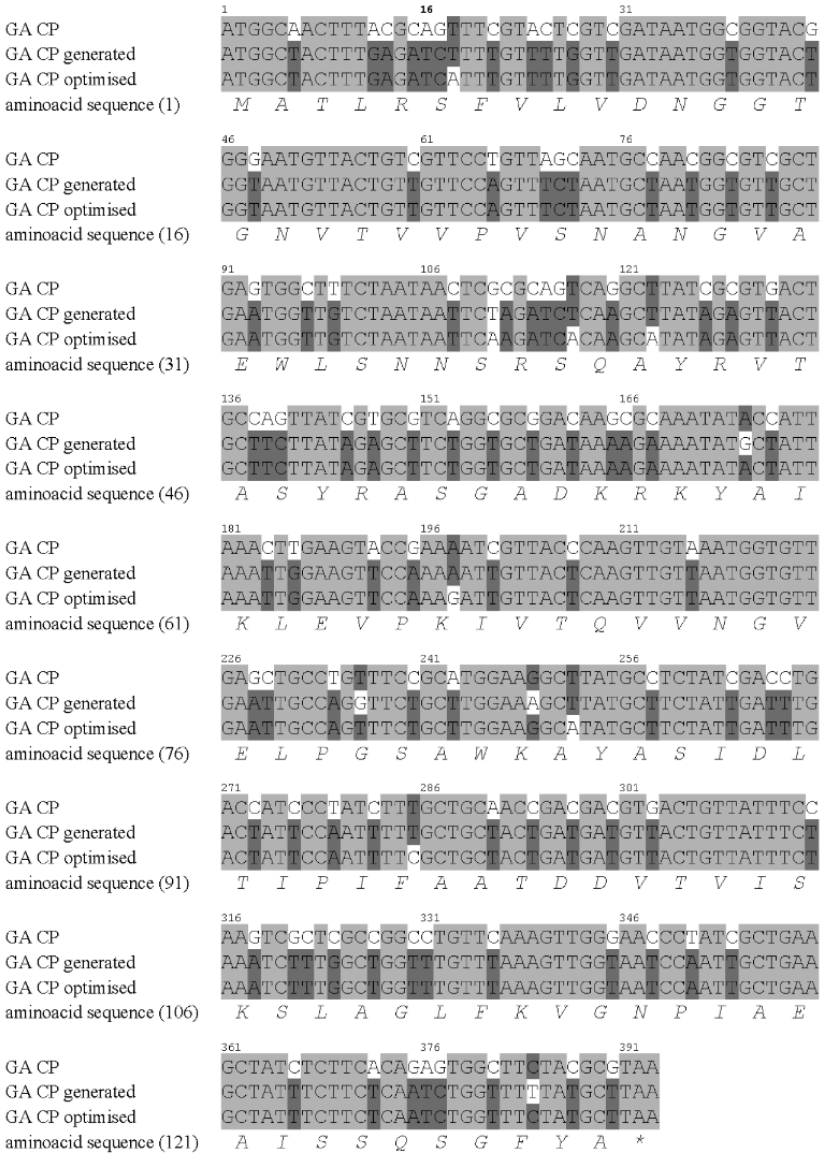

Fig. 1. Comparison of GA CP original, software generated and optimised (manually corrected) codon sequences.

MATERIALS AND METHODS

Materials. The materials employed were: Anti-Interleukin-2 Antikörper (online-antibodies GmbH); Pro-Q® Diamond Phosphoprotein Gel Stain (Molecular Probes, Invitrogen); Shrimp Alkaline Phosphatase (Fermentas); pESC Yeast Epitope Tagging Vectors (Stratagene); plasmid pUC57-GA containing GA coat protein sequence encoded with yeast optimized codons (GeneScript); Yeast Transformation Kit (Sigma) and First Strand cDNA Synthesis Kit (Fermentas).

Plasmids and constructions. All used constructions made by ligation of vectors and appropriate fragments (synthesised in PCR reaction and digested with vector-consistent restriction endonucleases), are summarised in Table 1. Two *S. cerevisiae* plasmids with original GA CP gene sequences were already available — pESC-GA was obtained from previous experiments (Freivalds *et al*., 2008) and pFX-GA was a kind gift from Dr. Andris Kazāks (Freivalds *et al*., 2008). Constructions with optimised codons were prepared on the basis of those two plasmids:

(1) for expression in yeast AH22, the construction pAS66 was made by cutting the coat protein gene from plasmid pUC57-GA and inserting it in the vector derived from pFX-GA;

(2) for expression in yeast YPH499, constructions pAS65 and pIC971 were synthesised by cloning out the GA CP coding sequence from plasmid pUC57-GA by PCR reaction

Table 1

OVERVIEW OF SYNTHESISED PLASMIDS

Construct	Input vector	Fragment or insert		
		source plasmid	forward primer	reverse primer
pAS66	pFX-GA digested with XbaI and BglII	pUC57-GA digested with XbaI and BglII	-	-
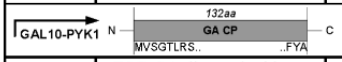				
pAS65	pESC-GA digested with BamHI and HindIII	pUC57-GA	pARS24	pARS25
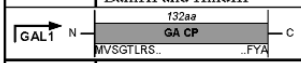				
pIC971	pESC-URA digested with EcoRI and NotI	pAS65	pINC402	pINC403
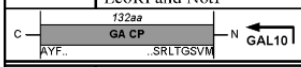				
pIC562	pAP409 digested with Kpn2I and Mph1103I	pTRHis2A-WNV	pWNV-Kpn	pWNV-Mph
pDA21	pESC-GA digested with EcoRI and NotI	pAK5	pDAR1	pARS18
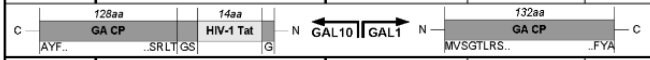				
pIC929	pAS65 digested with EcoRI and NotI	pAS65	pINC354	pINC355
pIC930	pIC929 digested with Kpn2I and NotI	pIC562	pWNV-Kpn	pINC356
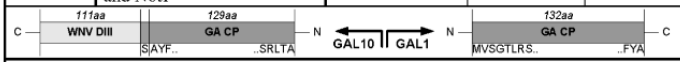				
pIC958	pAS65 digested with EcoRI and NotI	pAC262	pINC324	pINC325
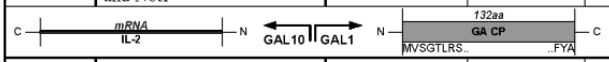				
pIC972	pIC971 digested with BamHI and HindIII	pAC262	pINC413	pINC414
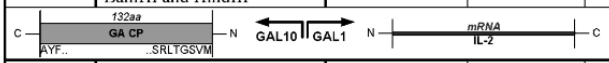				
pIC984	pAS65 digested with EcoRI and NotI	pCEP4-CXCR4-eGFP	pJAR18	pJAR19
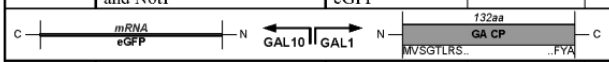				
pIC921	pIC971 digested with BamHI and HindIII	pCEP4-CXCR4-eGFP	pINC434	pINC435
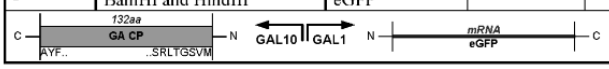				

and inserting it in plasmid pESC-URA; other plasmids were derived from those two plasmids.

Plasmid pIC562 was constructed to "stick" the West-Nile virus envelope protein domain III (WNV-EDIII) sequence to the C-terminus of Acinetobacter phage AP205 coat protein. The WNV-DIII sequence was cloned from pTRHis2A-WNV plasmid (Martina *et al*., 2008), inserted in vector plasmid pAP409 (Tissot *et al*., 2010) and expressed in *E. coli* JM109 cells.

In the first step, to obtain mosaic virus-like particles, the construction pIC929 was created in which GA CP sequences were inserted under control of both promoters (Gal1 and Gal10). GA CP under control of Gal10 promoter was C-terminally fused with the WNV-EDIII sequence, which was cloned out from construction pIC562. In the case of construction pDA21, pESC-GA plasmid (Freivalds *et al*., 2008) was modified by inserting, under control of the Gal10 promoter, the GA CP gene that was previously N-terminally prolonged with the HIV-Tat (48-60) sequence (from construction pAK5 for expression in *E. coli* system). Therefore, this construct was made with *E. coli*-specific codons.

For *in vivo* packaging, four constructions were made — two with the interleukin 2 (IL2) sequence cloned from plasmid pAC262 (Avots *et al*., 1990) and two with the eGFP sequence cloned from plasmid pCEP4-CXCR4-eGFP (Strods *et al*., 2010). Each of the genes was cloned in GA CP containing pESC-URA plasmid, under control of either under Gal1 or Gal10 promoter.

Transformation and protein production. *S. cerevisiae* strain AH22 competent yeast cells were transformed with

appropriate plasmids (pFX or pAS66) and cultivated for GA CP expression as described by Freivalds *et al.*, 2008.

S. cerevisiae strain YPH499 competent cells were transformed with appropriate pESC-URA plasmids by using standard lithium acetate/polyethylene glycol procedure (by using Yeast Transformation Kit (Sigma)) as described by Gietz *et al.* (1992). Transformants were selected on uracil-free agarised synthetic dextrose minimal medium (SDU^-) according to the manufacturer's protocol. Analytic expression was performed for clone selection. For cell multiplication, 5 mL SDU^- medium and incubation in 30 ^oC for 24 h were used. For expression, 1 mL inoculum and 5 mL uracil-free synthetic galactose minimal medium (SGU^-) and incubation in 30 ^oC, 200 rpm for 24 hours were used. Protein content in cells was determined with Western blotting. Selected clones were cultivated for preparative protein expression. 5 mL of inoculum were incubated in 100 mL SDU^- in 30 ^oC, 200 rpm for 24 hours; the cells were collected by centrifugation (3000 rpm, 5 min) and resuspended in 200 mL SGU^- and cultivated for 48h. Preparative cultivation was conducted in 1 L flasks.

Purification of VLPs. For purification, 3–8 grams of yeast cells were resuspended in 10 mL of buffer solution B (20 mM Tris-HCl, 5 mM EDTA, 0.65 M NaCl, pH7.8) supplemented with 0.03 mM PMSF. For cell disruption, suspension was subjected to the *French* press (three strokes, 20 000 psi), then stirred with 5mL glass beads (Sigma) (30 sec of stirring and 1 min of cooling on ice, 15 cycles) and, finally, sonicated with 22 kHz ultrasound (15 sec of sonication and 1 min of cooling on ice, 5 cycles). Insoluble cell debris was avoided by centrifugation (30 min, 12 000 rpm). The pellet wash (with 5 ml of buffer solution B) was added to the previous supernatant for concentration by dialysis against buffer solution B : glycerol (1 : 1) for 24 hours. Concentrated material was loaded onto a Sepharose CL-4B gelfiltration column (2 × 63 cm) with buffer solution B flow rate approximately 2 $mL{\cdot}h^{-1}$.

Capsids were pooled and concentrated by addition of solid ammonium sulphate to 60% of saturation and incubation overnight at –18 ^oC. After centrifugation (15 min, 10 000 rpm), the sediment was solubilised into 1 mL buffer B and dialysed against buffer TEN (20 mM Tris-HCl, 5 mM EDTA, 0.15 M NaCl, pH7.8) with a lower amount of sodium chloride. Contaminant nucleic acids were removed by passing through a short DEAE-Sephadex A50 ion-exchange column according to Rūmnieks *et al.*, 2008.

Final purification of VLPs was performed by sucrose density gradient ultracentrifugation on an ultracentrifuge Optima L-100XP with SW32Ti rotor at 20 500 rpm 13 hours. Centrifuge tubes were filled with layers of descending concentrations of sucrose solutions, starting with 36% on bottom till 5% on top. After fractionation and analysis, capsids were collected and dialysed against buffer solution B : glycerol (1 : 1) and stored.

Analysis of incapsided nucleic acids. Nucleic acids from 0.2 mg of purified capsids were extracted using phenol as described by Rūmnieks *et al.*, 2008. Synthesis of the first strand cDNA was conducted using the First strand cDNA synthesis kit (Fermentas) according to the manufacturer's protocol; 1/10 of extracted RNA was used as a template for each of the corresponding primers — random hexamers, $oligo(dT)_{18}$, forward primer against GA CP, and forward primer against IL-2 or against eGFP gene sequence. For second strand cDNA synthesis by PCR reaction, both forward and reverse primers were added to 2 µL of each mixture and products were analysed in agarose gel electrophoresis (Fig. 5).

Polyclonal antibodies against West-Nile virus E protein DIII sequence. Plasmid pIC562 was expressed in *E. coli* JM109. After ultrasonification of cells in lysis buffer (10 mM Tris-HCl, 5 mM EDTA, 0.03 mM PMSF, pH7.8), soluble proteins were removed by centrifugation at 12 000 rpm for 45 min. Fusion protein P562 (AP205 CP – WNV EDIII fragment) was extracted from the pellet with 7M urea in water and placed on a column with DEAE-cellulose, pre-equilibrated with 0.02 M Tris-HCl, pH8.6. Protein P562 did not absorb and was collected by washing out with equilibration buffer and sedimented with equal volume of saturated ammonium sulphate. For immunisation, a solution of P562 in 7 M urea was prepared.

The immunisation of five Balb/c mice was conducted by simultaneous peritoneal and subcutaneous injections of 25 µg of purified virus-like particles in total volume 200 mµL, supplemented with complete Freund's adjuvant (Sigma) in equal amounts. Two re-immunisations were conducted after 14 and 28 days in the same manner, but by using incomplete Freund's adjuvant (Sigma) instead of complete Freund's adjuvant. Mice were bled after 42 days and the collected blood was incubated for 30 min at +37 °C and for 20 min at +4 °C. After centrifugation serum was collected and mixed with glycerol (1 : 1) for storage in –20 °C.

Permission from the Food and Veterinary Service was obtained.

Polyacrylamide gel elecrophoresis and Western blotting. PAGE was performed in Tris-glycine buffer with 21% resolution gel and 6% stacking gel, and bands were silver-stained according to standard procedure. Western-blots were made with rabbit polyclonal anti – GA CP VLPs (as an antigen for antibody production, GA CP VLPs produced in *E. coli* (from construction pGA-355-24) and protein A – HR peroxidase conjugate (Sigma)) were used.

RESULTS

A set of plasmids was created to construct GA CP-based mosaic particles and to develop *in vivo* packaging of VLPs with the desired mRNAs (Table 1). The advantage of the used commercial expression system pESC-URA is it universality, which allows to manufacture plasmids in *E. coli*

Table 2

OLIGONUCLEOTIDE PRIMERS USED FOR THE CONSTRUCTION OF PLASMIDS AND RT-PCR

Oligonucleotide	Nucleotide sequence (5' to 3')
pARS24	TTGGATCCACAA**ATG**GCTACTTTGAGATCATTTGTTTTGGT
pARS25	TTTAAGCT**TA**AGCATAGAAACCAGATTGAGAAGAAATA
pINC402	CCGAATTCACAA**ATG**GCTACTTTGAGATCA
pINC403	TAGCGGCCGC**TTA**AGCATAGAAACCAGATTGAGA
pDAR1	ATGAATTCGGATCCCC**ATG**GGATATGGTCGTAAGAAAC
pARS18	TAGCGGCCGCAAGC**TTA**CGCGTAGAAGCCACTCTGT
pINC354	TCGAATTC**ATG**GCCCCTACTTCAAGTTCTAC
pINC355	ATGCGGCCGC**TTA**AGTCAGTGTTGAGATGATGC
pWNV-Kpn	CATCCGGACAGTTGAAGGGAACAAC
pWNV-Mph	GTATGCAT**TA**TTTGCCAATGCTGCTTCC
pINC356	ATGCGGCCGC**TTA**TTTGCCAATGCTGCTTCC
pINC324	TCGAATTC**ATG**GCCCCTACTTCAAGTTCTAC
pINC325	ATGCGGCCGC**TTA**AGTCAGTGTTGAGATGATGC
pINC413	TAGGATCCACAA**ATG**GCCCCTACTTCAAGTTCTAC
pINC414	TACAAGCT**TA**AGTCAGTGTTGAGATGATGC
pINC434	TAGGATCC**ATG**GTGAGCAAGGGCGAGGA
pINC435	TCTAAGCT**TA**CTTGTACAGCTCGTCCATGCC
pJAR18	TCGAATTCC**ATG**GTGAGCAAGGGCGAGGA
pJAR19	GAGCGGCCGCAAGC**TTA**CTTGTACAGCTCGTCCAT
p1.561	TGCC**ATG**GCAACTTTACGCAGTTTCG
p1.562	TGAAGC**TTA**CGCGTAGAAGCCACTCTG

Restriction endonuclease sites are underlined; initiation and termination codons are in bold

as a host and therefore to involve vectors for expression of VLPs in bacteria. Table 2 represents sequences of oligonucleotide primers used to create constructs for VLP production. To check the effect of codon changes made in the CP coding part of the plasmid on the production of GA CP VLP, we compared yields of capsids with previously exploited construction pFX-GA and the new construct pAS66 (Table 1).

Previous work had shown that, comparing the used *S. cerevisiae* systems AH22/pFX-GA and YPH499/pESC-URA, the first of them, which was formaldehyde inducible, gave slightly higher yield of particles (Freivalds *et al.*, 2008). Hence just this system was chosen to compare yield of the product coded by the original *E. coli*-specific sequence and our „improved" plasmid pAS66. Using pAS66 we obtained stably higher yield of particles, the process became more repeatable, and production reached two milligrams per one gram of yeast cells. Therefore, in our further constructs for the system of interest YPH499/pESC-URA (uracil auxotrophy), new CP coding sequences were exploited, excepting construct pDA21 with *E. coli* origin codons (Table 3). We focused on two-promoter system possibilities, rather than on the yield of products, as it is well known that *S. cerevisiae* prefers glucose as a carbon source and its growth rate is much higher in glucose than in galactose-containing media, which is necessary for activation of both promoters in pESC-URA. In all cases investigated till now, yield of purified capsids was at least 1 mg per gram of yeast cells.

Table 3

CHARACTERISTICS OF CONSTRUCTIONS EXPRESSED IN THE SYSTEM *Saccharomyces cerevisiae* YPH499/PESC-URA FOR PRODUCTION OF VLPS

Purpose	Construction, number	Promoters	Genes
VLPs yields	pAS65	GAL1	GA CP
	pIC971	GAL10	GA CP
mosaic particles	pDA21*	GAL1 GAL10	GA CP HIV-Tat(48-60) + GA CP
	pIC930	GAL1 GAL10	GA CP GA CP + WNV DIII
packaging *in vivo* of mRNAs	pIC958	GAL1 GAL10	GA CP IL2
	pIC972	GAL1 GAL10	IL2 GA CP
	pIC921	GAL1 GAL10	GA CP GFP
	pIC984	GAL1 GAL10	GFP GA CP

* both GA CP coding sequences are *E. coli* origin

Protein modifications can occur in yeast — particularly phosphorylation, which can affect up to 30% of the proteome (Ptacek *et al.*, 2005) and usually affects serine residues (Cobitz *et al.*, 1989). Phosphorylation of GA CP in our cases was not observed, which is surprising, as each 129-aminoacid-long GA CP molecule contains 14 serines. In the cases of VLPs produced from plasmids pAS65,

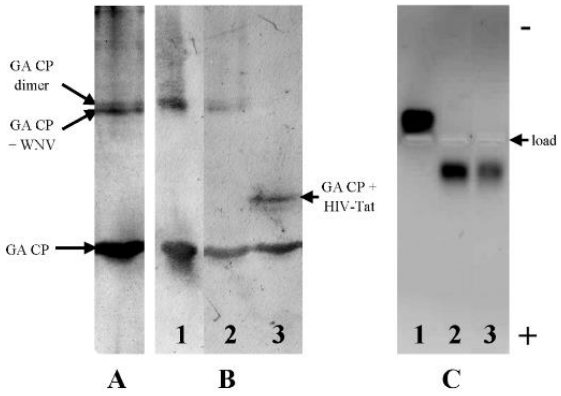

Fig. 2. Analysis of VLPs by PAAG (A and B) and agarose gel (C) electrophoresis: A – silver staining of purified construction IC930 VLPs; B – Western blotting of constructions 355-24 (1), IC930 (2) and DA21 (3); C – purified VLPs from constructions 355-24 (1), IC930 (2) and IC972 (3).

pAS66, pIC930 and pIC958, two tests (proQ Diamond phosphoprotein gel staining of CP in PAAG and incubation with PME with subsequent electrophoresis of capsids in native agarose gel) did not show phosphorylation of GA (data not shown). It is interesting that electrophoretic mobility of GA CP-formed capsids from *E. coli* (355-24) and from yeast (pIC930 and pIC972) was quite different in native agarose gels compared with that of coat protein in PAAG (Fig. 2C).

We attempted to obtain mosaic particles consisting of native CP and of CP fused with foreign sequences. Two such constructs, pDA21 and pIC930, were successfully expressed (Table 3). In both cases, N- terminal (DA21) and C-terminal (IC930) (Fig. 2A) fusions were involved (Fig. 3A). Two products were obtained: particles with HIV-1 Tat sequence 48-60 (Vivčs *et al*., 1997) and with West Nile EDIII sequence (Martina *et al*., 2008) (Fig. 4A). Western-blot analysis gave convincing evidence of mosaic particles, as besides monomers and dimers of GA CP, also bands of fused prolonged coat protein (Fig. 2B) were evident. Construct expression in pESC-URA vector allowed to obtain the HIV-1 Tat 48-60 sequence for study as a cell membrane-transducing address. Similar particles obtained by expression in *E. coli* were not formed (data not shown). However, use of another similar construct, in which GA CP was N-terminally fused with the vMIPII fragment (not shown) resulted in capsids in *E. coli*, but not in yeast. Therefore, the use of both bacterial and yeast expression systems allow us to broaden the set of mosaic virus like particles.

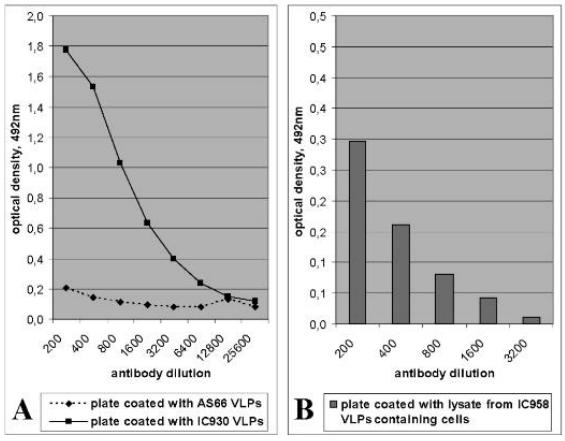

Fig. 3. ELISA immunodetection: A – AS66 and IC930 VLPs with murine polyclonal 562 antibodies against WNV EDIII; B – lysates from cells with expressed construction pIC958 VLPs with anti-interleukin-2 antibodies; displayed values are after subtraction of control (e.g., lysate from untransformed YPH499 cells).

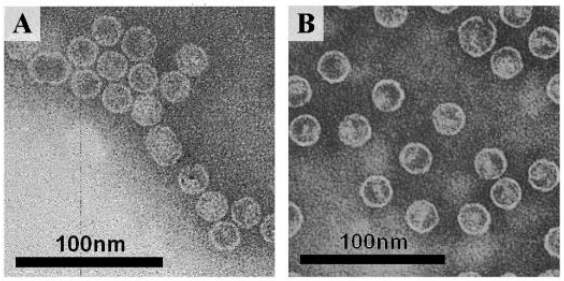

Fig. 4. Electronmicroscopy of mosaic VLPs – construction IC930 (A) and of VLPs with packaged IL-2 mRNA - construction IC972 (B).

While considering that in the future we need packaged GFP mRNA as a reporter for delivery experiments, two sorts of mRNAs were packaged under control of both promoters that resulted in four constructions: two for packaging of green fluorescent protein (GFP) mRNA (constructions IC984 and IC921) and two for packaging of IL2 mRNA (constructions IC958 un IC972). After accurate purification of produced VLPs, including sucrose density gradient ultracentrifugation to avoid even traces of "stuck" nucleic acids, capsids were treated with phenol and internal nucleic acid was collected. Random hexamer primers indicate the total RNA pool (Fig. 5, lines 1). Primer oligo(dT) allows to visualise all mRNAs, as they have poly(A) tracts (Fig. 5, lines 2). The utilised experimental conditions allowed us to compare amounts of mRNA by comparing material in specific PCR product bands. Lines 3 (Fig. 5) showed negligible amounts of GA coat protein mRNA, but cogent bands corresponding to GFP and IL2 coding sequences (Fig. 5, lines 4a–4d) demonstrated packaging of desired mRNAs *in vivo* into particles.

DISCUSSION

Yeast provides a source of eukaryotic 5'-capped and 3'-poly(A)-tailed mRNAs, which is attractive considering our goal to use GA VLPs as RNA packaging and delivery tools in mammalian cells. Also, the absence of bacterial endotoxins in yeast preparations is a good reason to choose this system for *in vivo* packaging studies. In previous studies, genes of interest for packaging were inserted under control of the Gal10 promoter (Legendre and Fastrez, 2005; Rūmnieks *et al*., 2008). We also used this method, but with

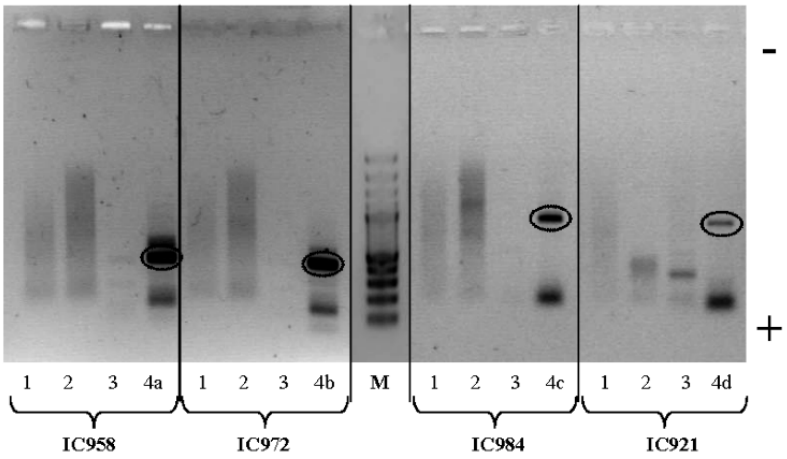

Fig. 5. Analysis of VLPs inner RNA contents by agarose gel electrophoresis. RT-PCR products for constructions IC958, IC972, IC984 and IC921 were compared with a set of different primers: 1 – random hexamer primers; 2 – oligo(dT)$_{18}$ primers; 3 – GA CP primers (p1.561 + p1.562); 4a – construction IC958 with IL2 specific primers pINC324 and pINC325; 4b – construction IC972 with IL2 specific primers pINC413 and pINC414; 4c – construction IC984 with eGFP specific primers pJAR18 and pJAR19; 4d – construction IC921 with eGFP specific primers pINC434 and pINC435. DNA Ladder 100bp (Fermentas) was used as a marker (M). Ellipses frame bands with densities corresponding to amounts of IL2 mRNA (4a and 4b) and eGFP mRNA (4c and 4d).

substituted constructions (Table 1, constructions pIC972 and pIC984). It was previously shown that packaging of heterologous mRNAs into GA CP particles occurred independently of the presence or absence of the specific stem-loop operator sequence (Rūmnieks *et al*., 2008). This is consistent with the rather low specificity of GA coat protein to structure of the operator (Gott *et al*., 1991) and explains the encapsidation of different RNAs. Even in the case of MS2 coat protein, which is well known as to form stable replicative complex I (coat protein + operator sequence of RNA), encapsidation efficiency and specificity to a greater extent affects the concentration of mRNA rather than its source (Picket and Peabody, 1993). Therefore, we were interested in examining the yield of GA CP particles and their RNA packaging capacity and specificity by changing promoters for expression of structural coat protein and corresponding mRNA.

Interleukin-2 is a secreted cytokine that is important for T- and B- lymphocyte proliferation. IL2 is produced by T-cells in response to antigenic and mitogenic stimulation and is required for T-cell proliferation and other activities crucial to regulation of the immune response. IL2 can stimulate B-cells, monocytes, lymphokine-activated killer cells and natural killer cells. Despite of unclear, even negative or contradictory results, IL2 still remains a promising therapeutic tool for melanoma and glioma treatment (Fenstermaker and Ciesielski, 2004; Albertini *et al*., 2008). In VLPs packaged IL2, mRNA is foreseen for local treatment, when VLPs will be able to deliver it into cells. Beside the liposomal intracellular delivery system (Pakunlu *et al.*, 2006), RNA phage MS2 coat protein formed particles were demonstrated as candidates for delivery of mRNAs into eukaryotic cells (Legendre and Fastrez, 2005; Sun *et al*., 2011). These studies suggest that we are on the path to creating a drug delivery vehicle based on GA coat protein capsids.

ACKNOWLEDGEMENTS

We wish to thank Prof. Pauls Pumpēns for the idea to use optimised codons for coat protein expression in yeast cells. We thank also Dr. Velta Ose-Klinklāva for electron microscopy imaging, and Dr. Dace Skrastiņa for performing mouse immunisation procedures.

We are very grateful to Prof. Kęstutis Sasnauskas and Dr. Aistė Bulavaitė from the Institute of Biotechnology, Vilnius University, for the possibility to obtain experience in work with yeasts.

This work was supported by Latvian National Research Programme No. 4 "BIOMEDICINE" project 2010-7/7.2.

REFERENCES

Albertini, M. R., Hank, J. A., Schalch, H., Kostlevy, J., Cassaday, R., Gan, J., Kim, K., Clements, B., Gillies, S. D., Sondel, P. M. (2008). Phase II trial of hu14.18-IL2 (EMD 273063) for patients with metastatic melanoma. *J. Clin. Oncol.,* **26**, May 20 Supplement, abstr. 9039.

Chen, H., Lü, J. H., Liang, W. Q., Huang, Y. H., Zhang, W. J.. Zhang, D. B. (2004). Purification of the recombinant hepatitis B virus core antigen (rHBcAg) produced in the yeast *Saccharomyces cerevisiae* and comparative observation of its particles by transmission electron microscopy (TEM) and atomic force microscopy (AFM). *Micron*, **35** (5), 311–318.

Cobitz, A. R., Yim, E. H., Brown, W. R., Perou, C. M., Tamanoi, F. (1989). Phosphorylation of RAS1 and RAS2 proteins in *Saccharomyces cerevisiae*. *Proc. Nat. Acad. Sci. USA*, **86** (3), 858–862.

Fenstermaker, R. A., Ciesielski, M. J. (2004). Immunotherapeutic strategies for malignant glioma. *Cancer Control*, **11** (3), 181–191.

Freivalds, J., Dislers, A., Ose, V., Skrastina, D., Cielens, I., Pumpens, P., Sasnauskas, K., Kazaks, A. (2006). Assembly of bacteriophage Qbeta virus-like particles in yeast *Saccharomyces cerevisiae* and *Pichia pastoris*. *J. Biotechnol.*, **123** (3), 297–303.

Freivalds, J., Rūmnieks, J., Ose, V., Renhofa, R., Kazāks, A. (2008). High-level expression and purification of bacteriophage GA virus-like particles from yeast *Saccharomyces cerevisiae* and *Pichia pastoris*. *Acta Univ. Latv.*, **745**, Biology, 75–85.

Freivalds, J., Dislers, A., Ose, V., Pumpens, P., Tars, K., Kazaks, A. (2011). High efficient production of phosphorylated hepatitis B core particles in yeast *Pichia pastoris*. *Protein Expr. Purif.*, **75**, 218–224.

Gietz, D., Jean, A. S., Woods, R. A., Schiestl, R. H. (1992). Improved method for high efficiency transformation of intact yeast cells. *Nucl. Acids Res.*, **20** (6), 1425.

Gott, J. M., Wilhelm, L. J., Uhlenbeck, O. C. (1991). RNA binding properties of the coat protein from bacteriophage GA. *Nucl. Acids Res.*, **19** (23), 6499–6503.

Juozapaitis, M., Slibinskas, R., Staniulis, J., Sakaguchi, T., Sasnauskas, K. (2005). Generation of Sendai virus nucleocapsid-like particles in yeast. *Virus Res.*, **108** (1–2), 221–224.

Klump, H. H., Maeder, D. L. (1991). The thermodynamic basis of the genetic code. *Pure Appl. Chem.*, **63** (10), 1357–1366.

Legendre, D., Fastrez, J. (2005). Production in *Saccharomyces cerevisiae* of MS2 virus-like particles packaging functional heterologous mRNAs. *J. Biotechnol.*, **117** (2), 183–194.

Mach, H., Volkin, D. B., Troutman, R. D., Wang, B., Luo, Z., Jansen, K. U., Shi, L. (2006). Disassembly and reassembly of yeast-derived recombinant human papilloma virus-like particles (HPV VLPs). *J. Pharmaceut. Sci.*, **95** (10), 2195–2206.

Martina, B. E., Koraka, P., van den Doel, P., van Amerongen, G., Rimmelzwaan, G. F., Osterhaus, A. D. (2008). Immunization with West Nile virus envelope domain III protects mice against lethal infection with homologous and heterologous virus. *Vaccine*, **26** (2), 153–157.

Pakunlu, R. I., Wang, Y., Saad, M., Khandare, J. J., Starovoytov, V., Minko, T. (2006). *In vitro* and *in vivo* intracellular liposomal delivery of antisense oligonucleotides and anticancer drug. *J. Contr. Release*, **114** (2), 153–162.

Picket, G. G., Peabody, D. S. (1993). Encapsidation of heterologous RNAs by bacteriophage MS2 coat protein. *Nucleic Acids Res.*, **21** (19), 4621–4626.

Ptacek, J., Devgan, G., Michaud, G., Zhu, H., Zhu, X., Fasolo, J., Guo, H., Jona, G., Breitkreutz, A., Sopko, R., McCartney, R. R., Schmidt, M. C., Rachidi, N., Lee S. J., Mah, A. S., Meng, L., Stark, M. J. R., Stern, D. F., De Virgilio, C., Tyers, M., Andrews, B., Gerstein, M., Schweitzer, B., Predki, P.F., Snyder, M. (2005). Global analysis of protein phosphorylation in yeast. *Nature Letters*, **438**, 679–684.

Rūmnieks, J., Freivalds, J., Cielēns, I., Renhofa, R. (2008). Specificity of packaging mRNAs in bacteriophage GA virus-like particles in yeast *Saccharomyces cerevisiae*. *Acta Univ. Latv.*, **745**, Biology, 145–154.

Received 3 April 2012

Strausberg, R. L., Strausberg, S. L. (2001). Overview of protein expression in *Saccharomyces cerevisiae*. *Curr. Protocols Protein Sci.* 5.6.1–5.6.7.

Sasnauskas, K., Bulavaite, A., Hale, A., Jin, L., Knowles, W. A., Gedvilaite, A., Dargeviciūte, A., Bartkeviciūte, D., Zvirbliene, A., Staniulis, J., Brown, D. W., Ulrich, R. (2002). Generation of recombinant virus-like particles of human and non-human polyomaviruses in yeast *Saccharomyces cerevisiae*. *Intervirology*, **45** (4–6), 308–317.

Strods, A., Petrovska, R., Jackeviča, L., Renhofa R. (2010). Cloning and expression of chemokine receptor CXCR4 in eukaryotic cells CHO, HEK293 and BHK21. *Proc. Latv. Acad. Sci. Section B,* **64** (3/4), 98–105.

Sun, S., Li, W., Sun, Y., Pan, Y., Li, J. (2011). A new RNA vaccine platform based on MS2 virus-like particles produced in *Saccharomyces cerevisiae*. *Biochem. Biophys. Res. Comm.*, **407** (1), 124–128.

Tars, T., Bundule, M., Fridborg, K., Liljas, L. (1997). The crystal structure of bacteriophage GA and a comparison of bacteriophages belonging to the major groups of *Escherichia coli* leviviruses. *J. Mol. Biol.*, **271**, 759–773.

Tissot, A. C., Renhofa, R., Schmitz, N., Cielens, I., Meijerink, E., Ose, V., Jennings, G. T., Saudan, P., Pumpens, P., Bachmann, M. F. (2010). Versatile virus-like particle carrier for epitope based vaccines. *PLoS One*, **5** (3), e9809.

Tsunetsugu-Yokota, Y., Morikawa, Y., Isogai, M., Kawana-Tachikawa, A., Odawara, T., Nakamura, T., Grassi, F., Autran, B., Iwamoto, A. (2003). Yeast-derived human immunodeficiency virus type 1 p55(gag) virus-like particles activate dendritic cells (DCs) and induce perforin expression in Gag-specific CD8(+) T cells by cross-presentation of DCs. *J. Virol.*, **77** (19), 10250–10259.

Vivčs, E., Brodin, P., Lebleu, B. (1997). A truncated HIV-1 Tat protein basic domain rapidly translocates through the plasma membrane and accumulates in the cell nucleus. *J. Biol. Chem.*, **272** (25), 16010–16017.

Авотс А., Бундулис Я., Осе В., Романчикова Н., Скривелис В., Янкевиц Е., Циманис А., Грен Е. (1990). [The expression of the human interleukin-2 gene in *Escherichia coli* bacteria]. *Докл. Акад. Наук СССР*, **315** (4), 994–996 (in Russian).

GA APVALKA PROTEĪNA ATVASINĀTO MOZAIKĀLO VĪRUSIEM LĪDZĪGO DAĻIŅU EKSPRESIJA *Saccharomyces cerevisiae* UN mRNS *in vivo* IEPAKOŠANA DAĻIŅĀS

Mūsu iepriekšējie pētījumi parādījuši, ka lielākais RNS bakteriofāga GA apvalka proteīna veidoto vīrusiem līdzīgo daļiņu (VLD) ieguvums ir ekspresējot tās raugos *Pichia pastoris*; savukārt, izmantojot *Saccharomyces cerevisiae* ekspresijas sistēmu, kapsīdu ieguvums ir daudz mazāks. Divi galvenie mērķi turpmākajām studijām raugos *Saccharomyces cerevisiae* bija paaugstināt GA apvalka proteīna veidoto VLD ieguvumu, izmantojot konstrukcijas ar optimizētu nukleotīdu tripletu sekvencēm, un izpētīt iespējas, ko varētu sniegt divu promoteru Gal1/Gal10 saturošs ekspresijas vektors pESC-URA vēlamo mozaīkveida VLD iegūšanai un mRNS iepakošanai VLD *in vivo*.

Conclusion

Bacteriophage GA coat protein based VLP production in yeast two-promoter expression system was optimized by changing nucleotide sequence according *S.cerevisiae* preferable codons without changing amino acid sequence. Mosaic particles containing GA coat protein and coat protein N-terminally supplemented with HIV-Tat (48-60) or C-terminally supplemented with WNV-DIII (296-406) sequence were produced. WNV-DIII sequence placement on the surface of VLPs was proofed by anti-WNV-DIII antibodies. To obtain particles packaged with desired nucleic acids, *in vivo* packaging method was tested by simultaneously expressing GA coat protein and IL-2 or GFP mRNA. Although the mRNAs of interest were packed, we tried to improve packaging specificity through adding MS2 operator sequence to mRNA and using modified GA VLPs, mimicking MS2 operator binding site. Nevertheless the packaging specificity was increased, still coat protein mRNA and possibly other RNA sequences were present in VLPs.

Thesis

- Yeast-produced bacteriophage GA coat protein derived VLPs are capable to form mosaic particles, including HIV-Tat (48-60) sequence and immunologically competent region of WNV domain III.
- Two-promoter system based on plasmid pESC-URA was used for *in vivo* packaging of IL-2 and GFP mRNA into GA coat protein particles; the packaging specifity was remarkably improved by supplementing MS2 operator sequence to GFP mRNA and using GA VLP mutants that mimicks MS2 operator binding site, however particles still contained its own coat protein mRNA.

3.2. Bacteriophage AP205 VLPs

Inspired by possibility to obtain specific antibodies using chemically coupled WNV epitope (Storni et al., 2004), we tried to make covalent attachment of WNV epitope by genetically fusing WNV protein to the C-terminus of bacteriophage AP205 coat protein (Cielens et al., 2014). Theoretically this method is better due to the uncompromised location of foreign sequence (EDIII), especially because EDIII sequence contains two cysteine at positions 305 and 336 (Figure 5) and therefore binding site to coat protein may alter.

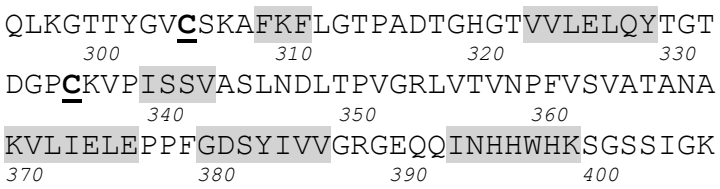

Figure 5 Amino acid sequence of the WNV envelope protein domain III (adaptation from (Nybakken et al., 2006)). Grey shaded sequence corresponds to the β-sheets A, B, C, E, F and G, respectively; in bold are denoted cysteine residues in positions 305 and 336.

Whole sequence from protein E domain III (specifically, amino acid residues 296-406) from West-Nile virus New York strain 385-99 were cloned at the C-terminal end of AP205 coat protein, separated by short linker and amber or opal suppressor. Mosaic VLPs synthesis was used as an alternative instead of full-epitope exposition on VLPs surface because self-assembly of C-terminal AP205-DIII fusion was failed both *in vivo* and *in vitro* (after refolding attempts) (Cielens et al., 2014).

After expression in *E.coli* cells carrying appropriate suppressor tRNA genes, AP205 coat protein based mosaic VLPs were produced, purified and mice were immunised in combination without or with different adjuvants – Alum or SiO_2 (Cielens et al., 2014). Immunisation data were generally similar for both AP205-op-DIII and AP205-am-DIII suppression variants. Along with VLPs, refolded WNV EDIII recombinant protein was also used for mice immunization. Direct ELISA tests showed that after immunisation without adjuvant addition, AP205-DIII VLPs induced evident anti-DIII response if compared with weak immunogenicity after immunization with DIII polyopeptide. Addition of adjuvants enhanced immune responses very strongly, reaching almost equal antibody titre levels after two boosts on 42nd day for both AP205-DIII VLPs and DIII peptide. As main positive aspect is switching of antibody subtype from IgM in case of DIII protein toward IgG in case of mosaic AP205/DIII VLPs in both adjuvant-free and adjuvant-added immunization variants (Cielens et al., 2014).

Mol Biotechnol
DOI 10.1007/s12033-014-9743-3

RESEARCH

Mosaic RNA Phage VLPs Carrying Domain III of the West Nile Virus E Protein

Indulis Cielens · Ludmila Jackevica · Arnis Strods · Andris Kazaks · Velta Ose · Janis Bogans · Paul Pumpens · Regina Renhofa

Abstract The virus-neutralising domain III (DIII) of the West Nile virus glycoprotein E was exposed on the surface of RNA phage AP205 virus-like particles (VLPs) in mosaic form. For this purpose, a 111 amino acid sequence of DIII was added via amber or opal termination codons to the C-terminus of the AP205 coat protein, and mosaic AP205-DIII VLPs were generated by cultivation in amber- or opal-suppressing *Escherichia coli* strains. After extensive purification to 95 % homogeneity, mosaic AP205-DIII VLPs retained up to 11–16 % monomers carrying DIII domains. The DIII domains appeared on the VLP surface because they were fully accessible to anti-DIII antibodies. Immunisation of BALB/c mice with AP205-DIII VLPs resulted in the induction of specific anti-DIII antibodies, of which the level was comparable to that of the anti-AP205 antibodies generated against the VLP carrier. The AP205-DIII-induced anti-DIII response was represented by a significant fraction of IgG2 isotype antibodies, in contrast to parallel immunisation with the DIII oligopeptide, which failed to induce IgG2 isotype antibodies. Formulation of AP-205-DIII VLPs in alum adjuvant stimulated the level of the anti-DIII response, but did not alter the fraction of IgG2 isotype antibodies. Mosaic AP205-DIII VLPs could be regarded as a promising prototype of a putative West Nile vaccine.

Keywords West Nile virus E glycoprotein · Domain DIII · RNA phage AP205 · Mosaic · Virus-like particles

I. Cielens · L. Jackevica · A. Strods · A. Kazaks · V. Ose · J. Bogans · P. Pumpens (✉) · R. Renhofa (✉)
Latvian Biomedical Research and Study Centre, Ratsupites Street 1, Riga 1067, Latvia
e-mail: paul@biomed.lu.lv

R. Renhofa
e-mail: regina@biomed.lu.lv

Published online: 26 February 2014

Introduction

West Nile virus (WNV) is a neurotropic, single-stranded and positive-sense RNA flavivirus that is transmitted to humans through the bite of an infected mosquito and has emerged globally as a significant cause of viral encephalitis (for recent reviews see [1, 2]). In the absence of a specific anti-viral treatment, the development of a safe and an efficient prophylactic vaccine against WNV is necessary.

Currently, most WNV vaccine candidates are live, attenuated viral vaccines based on chimeric viruses that incorporate the pre-membrane (prM) and E glycoproteins of the WNV envelope into the following viral vectors: yellow fever [3–6], fowlpox and canarypox [7], measles [8] and the modified vaccinia virus Ankara (MVA) strain of vaccinia virus [9]. The generation and preclinical efficacy of a hydrogen peroxide-inactivated WNV vaccine has been described [10]. A DNA vaccine encoding the prM and E proteins have been evaluated in healthy adults [11].

Recombinant subunit vaccine candidates are based on the structural WNV glycoprotein E because the protein may elicit a major neutralising antibody response [12, 13]. The recombinant E protein was purified from *Escherichia coli* and functioned as an efficient WNV vaccine in mice [14]. The WN-80E subunit vaccine, which is produced in a *Drosophila melanogaster* expression system, consists of the recombinant E protein truncated at the C-terminal end but contains 80 % of its N-terminal amino acids (aa) [15–17]. Recently, recombinant baculoviruses expressing WNV E protein, as well as prM protein, were constructed and tested successfully in mice [18, 19].

Within the E glycoprotein, domain III (DIII) is the region that is exposed on the viral surface [20] and is implicated in receptor binding [21]. DIII is a target of the most WNV neutralising antibodies [22–26], and passive transfer of DIII-

specific antibodies may protect mice from WNV challenge [27]. Subunit vaccines based on recombinantly expressed DIII have been tested in animal models and have proven effective in protecting against WNV infection [28–32].

The immunogenicity of DIII was strongly enhanced by chemical conjugation to virus-like particles (VLPs) of the bacteriophage AP205 [33], in accordance with the general acceptance of VLPs as highly ordered carriers for foreign epitopes (for recent reviews see [34, 35]).

In the present study, construction of a novel type of putative VLP-based DIII vaccine is described. RNA bacteriophage AP205 VLPs [36] are used to expose the DIII sequence on the mosaic VLPs. In contrast to the previous chemically conjugated vaccine [33], mosaic AP205 VLPs are generated by genetic fusion of the DIII sequence to the C-terminus of the AP205 coat protein (CP) via the termination codons UAG and UGA under codon-suppression conditions. Uniform fusions of the DIII sequence, without any read-through termination codons, to AP205 CP as well as to the CP of a similar RNA bacteriophage, GA, do not lead to self-assembly and formation of VLPs. Direct expression of the DIII sequence is used as a source of the highly purified recombinant DIII protein. Overall, we present efficient production and purification of mosaic AP205-DIII VLPs in *E. coli* cells and show the ability of mosaic VLPs to induce specific anti-DIII antibodies in mice.

Materials and Methods

Bacterial Strains

Escherichia coli strain RR1 [F- rB- mB- *leuB6 proA2 thi-1 araC14 lacY1 galK2 xyl-5 mtl-1 rpsL20* (Strr) *glnV44* Δ (*mcrC-mrr*)] was used for the cloning and selection of recombinant plasmids. *E. coli* C2566 was used for the direct expression of the DIII gene. *E. coli* JM109 was used to express the fused AP205-DIII and GA-DIII genes. For the expression of mosaic AP205-am-DIII and AP205-op-DIII VLPs, the amber suppressor *E. coli* JM109 (pISM579) and the opal suppressor *E. coli* JM109 (pISM3001) carrying resident suppressor tRNA genes were used. The plasmid pISM3001 [37] was a kind gift from Dr. F.C. Minion (USA), while strain MY579 harbouring amber suppressor tRNA was obtained from Dr. M. Yarus (USA). The plasmid pISM579 encoding tRNA for amber (UAG) codon suppression was constructed on the basis of the plasmid pISM3001, where the opal (UGA) suppressor tRNA encoding gene trpT176 was replaced with analogous DNA sequence encoding the Hirsh amber suppressor tRNA. The latter was isolated from plasmid pBE621 [38] that encodes the trpT178 derivative, which, in addition to Hirsh mutation G24 → A, also contains mutations U33 → G and C35 → U. Because the respective tRNA genes are flanked by *Eco*RI sites, the substitution was carried out by partial *Eco*RI cleavage and religation and then confirmed by sequencing.

Construction of the WNV Protein E Domain DIII-Expressing Plasmids

The construction map of the WNV protein E domain DIII-expressing plasmids is shown in Fig. 1. To construct the AP205-DIII expression units, a set of cloning vectors (Fig. 1, on the left) was generated on the basis of a pAP283-58 plasmid that expresses the CP gene of the RNA bacteriophage AP205 under the control of the *E. coli* tryptophan operon promoter Ptrp [36]. The following oligonucleotides were used as PCR primers to insert the sequences encoding the linker aa residues together with the appropriate cloning sites and the suppression codons (underlined) at the C-terminus of the AP205 CP gene:

5′-TGTCTAGAATTTTCTGCGCACCCATCCCGG-3′;
5′-TGATGCATCCTCCGGATCCAGCAGTAGTATC AGACGATAC-3′;
5′-TACCATGGCAAATAAGCCAATGCAACCG-3′;
5′-GTAAGCTTAGATGCATTATCCGGATCCCTA AGCAGTAGTATCAGACGATACG-3′;
5′-GTAAGCTTAGATGCATTATCCGGATCCTCA AGCAGTAGTATCAGACGATACG-3′.

The WNV protein E DIII fragment encompassing aa residues 296–406 was PCR-amplified from the plasmid pTrcHis2-WNVclone F101 New York strain 385–399 (kindly supplied by B. E. E. Martina, Erasmus MC, Rotterdam) and cloned into the previously constructed vectors at the appropriate restriction sites (Fig. 1, on the right).

The following oligonucleotides were used as cloning primers for the PCR:

5′-CATCCGGACAGTTGAAGGGAACAAC-3′;
5′-GTATGCATTTGCCAATGCTGCTTCC-3′;
5′-CATCCGGACAGTTGAAGGGAACAAC-3′;
5′-GTAAGCTTATTTGCCAATGCTGCTTCC-3′

To construct the GA-DIII expression units, a pGA 355-24 plasmid expressing the CP gene of the RNA bacteriophage GA under control of the Ptrp [39, 40] was supplied with the appropriate linker at the C-terminus and used as a vector for cloning of the DIII sequence amplified with the following primers:

5′-CATCCGGACAGTTGAAGGGAACAAC-3′ and
5′-GTAAGCTTATTTGCCAATGCTGCTTCC-3′

For direct expression, the DIII sequence was amplified by the primers

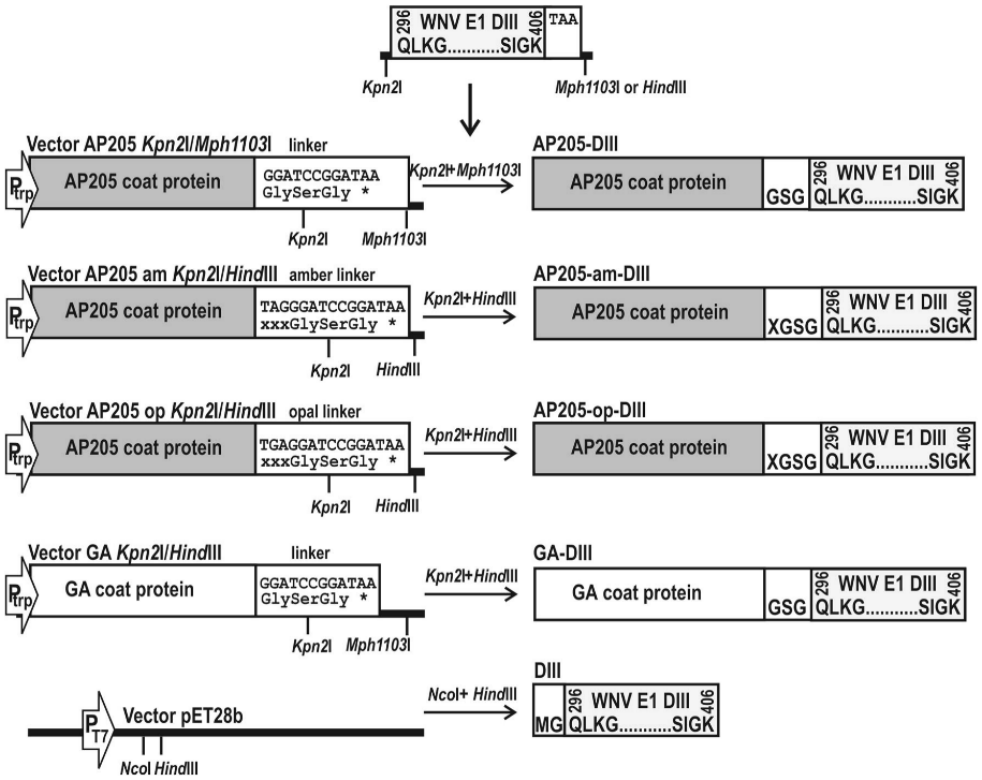

Fig. 1 Schematic representation of the recombinant DIII constructions. The nucleotide and aa sequences and the locations of restriction sites at the joining points are shown. Undefined aa residues are depicted by X

5′-TACCATGGGCCAGTTGAAGGGAACAACCTATGG-3′ and
5′-ATGAAGCTTATTTGCCAATGCTGCTTCC-3′

and inserted at the restriction sites *Nco*I and *Hin*dIII in the multicloning region of the plasmid pET-28+ under control of the IPTG-inducible T7 promoter. The plasmid structures were confirmed by sequencing.

Expression and Purification of AP205- and GA-DIII Derivatives

Escherichia coli JM109 cells were transformed with the pAP205-DIII and pGA-DIII plasmids. *E. coli* JM109 strains carrying resident suppressor tRNA plasmids were used for the expression of AP205-DIII mosaics. *E. coli* JM109 with a resident amber suppression tRNA gene (pISM579) was transformed with the pAP205-am-DIII plasmid. *E. coli* JM109 with a resident opal suppression tRNA gene (pISM3001) was transformed with the pAP205-op-DIII plasmid. Single colonies were suspended in tubes containing 5 mL of LB medium with 50 μg/mL of ampicillin and 10 μg/mL of chloramphenicol and grown without shaking at 37 °C for 16 h. The prepared inoculum was diluted tenfold in M9 medium supplemented with 10 g/L of casamino acids, 2 g/L of glucose (BD, USA), 25 μg/mL of vitamin B1, 20 mM magnesium sulphate, ampicillin (50 μg/mL) and chloramphenicol (10 μg/mL) grown in 3 L Erlenmeyer flasks on an Infors shaker (200 rpm) at 37 °C to an OD_{540} of 0.8–1.0, induced with 100 μg/mL of IPTG and cultivated for 4 h. Cells were harvested by centrifugation.

To purify the mosaic AP205-am-DIII and AP205-op-DIII VLPs, 3 g of wet, fresh cells were homogenised in 9 mL of lysis buffer containing 50 mM Tris–HCl (pH 8.0), 5 mM EDTA, 50 μg/mL PMSF and 0.1 % Triton X-100 and then ultrasonicated five times for 15 s each time at 22 kHz at 45 s intervals, while keeping the cells on ice. After centrifugation at 10,000 rpm for 30 min, the supernatant was loaded onto a Sepharose CL-2B column (70 × 2 cm). NET buffer [0.15 M NaCl, 20 mM Tris–HCl (pH 7.8), 5 mM EDTA] with 0.02 % Brij58 was used for elution at a velocity of 2 mL/h, 90 min/3-mL fraction. VLP-containing fractions were detected by native 0.8 %

agarose (TopVision LE GQ, Fermentas, Lithuania) gel electrophoresis in 1xTAE buffer [40 mM Tris (pH 8.4), 20 mM acetic acid, 1 mM EDTA] (Fermentas). The VLP-containing fractions (typically fractions 15–28) were pooled and the material was loaded onto a Sephadex A50 (5–7 × 1 cm) column, which does not retard VLPs, to remove nucleic acids. Unbound material containing VLPs was washed out with NET buffer (without Brij58) under spectrophotometric control. After concentration on an Amicon Ultra-15 centrifugal filter device (MWCO 30,000; Merck Millipore, USA), the samples were loaded onto a Sepharose CL-4B column (48 × 1.5 cm) and eluted with NET buffer at a velocity of 2 mL/h/fraction. The fractions detected by native agarose gel electrophoresis (NAGE) (typically fractions 17–25) were pooled, concentrated on the Amicon device as described above, and subjected again to gel filtration on the Sepharose CL-2B column (60 × 1.5 cm) in NET buffer by collection of 2-mL fractions. The VLP-containing fractions (typically fractions 24–33) were pooled, concentrated on the Amicon device to 3 mL, and loaded onto a pre-formed 5–36 % sucrose gradient (sucrose concentration (w/w) layers: 36 % to 3 mL; 30 % to 3 mL; 25 % to 6 mL; 20 % to 8 mL; 15 % to 6 mL; 10 % to 6 mL; 5 % to 3 mL; in Polyallomer 25 × 89 mm tubes) for centrifugation in a Beckman Coulter Optima L-100XP ultracentrifuge (rotor SW32 Ti) at 20,500 rpm for 13 h at +4 °C. Fractions of 1 mL were collected from the pierced bottom of the tube. The VLPs usually appeared around fraction 12, which was in the first third from the bottom. Sucrose was removed by Amicon concentrator to a volume of 1.5 mL in NET buffer and 1.5 mL of glycerol was added. VLP preparations with a typical protein concentration of 8 mg/mL (31 OD_{260} units/mL) were stored at −18 °C. The yield of VLPs reached 8 mg/g of wet cells.

To purify the GA-DIII derivative, the debris of the cell lysate prepared as described above and centrifuged at 10,000 rpm for 30 min was eluted by 7 M urea in water and loaded onto a DEAE cellulose column (1 × 5 cm) in 20 mM Tris–HCl (pH 8.6). The unbound material was collected in fractions of 3 mL. The most pure fractions were pooled, subjected to ammonium sulphate precipitation at 50 % saturation, dissolved in 7 M urea and diluted to 10 μg/mL in a 50 mM sodium carbonate buffer, pH 9.6, for coating on ELISA plates.

Expression and Purification of the DIII Protein

Escherichia coli C2566 cells were transformed with the pET28b-DIII plasmid (Fig. 1). Single colonies were suspended in tubes containing 5 mL of LB medium with 50 μg/mL of ampicillin and grown without shaking at 37 °C for 16 h. The prepared inoculum was diluted tenfold in 2TY medium containing 20 μg/mL of ampicillin in 2 L flasks, incubated on an Infors shaker (200 rpm) at 37 °C to an OD_{540} of 0.8–1.0, induced by adding IPTG to 100 μg/mL and cultivated for 3.5–4.5 h. Cells were harvested by centrifugation.

To purify the DIII protein, 1 g of cells was homogenised and ultrasonicated in 4 mL of lysis buffer, and the supernatant was discarded. The pellet was extracted with 4 mL of 7 M urea in water. To remove the nucleic acids, two alternative techniques were used: (i) proteins in the supernatant were precipitated by adding ammonium sulphate to 50 % saturation for 20 h at 4 °C, the debris was dissolved in 7 M urea and the ammonium sulphate precipitation was repeated and (ii) the supernatant was loaded onto a DEAE cellulose column equilibrated with 20 mM Tris–HCl (pH 8.6), and the unbound material was collected and precipitated with ammonium sulphate at 50 % saturation. The pellets obtained from both versions were washed by water portions of 200 μL to remove any remaining nucleic acids. After centrifugation at 10,000 rpm for 30 min, the samples were resuspended in a minimal volume of 7 M urea containing 5 mM dithiotreitol (Sigma-Aldrich, USA), clarified by centrifugation at 6,000 rpm, and refolded by dialysing the 3 mL sample for 3–4 days against 4–5 changes of 50 mL of buffer containing 2 M urea and 0.5 M arginine-HCl (pH 8.0) [41]. After clarifying at 6,000 rpm for 15–20 min, the sample was subjected to gel filtration on a Sepharose CL-4B column (30 × 1 cm) and eluted in PBS buffer (0.01 M phosphate, pH 7.4, 0.138 M NaCl, 0.0027 M KCl) at a velocity of 1 mL/h, 90 min/1.5-mL fraction. The final samples were stored frozen at −18 °C.

Detection of Protein and Nucleic Acids

All measurements were performed on Biochrom (Biochrom Ltd., UK) and Nanodrop (Thermo Scientifics, USA) spectrophotometers. The amount of protein (in the presence of nucleic acids) was estimated according to [42]. The VLP preparations were compared with respect to the presence of protein and nucleic acids using NAGE and double radial immunodiffusion (DRI) according to the method of Ouchterlony using rabbit polyclonal anti-AP205 antibodies. For NAGE and DRI, 1 and 0.8 % TopVision LE GQ Agarose (Fermentas) in TBE buffer and in PBS buffer were used, respectively, with subsequent Coomassie Blue R-250 (60 μg/mL of Coomassie Blue R-250 in 10 % acetic acid) staining of the gels.

Protein samples were analysed on 15 % SDS-PAGE gels with subsequent Coomassie staining. For Western blots, the polyclonal rabbit anti-AP205 was used at a 1:1000 dilution. All chemicals were from Sigma-Aldrich.

The ratio of DIII-containing versus initial AP205 proteins was determined by analysis of Coomassie-stained gels with the free ImageJ program (http://rsbweb.nih.gov/ij/).

Electron Microscopy and Dynamic Light Scattering Analysis

For electron microscopy, VLPs in suspension were adsorbed to carbon-Formvar coated copper grids and negatively stained with a 1 % uranyl acetate aqueous solution. The grids were examined with a JEM-1230 electron microscope (Jeol Ltd., Tokyo, Japan) at 100 kV.

The size of the particles was detected by dynamic light scattering (DLS) in a Zetasizer Nano ZS (Malvern Instruments Ltd, UK) instrument.

Immunogenicity of the DIII-Containing Proteins

Female BALB/c mice, 6–8 weeks of age and obtained from the Latvian Experimental Animal Laboratory (Riga Stradins University), were maintained at the Biomedical Research and Study Centre under pathogen-free conditions. The experiments were approved by the Latvian Animal Protection Ethics Committee and the Latvian Food and Veterinary service, permission No. 31/23.10.2010. Groups of five mice were immunised sub-dermally on the back of the animals with 25 μg of protein (diluted in 0.2 mL of PBS) per mouse on days 0, 14 and 28. For immunisation with adjuvants, 250 μg of Alum for all three immunisations and 100, 250 and 500 μg of SiO_2 for the first, second and third immunisation, respectively, were used. To assess the humoral response, the animals were bled on days 7, 14 and 28, reimmunised on days 15 and 29, and sacrificed on day 42. The anti-DIII titres in the sera were determined with a direct ELISA using plates coated with DIII protein or GA-DIII fusion protein. The anti-AP205 titres were determined with a direct ELISA using plates coated with the AP205 VLPs.

For the direct ELISA, 96-well microplates (Nunc, USA) were coated with the appropriate proteins using 100 μL of protein solution (10 μg/mL in 50 mM sodium carbonate buffer, pH 9.6) per well. The plates were incubated with the protein solution overnight at 4 °C. After the plates were blocked with 1 % BSA in PBS for 1 h at 37 °C, serial dilutions of the sera were added to the wells, and the plates were incubated at 37 °C for an additional 1 h. After washing three times with PBS containing 0.05 % Tween-20, 100 μL of horseradish peroxidase conjugated anti-mouse antibody (Sigma-Aldrich) was added at a 1:10,000 dilution. After incubation at 37 °C for 1 h, the plates were washed, and OPD substrate (Sigma-Aldrich) was added for colour development. A Multiskan (Sweden) was used to measure the absorbance at 492 nm. The end-point titres were defined as the highest serum dilution that resulted in an absorbance value three times greater than that of the control sera obtained from unimmunised mice.

The IgM and IgG subsets in the sera of the immunised mice were detected with isotype specific ELISAs using a mouse monoclonal antibody isotyping reagent and an anti-goat/sheep IgG peroxidase conjugate (Sigma-Aldrich).

For the competitive ELISA, 96-well microplates were coated with the DIII protein using 100 μL of protein solution (10 μg/mL) per well. After the plates had been coated, 50 μL aliquots of serial dilutions of competing protein AP205-am-DIII and 50 μL of the anti-DIII were added to the wells simultaneously. The 1:800 dilution of the anti-DIII with an OD492 value within the range of 0.5–0.6 in the control samples without competing protein was used. After incubation at 37 °C for 1 h, the microplates were processed as described above. The percent inhibition (I%) of antibody binding by the competing protein was calculated as follows:

$$I\% = [(\text{OD492 test sample} - \text{OD492 negative control})/(\text{OD492 positive control} - \text{OD492 negative control})] \times 100.$$

The molar amounts of the proteins necessary for 50 % inhibition (I50) were calculated.

Results

Construction, Expression and Purification of Recombinant AP205 Variants Carrying the DIII Epitope

The construction of the recombinant AP205-am-DIII and AP205-op-DIII genes, where the DIII sequence is C-terminally fused to the AP205 CP over amber or opal translation termination codons, is depicted in Fig. 1. Direct expression of the DIII sequence (Fig. 1) was performed to have a source of the DIII for ELISA testing after immunisation of mice with AP205 VLPs carrying the DIII sequence. Furthermore, we used highly purified and refolded DIII protein as a congruent for immunisation of mice in parallel with the mosaic AP205-derived VLPs.

The expression level of both AP205-am-DIII and AP205-op-DIII polypeptides, as determined from SDS-PAGE of total SDS-mercaptoethanol cell lysates, corresponded, in general, to the suppressor capacity of the appropriate *E. coli* strains (Fig. 2a). Approximately 50 % of the total target proteins appeared in the soluble cell fraction, similar to the separation that occurs during expression of non-chimeric AP205 or other VLP-producing (RNA phage Qβ, hepatitis B core antigen) genes (not shown). The non-chimeric AP205 carrier did not demonstrate any difference in solubility in comparison to the AP205-DIII fusions. The ratio of AP205-DIII fusions to

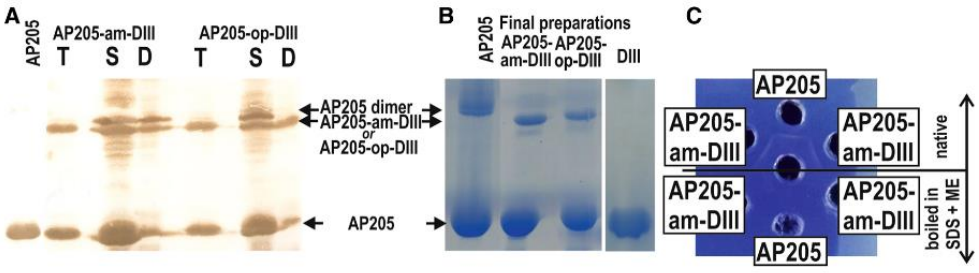

Fig. 2 Monitoring of the expression and purification process of the mosaic AP205-DIII VLP variants. **a** SDS-PAGE Western blot (with polyclonal anti-AP205 antibody) of total protein in SDS-mercaptoethanol lysed cell samples (T), supernatants of the ultrasonicated cell lysates (S), and debris of the ultrasonicated cell lysates after solubilisation in 7 M urea (D). **b** Coomassie stained SDS-PAGE of the final purified preparations of the mosaic AP205-DIII particles, **c** double radial Ouchterlony's immunoprecipitation analysis of AP205-DIII mosaics: native VLPs (*top*), VLPs boiled in Laemmli's buffer (*bottom*). The polyclonal anti-AP205 antibody was placed in the central hole

AP205 in the initial *E. coli* lysates was ~50 %. During the preparation of ultrasonicated cell lysates, a fraction of AP205 dimers appeared and remained relatively stable during boiling in Laemmli's buffer; however, extensive boiling of the final purified samples led to the disappearance of the AP205 dimer band (Fig. 2b).

The mosaic VLPs yielded, on average, ~8 mg of purified AP205-DIII per gram of wet cells. After extensive purification, the mosaic AP205-DIII VLPs demonstrated a high purity of the target proteins (up to 90 %) with a ratio of AP205-DIII to AP205 carrier of ~0.12–0.17 to 1 within the particles.

The minimal contamination of purified AP205-DIII VLPs with host proteins (Fig. 2b) can be explained by intra-particle occlusion of bacterial proteins rather than by adherence on the VLP surface. A gradual loss of the chimeric AP205-DIII component of VLPs was observed during the purification process. This gradual loss would happen if VLPs enriched with chimeric DIII-harbouring monomers are less stable than VLPs with a lower content of chimeric monomers and are therefore preferentially destroyed during purification.

Properties of Mosaic AP205 VLPs Carrying the DIII Epitope

Double radial Ouchterlony immunoprecipitation, which could be regarded as the most specific test for the existence of the VLPs, demonstrated full confluence, without any 'spurs', of the precipitation lines formed by the AP205-am-DIII and AP205-op-DIII VLPs with the precipitation line produced by the non-chimeric AP205 VLPs (Fig. 2c, top). Therefore, full 'Ouchterlony identity' of the AP205-derived VLPs was demonstrated even though they differed with respect to the presence of the AP205-DIII fusions. Disruption of the VLPs by boiling in Laemmli's buffer prevented formation of the precipitation lines in the Ouchterlony's test (Fig. 2c, bottom).

According to electron microscopy analysis, purified mosaic AP205-derived particles were indistinguishable from non-purified items observed in the initial *E. coli* lysates (not shown), as well as from the original AP205 carrier particles (Fig. 3).

Direct measurement of the particle size in solution using the DLS method revealed particles with a close-to-expected diameter of 32.7 nm in the case of the control AP205, but slightly differing diameters of 32.7 and 37.8 nm for AP205-am-DIII and AP205-op-DIII, respectively (Fig. 4).

The DIII sequence appeared on the surface of the VLPs because it was fully accessible to anti-DIII antibodies in a competitive ELISA test (not shown).

The content of the encapsidated RNA within purified mosaic AP205-DIII VLPs was estimated as 1,180 nucleotides per particle; the estimated RNA content remained constant after additional purification steps.

Double radial Ouchterlony immunodiffusion using polyclonal rabbit anti-AP205 antibodies and NAGE confirmed stable association of the encapsidated RNA with the VLPs (not shown). Therefore, we think that the residual nucleic acids are not placed on the surface of mosaic particles, since nucleic acids are resistant to ribonuclease treatment (not shown) and are not removed not only during Ouchterlony immunodiffusion process, but also by DEAE Sephadex chromatography, sucrose gradient centrifugation or ammonium sulphate precipitation.

Properties of Regular AP205-DIII and GA-DIII Fusions, and Purification of the Directly Expressed DIII Protein

We were motivated to generate mosaic AP205-derived particles because our early efforts to generate regular

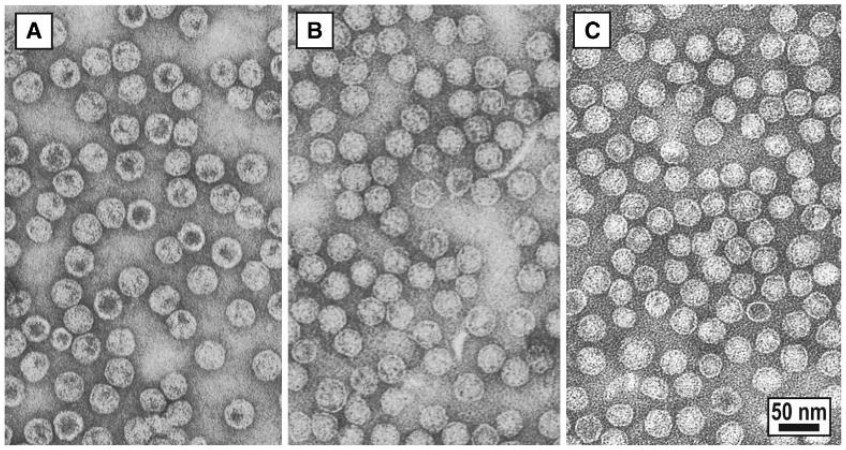

Fig. 3 Electron microscopy analysis of the purified mosaic AP205-DIII VLPs. **a** AP205-am-DIII, **b** AP205-op-DIII, **c** AP205 VLPs as a control. *Scale bar* 50 nm

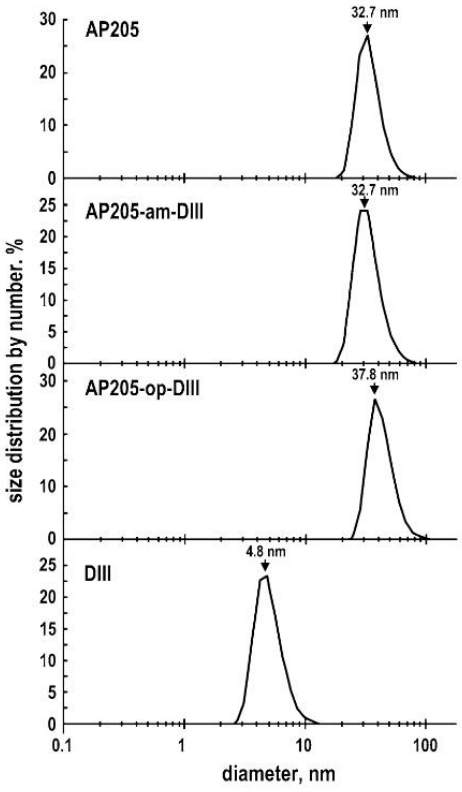

Fig. 4 The size of particles in the purified samples measured by DLS analysis. The results of the DLS size distribution are shown with the particle radius in nm on the *x*-axis and the number of particles in % on the *y*-axis. The *arrows* indicate the radius of the particles

AP205-DIII and/or GA-DIII VLPs were unsuccessful. When regularly fused AP205-DIII or GA-DIII genes without any intervening suppressor codons (Fig. 1) were expressed, chimeric target proteins appeared as insoluble products without any signs of self-assembly in bacterial cells (not shown). The attempts to refold them in vitro, also in the presence of the initial AP205 as a helper, failed (not shown).

Direct expression of DIII protein led to a substantial yield, 12 mg/g of cells, of insoluble recombinant product. The DIII protein was purified and refolded by an arginine-mediated renaturation procedure [41], as described in the Materials and Methods. The final yield of the renatured product after CL4B column chromatography reached 3 mg/g of cells. The quality of the refolded DIII protein is shown in Fig. 2b. The purified DIII protein did not form aggregates in solution and DLS analysis demonstrated particles with a radius of 4.8 nm (Fig. 4).

Immunisation of Mice with DIII-Carrying Proteins

In Fig. 5, we present immunisation data on the AP205-op-DIII VLPs only because analogous data on the immunisation of mice with the AP205-am-DIII VLPs demonstrate general similarities with the presented data.

The antibody response in mice against the DIII epitope was demonstrated by direct ELISA on two different antigens coated onto solid support: (i) purified DIII protein and (ii) purified regular GA-DIII fusion, where DIII was added C-terminally to the CP of RNA phage GA. RNA phage GA is not cross-reactive immunologically with RNA phage AP205. Titration on differently coated solid supports led to the conclusion that the fused GA-DIII protein was more

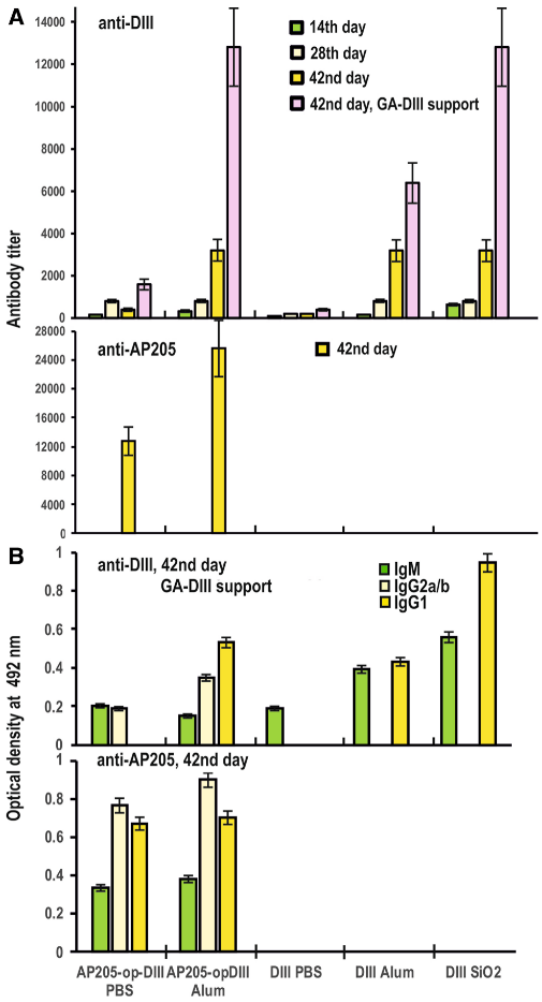

Fig. 5 Immunogenicity of the DIII-carrying proteins. **a** Average antibody titres to DIII (*top*) and AP205 carrier (*bottom*) for the sera from five animals are shown. **b** Isotyping of the antibodies induced against DIII (*top*) and AP205 carrier (*bottom*) after the immunisation of mice with DIII-carrying proteins. Antibodies were diluted 1:50 with PBS

sensitive (up to four times) as a support for anti-DIII antibody detection than the purified DIII polypeptide (Fig. 5a).

After immunisation of mice without any adjuvants, the AP205-op-DIII VLPs induced an evident anti-DIII response (Fig. 5a, top, slot 1); however, the response was about four times weaker than the appropriate anti-AP205 carrier response (Fig. 5a, bottom, slot 1). Formulation of the AP205-DIII VLPs in the Alhydrogel adjuvant preferably enhanced anti-DIII (Fig. 5a, top, slot 2). In all cases, the maximal anti-DIII response was found after two boosts on day 42 of immunisation (Fig. 5a, top).

The DIII polypeptide appears to be a weak immunogen after immunisation of mice without any adjuvant (Fig. 5a, top, slot 3). Formulation of the DIII polypeptide in Alhydrogel (Fig. 5a, top, slot 4) or silicon dioxide (Fig. 5A, top, slot 5) enhanced the anti-DIII response to the level of the anti-DIII response induced by the AP205-op-DIII VLPs in Alhydrogel (Fig. 5a, top, slot 2).

Isotyping of the induced antibodies revealed a remarkable increased ability of the AP205-op-DIII VLPs over the DIII protein to induce anti-DIII antibodies of the IgG and, specifically, the IgG2a isotype without any adjuvants (Fig. 5b, top, slots 1 and 3). Without adjuvants, the DIII polypeptide was unable to switch antibody production from the IgM to the IgG isotype (Fig. 5b, top, slot 3). By immunising with adjuvants, the DIII protein acquired the ability to perform this switch and induce IgG1 antibodies (Fig. 5b, top, slots 4 and 5), whereas the AP205-op-DIII VLPs demonstrated clear competence to induce anti-DIII antibodies of both IgG1 and IgG2a/b isotypes (Fig. 5b, top, slots 2, 4, and 5).

The AP205 carrier within the AP205-op-DIII VLPs induced a broad spectrum of IgM, IgG1 and IgG2a/b antibodies both in the absence and presence of the adjuvant (Fig. 5b, bottom, slots 1 and 2).

Discussion

After the WNV-neutralising efficacy of AP205 VLPs decorated by chemically coupled WNV DIII sequence was shown [33], it seemed intriguing to achieve RNA phage coat-driven VLPs carrying the DIII sequence by fusion of the appropriate genes. Moreover, AP205-DIII fusions may eliminate the potential uncertainty of the chemical coupling [33], because the DIII sequence contains two internal cysteine residues. Because self-assembly of the C-terminal AP205-DIII and GA-DIII fusions in vivo and attempts to refold them in vitro failed, construction of mosaic AP205 VLPs bearing the DIII epitope on the VLP surface was performed in the present study.

The idea that the assembly non-competent VLP monomers might be rescued into mixed or mosaic particles in the presence of native VLP monomers as helpers was first described for the hepatitis B virus (HBV) surface antigen (HBsAg) [43]. By simultaneous expression of two genes, mosaic HBsAg particles carrying poliovirus [44] and malaria [45, 46] epitopes have been purified and successfully applied as vaccine candidates. Interestingly, mosaic HBsAg-poliovirus particles induced much higher titres of neutralising antibodies to poliovirus than did the homogenous ones [44]. Additionally, mosaic V3:Ty-VLPs have been produced that carry various V3 loops of different HIV isolates on the same Ty particle [47]. Furthermore, incorporation of mutated VLP

monomers into well characterised, highly symmetric icosahedral VLPs has been described for the hepatitis B core antigen (HBcAg) [48, 49]. In the case of HBcAg, the real presence of both homo- and hetero-dimers within mosaic particles has been documented [50].

A strategy for constructing mosaic particles was started by introducing a linker containing translational stop codons (UGA or UAG) between the sequences encoding a monomer body and a foreign protein sequence, with subsequent simultaneous synthesis of both the initial VLP monomer as a helper moiety and a read-through fusion protein containing a foreign sequence. This strategy was applied for RNA phage Qβ coats [51–53] and C-terminally truncated HBcAg for exposition of hantavirus [54–56] and HBV preS [57] epitopes.

The same mosaic VLP strategy was used here in the case of the RNA phage AP205 coats, which demonstrated definite advantages as promising VLP carriers by construction of putative prophylactic and therapeutic vaccine candidates [36].

It is noteworthy that in the present study, both amber and opal suppressions demonstrated similar outcomes of the target proteins, a situation that is not always the case. For example, the yields of analogous AP205 mosaics with Affibody differed strongly between the amber and opal suppression variants (Renhofa et al. personal communication).

One of the most prospective features of the mosaic AP205 derivatives carrying the DIII epitope is their ability to induce IgG2 antibodies, which is a result of Th1 pathway activation. As is known for other VLP carriers, e.g. for HBcAg VLPs, the Th1 priming and induction of IgG2 isotype antibodies correlates with the presence of encapsidated RNA [58, 59]. The similar Th1/Th2 switch connected with the loss of encapsidated RNA has been described for full-length and C-terminally truncated HBc variants carrying HBV preS1 [60] and HCV [61] epitopes. Encapsidated RNA functions in this case as a TLR-7 ligand [62]. The cause of similar behaviour of AP205 mosaics carrying the DIII epitope could be a subject of further immunological studies.

Acknowledgments We wish to thank Dr. B. E. Martina for providing us with the pTrcHis2-WNV plasmid, Juris Ozols, Guntars Zarins, Dace Priede, and Inara Akopjana for excellent technical assistance. This work was supported by a Latvian grant 2010/0261/2DP/2.1.1.1.0/10/APIA/VIAA/052 and FP7 Grant 261466 Vectorie.

References

1. Lim, S. M., Koraka, P., Osterhaus, A. D., & Martina, B. E. (2011). West Nile virus: Immunity and pathogenesis. *Viruses, 3*, 811–828.
2. Suthar, M. S., Diamond, M. S., & Gale, M, Jr. (2013). West Nile virus infection and immunity. *Nature Reviews Microbiology, 11*, 115–128.
3. Arroyo, J., Miller, C., Catalan, J., Myers, G. A., Ratterree, M. S., Trent, D. W., et al. (2004). ChimeriVax-West Nile virus live-attenuated vaccine: Preclinical evaluation of safety, immunogenicity, and efficacy. *Journal of Virology, 78*, 12497–12507.
4. Monath, T. P., Liu, J., Kanesa-Thasan, N., Myers, G. A., Nichols, R., Deary, A., et al. (2006). A live, attenuated recombinant West Nile virus vaccine. *Proceedings of the National Academy of Sciences United States of America, 103*, 6694–6699.
5. Guy, B., Guirakhoo, F., Barban, V., Higgs, S., Monath, T. P., & Lang, J. (2010). Preclinical and clinical development of YFV 17D-based chimeric vaccines against dengue, West Nile and Japanese encephalitis viruses. *Vaccine, 28*, 632–649.
6. Dayan, G. H., Bevilacqua, J., Coleman, D., Buldo, A., & Risi, G. (2012). Phase II, dose ranging study of the safety and immunogenicity of single dose West Nile vaccine in healthy adults ≥50 years of age. *Vaccine, 30*, 6656–6664.
7. Sá E Silva, M., Ellis, A., Karaca, K., Minke, J., Nordgren, R., et al. (2013). Domestic goose as a model for West Nile virus vaccine efficacy. *Vaccine, 31*, 1045–1050.
8. Brandler, S., Marianneau, P., Loth, P., Lacôte, S., Combredet, C., Frenkiel, M. P., et al. (2012). Measles vaccine expressing the secreted form of West Nile virus envelope glycoprotein induces protective immunity in squirrel monkeys, a new model of West Nile virus infection. *Journal of Infectious Diseases, 206*, 212–219.
9. Volz, A., & Sutter, G. (2013). Protective efficacy of modified vaccinia virus Ankara in preclinical studies. *Vaccine, 31*, 4235–4240.
10. Pinto, A. K., Richner, J. M., Poore, E. A., Patil, P. P., Amanna, I. J., Slifka, M. K., et al. (2013). A hydrogen peroxide-inactivated virus vaccine elicits humoral and cellular immunity and protects against lethal West Nile virus infection in aged mice. *Journal of Virology, 87*, 1926–1936.
11. Ledgerwood, J. E., Pierson, T. C., Hubka, S. A., Desai, N., Rucker, S., Gordon, I. J., et al. (2011). A West Nile virus DNA vaccine utilizing a modified promoter induces neutralizing antibody in younger and older healthy adults in a phase I clinical trial. *Journal of Infectious Diseases, 203*, 1396–1404.
12. Roehrig, J. T. (2003). Antigenic structure of flavivirus proteins. *Advances in Virus Research, 59*, 141–175.
13. Heinz, F. X., & Stiasny, K. (2012). Flaviviruses and their antigenic structure. *Journal of Clinical Virology, 55*, 289–295.
14. Wang, T., Anderson, J. F., Magnarelli, L. A., Wong, S. J., Koski, R. A., & Fikrig, E. (2001). Immunization of mice against West Nile virus with recombinant envelope protein. *The Journal of Immunology, 167*, 5273–5277.
15. Siirin, M. T., Travassos da Rosa, A. P., Newman, P., Weeks-Levy, C., Coller, B. A., Xiao, S. Y., et al. (2008). Evaluation of the efficacy of a recombinant subunit West Nile vaccine in Syrian golden hamsters. *American Journal of Tropical Medicine and Hygeine, 79*, 955–962.
16. Lieberman, M. M., Nerurkar, V. R., Luo, H., Cropp, B., Carrion, R., Jr, de la Garza, M., et al. (2009). Immunogenicity and protective efficacy of a recombinant subunit West Nile virus vaccine in rhesus monkeys. *Clinical and Vaccine Immunology, 16*, 1332–1337.
17. Jarvi, S. I., Hu, D., Misajon, K., Coller, B. A., Wong, T., & Lieberman, M. M. (2013). Vaccination of captive nēnē (Branta sandvicensis) against West Nile virus using a protein-based vaccine (WN-80E). *Journal of Wildlife Diseases, 49*, 152–156.
18. Metz, S. W., & Pijlman, G. P. (2011). Arbovirus vaccines; opportunities for the baculovirus-insect cell expression system. *Journal of Invertebrate Pathology, 107*, S16–S30.
19. Zhu, B., Ye, J., Lu, P., Jiang, R., Yang, X., Fu, Z. F., et al. (2012). Induction of antigen-specific immune responses in mice by recombinant baculovirus expressing premembrane and envelope proteins of West Nile virus. *Virology Journal, 9*, 132.

20. Kanai, R., Kar, K., Anthony, K., Gould, L. H., Ledizet, M., Fikrig, E., et al. (2006). Crystal structure of West nile virus envelope glycoprotein reveals viral surface epitopes. *Journal of Virology, 80*, 11000–11008.
21. Lee, J. W., Chu, J. J., & Ng, M. L. (2006). Quantifying the specific binding between West Nile virus envelope domain III protein and the cellular receptor alphaVbeta3 integrin. *Journal of Biological Chemistry, 281*, 1352–1360.
22. Beasley, D. W., & Barrett, A. D. (2002). Identification of neutralizing epitopes within structural domain III of the West Nile virus envelope protein. *Journal of Virology, 76*, 13097–13100.
23. Volk, D. E., Beasley, D. W., Kallick, D. A., Holbrook, M. R., Barrett, A. D., & Gorenstein, D. G. (2004). Solution structure and antibody binding studies of the envelope protein domain III from the New York strain of West Nile virus. *Journal of Biological Chemistry, 279*, 38755–38761.
24. Nybakken, G. E., Oliphant, T., Johnson, S., Burke, S., Diamond, M. S., & Fremont, D. H. (2005). Structural basis of West Nile virus neutralization by a therapeutic antibody. *Nature, 437*, 764–769.
25. Choi, K. S., Nah, J. J., Ko, Y. J., Kim, Y. J., & Joo, Y. S. (2007). The DE loop of the domain III of the envelope protein appears to be associated with West Nile virus neutralization. *Virus Research, 123*, 216–218.
26. Sánchez, M. D., Pierson, T. C., McAllister, D., Hanna, S. L., Puffer, B. A., Valentine, L. E., et al. (2005). Characterization of neutralizing antibodies to West Nile virus. *Virology, 336*, 70–82.
27. Oliphant, T., Engle, M., Nybakken, G. E., Doane, C., Johnson, S., Huang, L., et al. (2005). Development of a humanized monoclonal antibody with therapeutic potential against West Nile virus. *Nature Medicine, 11*, 522–530.
28. Chu, J. H., Chiang, C. C., & Ng, M. L. (2007). Immunization of flavivirus West Nile recombinant envelope domain III protein induced specific immune response and protection against West Nile virus infection. *The Journal of Immunology, 178*, 2699–2705.
29. McDonald, W. F., Huleatt, J. W., Foellmer, H. G., Hewitt, D., Tang, J., Desai, P., et al. (2007). A West Nile virus recombinant protein vaccine that coactivates innate and adaptive immunity. *Journal of Infectious Diseases, 195*, 1607–1617.
30. Martina, B. E., Koraka, P., van den Doel, P., van Amerongen, G., Rimmelzwaan, G. F., & Osterhaus, A. D. (2008). Immunization with West Nile virus envelope domain III protects mice against lethal infection with homologous and heterologous virus. *Vaccine, 26*, 153–157.
31. Ramanathan, M. P., Kutzler, M. A., Kuo, Y. C., Yan, J., Liu, H., Shah, V., et al. (2009). Communication with an optimized IL15 plasmid adjuvant enhances humoral immunity via stimulating B cells induced by genetically engineered DNA vaccines expressing consensus JEV and WNV E DIII. *Vaccine, 27*, 4370–4380.
32. Martina, B. E., van den Doel, P., Koraka, P., van Amerongen, G., Spohn, G., Haagmans, B. L., et al. (2011). A recombinant influenza A virus expressing domain III of West Nile virus induces protective immune responses against influenza and West Nile virus. *PLoS One, 6*, e18995.
33. Spohn, G., Jennings, G. T., Martina, B. E., Keller, I., Beck, M., Pumpens, P., et al. (2010). A VLP-based vaccine targeting domain III of the West Nile virus E protein protects from lethal infection in mice. *Virology Journal, 7*, 146.
34. Zeltins, A. (2013). Construction and characterization of virus-like particles: A review. *Molecular Biotechnology, 53*, 92–107.
35. Pushko, P., Pumpens, P., & Grens, E. (2013). Development of virus-like particle (VLP) technology from small highly-symmetric to large complex VLP structures. *Intervirology, 56*, 141–165.
36. Tissot, A. C., Renhofa, R., Schmitz, N., Cielens, I., Meijerink, E., Ose, V., et al. (2010). Versatile virus-like particle carrier for epitope based vaccines. *PLoS One, 5*, e9809.
37. Smiley, B. K., & Minion, F. C. (1993). Enhanced readthrough of opal (UGA) stop codons and production of *Mycoplasma pneumoniae* P1 epitopes in *Escherichia coli*. *Gene, 134*, 33–40.
38. Raftery, L. A., Egan, J. B., Cline, S. W., & Yarus, M. (1984). Defined set of cloned termination suppressors: *In vivo* activity of isogenetic UAG, UAA, and UGA suppressor tRNAs. *Journal of Bacteriology, 158*, 849–859.
39. Freivalds, J., Rūmnieks, J., Ose, V., Renhofa, R., & Kazāks, A. (2008). High-level expression and purification of bacteriophage GA virus-like particles from yeast *Saccharomyces cerevisiae* and *Pichia pastoris* Acta Univ. Latv. *Biology, 745*, 75–85.
40. Strods, A., Argule, D., Cielens, I., Jackeviča, L., & Renhofa, R. (2012). Expression of GA coat protein-derived mosaic virus-like particles in *Saccharomyces cerevisiae* and packaging *in vivo* of mRNAs into particles. *Proceedings of the Latvian Academy of Sciences Section B, 66*, 234–241.
41. Chen, J., Liu, Y., Li, X., Wang, Y., Ding, H., Ma, G., et al. (2009). Cooperative effects of urea and L-arginine on protein refolding. *Protein Expression and Purification, 66*, 82–90.
42. Ehresmann, B., Imbault, P., & Weil, J. H. (1973). Spectrophotometric determination of protein concentration in cell extracts containing tRNA's and rRNA's. *Analytical Biochemistry, 54*, 454–463.
43. Bruss, V., & Ganem, D. (1991). Mutational analysis of hepatitis B surface antigen particle assembly and secretion. *Journal of Virology, 65*, 3813–3820.
44. Delpeyroux, F., Peillon, N., Blondel, B., Crainic, R., & Streeck, R. E. (1988). Presentation and immunogenicity of the hepatitis B surface antigen and a poliovirus neutralization antigen on mixed empty envelope particles. *Journal of Virology, 62*, 1836–1839.
45. Moelans, I. I., Cohen, J., Marchand, M., Molitor, C., de Wilde, P., van Pelt, J. F., et al. (1995). Induction of *Plasmodium falciparum* sporozoite-neutralizing antibodies upon vaccination with recombinant Pfs16 vaccinia virus and/or recombinant Pfs16 protein produced in yeast. *Molecular and Biochemical Parasitology, 72*, 179–192.
46. Gordon, D. M., McGovern, T. W., Krzych, U., Cohen, J. C., Schneider, I., LaChance, R., et al. (1995). Safety, immunogenicity, and efficacy of a recombinantly produced *Plasmodium falciparum* circumsporozoite protein-hepatitis B surface antigen subunit vaccine. *Journal of Infectious Diseases, 171*, 1576–1585.
47. Layton, G. T., Harris, S. J., Gearing, A. J., Hill-Perkins, M., Cole, J. S., Griffiths, J. C., et al. (1993). Induction of HIV-specific cytotoxic T lymphocytes in vivo with hybrid HIV-1 V3:Ty-virus-like particles. *Journal of Immunology, 151*, 1097–1107.
48. Loktev, V. B., Ilyichev, A. A., Eroshkin, A. M., Karpenko, L. I., Pokrovsky, A. G., Pereboev, A. V., et al. (1996). Design of immunogens as components of a new generation of molecular vaccines. *Journal of Biotechnology, 44*, 129–137.
49. Beterams, G., Böttcher, B., & Nassal, M. (2000). Packaging of up to 240 subunits of a 17 kDa nuclease into the interior of recombinant hepatitis B virus capsids. *FEBS Letters, 481*, 169–176.
50. Kazaks, A., Dishlers, A., Pumpens, P., Ulrich, R., Krüger, D. H., & Meisel, H. (2003). Mosaic particles formed by wild-type HBV core protein and its deletion variants consist of both homo- and heterodimers. *FEBS Letters, 549*, 157–162.
51. Kozlovska, T. M., Cielens, I., Vasiljeva, I., Strelnikova, A., Kazaks, A., Dislers, A., et al. (1996). RNA phage Q beta coat protein as a carrier for foreign epitopes. *Intervirology, 39*, 9–15.
52. Kozlovska, T. M., Cielens, I., Vasiljeva, I., Bundule, M., Strelnikova, A., Kazaks, A., et al. (1997). Display vectors. II. Recombinant capsid of RNA bacteriophage Qβ as a display moiety. *Proceedings of the Latvian Academy of Sciences, 51*, 8–12.
53. Vasiljeva, I., Kozlovska, T., Cielens, I., Strelnikova, A., Kazaks, A., Ose, V., et al. (1998). Mosaic Qbeta coats as a new presentation model. *FEBS Letters, 431*, 7–11.

54. Koletzki, D., Zankl, A., Gelderblom, H. R., Meisel, H., Dislers, A., Borisova, G., et al. (1997). Mosaic hepatitis B virus core particles allow insertion of extended foreign protein segments. *Journal of General Virology, 78*, 2049–2053.
55. Ulrich, R., Koletzki, D., Lachmann, S., Lundkvist, A., Zankl, A., Kazaks, A., et al. (1999). New chimaeric hepatitis B virus core particles carrying hantavirus (serotype Puumala) epitopes: Immunogenicity and protection against virus challenge. *Journal of Biotechnology, 73*, 141–153.
56. Kazaks, A., Lachmann, S., Koletzki, D., Petrovskis, I., Dislers, A., Ose, V., et al. (2002). Stop-codon insertion restores the particle formation ability of hepatitis B virus core-hantavirus nucleocapsid protein fusions. *Intervirology, 45*, 340–349.
57. Kazaks, A., Borisova, G., Cvetkova, S., Kovalevska, L., Ose, V., Sominskaya, I., et al. (2004). Mosaic hepatitis B virus core particles presenting the complete preS sequence of the viral envelope on their surface. *Journal of General Virology, 85*, 2665–2670.
58. Riedl, P., Stober, D., Oehninger, C., Melber, K., Reimann, J., & Schirmbeck, R. (2002). Priming Th1 immunity to viral core particles is facilitated by trace amounts of RNA bound to its arginine-rich domain. *Journal of Immunology, 168*, 4951–4959.
59. Sominskaya, I., Skrastina, D., Petrovskis, I., Dishlers, A., Berza, I., Mihailova, M., et al. (2013). A VLP library of C-terminally truncated hepatitis B core proteins: Correlation of RNA encapsidation with a Th1/Th2 switch in the immune responses of mice. *PLoS One, 8*, e75938.
60. Skrastina, D., Bulavaite, A., Sominskaya, I., Kovalevska, L., Ose, V., Priede, D., et al. (2008). High immunogenicity of a hydrophilic component of the hepatitis B virus preS1 sequence exposed on the surface of three virus-like particle carriers. *Vaccine, 26*, 1972–1981.
61. Sominskaya, I., Skrastina, D., Dislers, A., Vasiljev, D., Mihailova, M., Ose, V., et al. (2010). Construction and immunological evaluation of multivalent hepatitis B virus (HBV) core virus-like particles carrying HBV and HCV epitopes. *Clinical and Vaccine Immunology, 17*, 1027–1033.
62. Lee, B. O., Tucker, A., Frelin, L., Sallberg, M., Jones, J., Peters, C., et al. (2009). Interaction of the hepatitis B core antigen and the innate immune system. *Journal of Immunology, 182*, 6670–6681.

Conclusion

Our antibody titres obtained after immunization with genetically fused WNV protein fragment were comparable to those obtained by immunization with AP205 VLPs carrying WNV sequence through chemical attachment (Spohn et al., 2010). Chemical binding procedure is tricky because of two cysteines in WNV sequence, whereas genetic fusion is easier for production of particles at the same time providing determined place and orientation of attached sequence. Abovementioned facts shows possible role of such mosaic VLPs to be used as a perspective and safe prophylactic vaccine against WNV infection.

Thesis

- Mosaic particles containing phage AP205 coat protein and protein C-terminally fused with 111 amino acids long WNV envelope protein E domain III sequence can be obtained in *E.coli* expression system.
- Bacteriophage AP205 WNV DIII sequence containing mosaic VLPs elicit WNV specific antibody response after immunisation in mice.

3.3. Hepatitis B virus core VLPs

Hepatitis B virus core protein formed recombinant particles were obtained by expressing full-length (183 amino acids) core protein either in bacteria (*E.coli*) or yeasts (*P.pastoris*). In *E.coli* were expressed also four point-mutants with amino acids 75, 77, 79 and 80 substituted by lysine residues, all capable to self-assemble into VLPs (Figure 6).

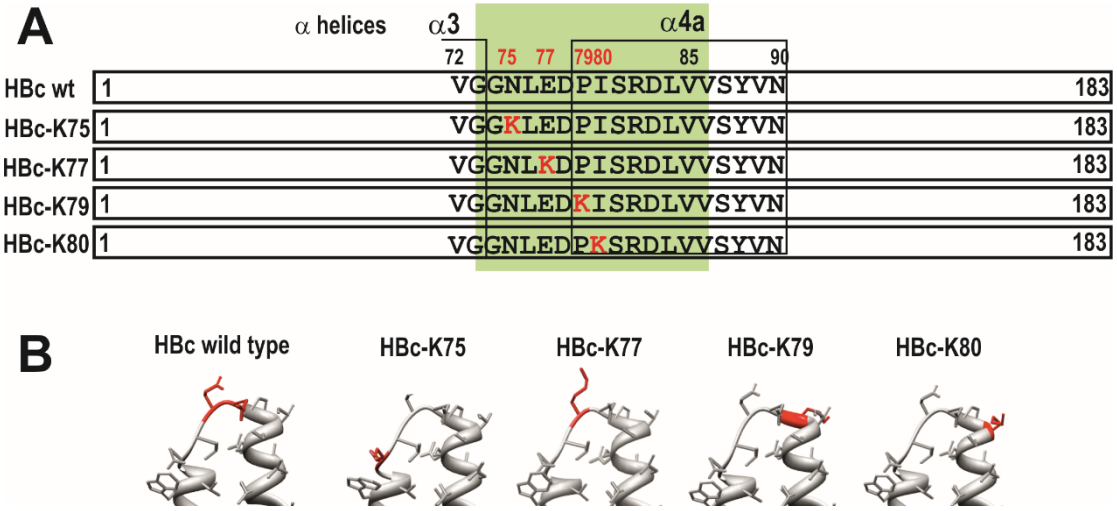

Figure 6 Amino acid sequence and spatial structure of wild-type HBc protein monomer and four lysine mutant variants. (**A**) Primary structure of the central part of spike of the HBc molecule, (**B**) 3D structure for the spikes of wild-type HBc protein monomer and four lysine-exchanged HBc mutants with appropriate innate amino acid marked red. The crystal structure 3D projections of the tips of MIR spikes are from recombinant bacteria-produced HBc VLPs (Wynne et al., 1999).

To our knowledge, two "innate" lysines in core protein are located at the positions 7 (N-terminus) and 96 (middle of spike), therefore additional lysines exposed on the tip of the MIR region possibly could be used for chemical coupling purposes. During thoroughly purification procedures, sodium dodecyl sulfate PAGE (SDS-PAGE) and NAGE were used to control process and ascertain for quality of preparations. Point-mutant VLPs after analysis in NAGE showed slower movement that they both (bacteria-/yeast-produced) un-mutated counterparts. Especially can be mentioned HBc-K77 mutant, bearing rather positive charge at pH7.5 and pH8.3 and therefore moving even backwards in NAGE (Strods et al., 2015a). After purification, four novel VLPs were obtained for addressing purposes. In one case for HBc-K75 VLPs, T lymphocyte specific aptamer sgc-8 containing 3' attached thiol group was chemically coupled to particles (Renhofa et al., 2014).

To obtain empty VLPs suitable for encapsidation of various materials, all abovementioned VLPs were subjected to alkaline treatment at pH12 – procedure (described in Materials and Methods) to get nucleic acid empty HBc particles without impairing their structure. Despite the simplicity of method, empty VLPs needs to be purified through gelfiltration chromatography in order to separate aggregates from discrete empty capsids. In all cases after chromatography empty non-aggregated bacteria- and yeast-produced particles as well as all mutant (HBc-K75, HBc-K77, HBc-K79 and HBc-K80) particles were obtained. In

two cases for mutant VLPs HBc-K75 and HBc-K77 increased disposition for aggregate formation was shown (Strods et al., 2015a).

Our further interest was devoted only to this "qualitative" part, particularly analysing them by wide variety of methods, including optical absorbance measurements, SDS-PAGE, NAGE at different pH, dynamic light scattering (DLS), electron microscopy (EM), monoclonal HBe/anti-HBe and HBc/anti-HBc kits and Ouchterlony's double radial immune diffusion tests. DLS measurements showed size and homogeneity of empty particles similar to full ones, SDS-PAGE and EM analysis proofed integrity of core protein and capsids, respectively.

Despite the fact that EM can be used to discriminate between intact and empty particles, we used other methods – mainly optical absorbance measurements and NAGE analysis. Absorbance spectra analysis of empty bacteria-source and yeast-source particles showed ratio A260/A280 approximately 0.7, indicating absence of nucleic acids comparable to pure protein (HBc protein dimers analysed by (Porterfield et al., 2010)). NAGE analysis was also used to proof the loss of nucleic acids by comparing ethidium bromide and Coomassie blue stained gels for both alkaline un-treated and empty HBc VLPs. Movement of empty particles was generally slower (less negatively charged) for both bacteria- and yeast-produced VLPs in almost all tested pH conditions if compared with native particles, once again confirming the lack of inner negatively charged RNA filling in empty ones (Strods et al., 2015a). It can be also noticed that empty yeast-produced HBc VLPs were faster moving in NAGE compared to *E.coli* expressed, possibly due to the yeast provided phosphorylation (Freivalds et al., 2011). Alkali treatment method was used to make empty phage origin VLPs – for MS2 (Hooker et al., 2004) and PP7 (Tumban et al., 2013).

Empty HBc VLPs were combined with different types of RNAs and DNAs, using either simply mixing or urea scarification step for disruption and reassembly of particles. First, *E.coli* tRNA and rRNA bound firmly with both empty bacteria- and yeast-produced VLPs. Our experiments pointed to the lower packaging capability of yeast-derived VLPs compared with bacteria-produced ones, possibly due to the occupied inner compartment by phospho groups. Specifically, each bacteria-produced empty VLP seized almost 25 tRNA molecules whereas yeast-produced – less than 10 (Strods et al., 2015a). This fact corresponds also to nucleotide content in non-emptied particles, wherein bacteria-produced contains approximately 636 nt per particle more that yeast-produced, according to our optical density based calculations from simplified (Porterfield and Zlotnick, 2010) method. RNA packaged particles demonstrated similar NAGE and DLS pattern as native recombinant particles, however, phenol extraction of packaged material clearly demonstrated strong RNA degradation, determined by formaldehyde agarose gel electrophoresis, capillary electrophoresis and formaldehyde-PAGE. In comparison – RNA from recombinant bacteria-produced VLPs contained much longer fragments. Despite this fact, we packaged *in vitro* synthesized mRNA and after sequencing of extracted (and degraded) material with next-generation sequencing technology, at least 86.77% were mRNA specific sequences. There are known that nucleoprotein from Lassa and Tacaribe viruses and from Crimean-Congo haemorrhagic fever virus possess exoribonuclease (Hastie et al., 2011; Jiang et al., 2013) and endodeoxyribonuclease (Guo et al., 2012) activity, respectively. We assume that our empty particles also bear some kind of nuclease activity and thereby proposal for future would be packaging of native HBV genome, possibly, able to overcome this "face-control".

Second, DNA starting from short oligos to large plasmids were used. Oligodeoxynucleotides (ODNs) in length 21 and 63 nucleotides after mixing in large

superiority with empty particles showed the same high level packaging as in case with RNA, favouring bacteria-produced VLPs (Figure 7).

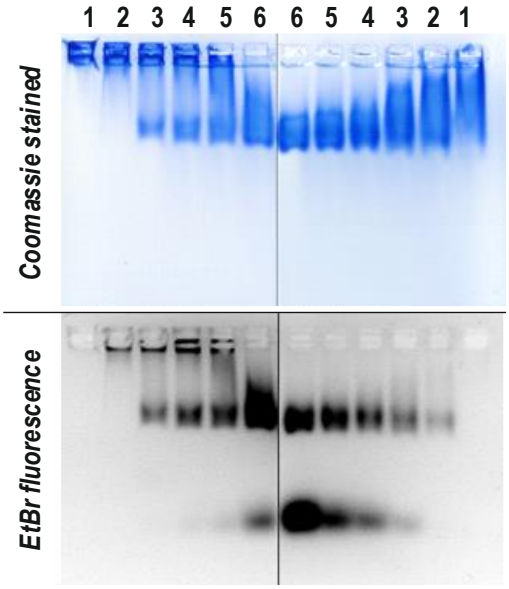

Figure 7 Contact titration of bacteria-produced (left) and yeast-produced (right) HBc VLPs by ODN63 at appropriate ODN molar superiority over VLP: 10 (2), 20 (3), 30 (4), 40 (5), 50 (6); appropriate empty HBc VLPs were used as a control (1).

Packaged VLPs resisted NAGE and CsCl and sucrose density centrifugations. For larger DNA fragments urea-treatment was used, and opposite to ODNs, long DNA fragments or plasmid DNA formed large complexes in molar superiority of empty VLPs. Those large complexes were seen in DLS, held in wells in NAGE and in EM they looked like chains, but at the same time DNA was protected against DNase cleavage. To explore the capacity of packaging functional sequences, empty VLPs were packaged at equimolar ratios with a set of different length discrete DNA fragments and then tested for DNAse resistance. Phenol extraction revealed the intactness of packaged 1289 base pair fragment but not the 1737 base pair fragment. This border of packaging (between 2578 and 3474 nucleotides) is nearly to our calculated theoretical packaging of 3844 and 3208 nucleotides per particle for bacteria- and yeast-produced HBc VLPs, respectively. This outcome could encourage in future for packaging of transcription/translation capable genes of interest.

To test the possibility to use HBV core VLPs as an immunisation moiety, mice were immunised with “native” HBc VLPs, empty HBc VLPs and re-packed with CpG HBc VLPs. Antibody titres on the 10^{th} day were markedly higher for both bacteria-produced HBc VLPs and bacteria-produced with CpG re-packed HBc VLPs, but not for the empty bacteria-produced VLPs, however, at 28^{th} day titres were equilibrated. Antibody isotyping showed markedly higher IgG1 and lower IgG2 antibody repertoire for empty VLPs, whereas IgG2 antibodies were more represented in non-empty HBc VLPs, especially in CpG containing. More convincible immune response was seen in INF-γ ELISpot after stimulation of lymphocytes, obtained from mice immunised with CpG-containing VLPs, if compared with HBc VLPs or empty HBc VLPs (Strods et al., 2015b).

SCIENTIFIC REPORTS

OPEN

Received: 08 February 2015
Accepted: 13 May 2015
Published: 26 June 2015

Preparation by alkaline treatment and detailed characterisation of empty hepatitis B virus core particles for vaccine and gene therapy applications

Arnis Strods, Velta Ose, Janis Bogans, Indulis Cielens, Gints Kalnins, Ilze Radovica, Andris Kazaks, Paul Pumpens & Regina Renhofa

Hepatitis B virus (HBV) core (HBc) virus-like particles (VLPs) are one of the most powerful protein engineering tools utilised to expose immunological epitopes and/or cell-targeting signals and for the packaging of genetic material and immune stimulatory sequences. Although HBc VLPs and their numerous derivatives are produced in highly efficient bacterial and yeast expression systems, the existing purification and packaging protocols are not sufficiently optimised and standardised. Here, a simple alkaline treatment method was employed for the complete removal of internal RNA from bacteria- and yeast-produced HBc VLPs and for the conversion of these VLPs into empty particles, without any damage to the VLP structure. The empty HBc VLPs were able to effectively package the added DNA and RNA sequences. Furthermore, the alkaline hydrolysis technology appeared efficient for the purification and packaging of four different HBc variants carrying lysine residues on the HBc VLP spikes. Utilising the introduced lysine residues and the intrinsic aspartic and glutamic acid residues exposed on the tips of the HBc spikes for chemical coupling of the chosen peptide and/or nucleic acid sequences ensured a standard and easy protocol for the further development of versatile HBc VLP-based vaccine and gene therapy applications.

Hepatitis B virus (HBV) core (HBc) protein p21, which is encoded by HBV gene C, acts in the viral life cycle as an icosahedral scaffold of the HBV nucleocapsid, which contains and carries genomic HBV DNA, polymerase (for a review, see[1]) and possibly protein kinase[2]. HBc protein spontaneously forms dimeric units[3] that self-assemble into two particle isomorphs[2,4] by allosterically controlled mechanisms[5] in HBV-infected eukaryotic cells. The spatial structure of HBc particles was previously resolved in *E. coli* due to the ability of HBc to undergo synthesis and self-assembly in these cells (for a review see[6]). Recombinant HBc particles are represented by the same two isomorphs with triangulation numbers T = 4 and T = 3[7]; they consist of 240 and 180 HBc monomers and are 35 and 32 nm in diameter[7,8], respectively. The three-dimensional structure of the T = 4 particles was resolved by X-ray crystallography[9], whereas a quasi-atomic pattern of the native T = 3 isomorph was reconstructed by docking the dimers of the T = 4 crystal structure[8].

HBc protein was also shown to self-assemble in multiple other efficient heterologous expression systems, including yeast *S. cerevisiae*[10,11] and *P. pastoris*[12,13]. The HBc protein linear structure splits into the following two clearly separated domains: the N-terminal self-assembly (SA) domain (1–140 aa) that is necessary and sufficient to perform the assembly function and the protamine-like arginine-rich

Latvian Biomedical Research and Study Centre, Ratsupites Str. 1 k-1, LV-1067, Riga, Latvia. Correspondence and requests for materials should be addressed to R.R. (email: regina@biomed.lu.lv)

C-terminal domain (CTD; 150-183 aa)[14]. These two domains are separated by a hinge peptide (141–149 aa)[15] that performs morphogenic functions and manages encapsidated nucleic acids[15,16]. The SA domain of HBc protein possesses a set of variable and conservative stretches that correspond to immunological B-cell epitopes and structural elements, respectively, whereas the CTD domain and hinge peptide are the most conserved HBc regions (for a review see[6,17]).

The intrinsic self-assembly function of the SA domain and its high capacity to accept foreign aa stretches are used to generate chimeric virus-like particles (VLPs), both full-length and C-terminally truncated, on the HBc scaffold (for review, see[6,18–20]). The CTD domain is responsible for the encapsidation of the 3.5-kilobase pregenomic HBV mRNA, which is converted into partially double-stranded HBV DNA[21]. Nucleic acid-binding sites in the CTD domain are located in four arginine blocks[22]. As a rather flexible structure, without any distinct tertiary outfit (although no 3D data are currently available), the CTD domain may appear inside[23] as well outside of HBc particles[24,25]. According to recent findings, a significant portion of the CTD is exposed at the surface of the RNA-containing immature nucleocapsid, and the CTD is mostly confined within the DNA-containing mature nucleocapsid[26].

Similar to natural HBc within viral nucleocapsids during the recognition of pregenomic HBV mRNA[21], recombinant VLPs prefer single-stranded RNA for packaging, whereas the elimination of the CTD domain prevents this type of packaging in *E. coli* cells[27,28]. Nevertheless, HBc possesses a definite ability to bind to both RNA and DNA *in vitro*[22]; however, dsDNA is regarded as a poor substrate for assembly[29].

Encapsidation of short hairpin RNAs by HBc nucleocapsids is performed *in vivo* in eukaryotic cells and results in the construction of the HBV "Trojan horse" vector that targets hepatocytes[30]. *In vitro* HBc encapsidation is regarded as a way to perform packaging of desired molecules, such as immunostimulatory (ISS) CpG sequences[31,32] and other short oligodeoxynucleotides (ODNs)[33], pregenomic mRNA and random ssRNA with similar efficiency irrespective of phosphorylation[34,35]. In addition, the packaging of ssDNA occurs to a lesser extent, and the packaging of dsDNA[34], other polyanions (poly-glutamic acid and polyacrylic acid but not low molecular mass anions (inositol triphosphate) or polycations (polylysine and polyethylenimine)[34], and magnetic nanoparticles[36] occurs minimally.

However, the controlled encapsidation and quality control of bacteria- and yeast-derived HBc VLPs are hindered by the presence of irregular internal RNA of host origin. In this study, we propose a novel experimental approach to completely remove the internal RNA from bacteria- and yeast-derived HBc VLPs by alkaline hydrolysis, without any loss of VLP quality. The empty HBc VLPs demonstrated the high efficiency of simple, so-called contact DNA and RNA packaging. The introduction of lysine residues on the surface of HBc VLPs enabled chemical coupling of foreign peptide and nucleic acid sequences and promoted the development of packaging and peptide exposure technologies to generate well-characterised HBc-derived vaccine and gene therapy tools[37,38].

Results

Preparation of empty HBc VLPs by alkaline treatment. Wild type (wt) HBc VLPs were produced in *E. coli* and *P. pastoris*. Four HBc VLP variants with amino acid (aa) positions 75, 77, 79, and 80 substituted by lysine residues (Fig. 1), in order to expose the lysines on the tips of the HBc spikes for further chemical coupling purposes, were produced in *E.coli*.

Efficient column chromatography purification steps before alkaline treatment (see Supplementary Fig. S1 online) led to VLP preparations that demonstrated high consistency but different mobility by native agarose gel electrophoresis (NAGE) analysis at pH 8.3 and 7.5 (see Supplementary Fig. S2 online). Calculations (see Supplementary Methods online) based on precise UV spectra measurements (see Supplementary Fig. S3 online) revealed the total amount of VLP-encapsidated RNA as approximately 3844 and 3208 nucleotides per particle for bacteria- and yeast-produced wt HBc VLPs, respectively.

Length analysis of RNA encapsidated by the wt HBc VLPs from bacteria revealed the presence of fragments ranging from approximately 30 to 2000 nt (mononucleotides) in size, with the prevalence of short oligoribonucleotides up to 500 nt in length (see Supplementary Fig. S4 online).

Sequence analysis of RNA encapsidated by the bacteria-produced wt HBc VLPs showed that 34.93% of the RNA was represented by transcripts of the expression plasmid, 98.49% of which were mRNAs encoding the HBc monomer from the pHBc183 plasmid (see Supplementary Fig. S5 and Table S1 online). Other encapsidated sequences were of *E. coli* origin and represented at least 332 genes (see Supplementary MS Excel spreadsheet online). Remarkably, most of the VLP-packaged RNAs were of mRNA origin; 23S and 16S rRNA-derived sequences constituted only 5.82 and 0.61% of the total, respectively.

RNA encapsidated by wt and four lysine-exposing HBc VLPs was fully hydrolysed by alkaline treatment, and characteristic VLP fractions were pooled after separation on Sepharose CL-4B (Fig. 2a). PAGE showed the maintenance of HBc during alkaline treatment (see Supplementary Fig. S1 online). The A fractions of the HBc VLPs corresponded by elution time to VLP aggregates and demonstrated contamination with RNA by UV spectra analysis (see Supplementary Fig. S6 online). Dynamic light scattering (DLS) measurements confirmed marked aggregation of VLPs, with the highest level of aggregation for HBc-K77 VLPs (Fig. 2b, left side). Nevertheless, EM of the A fractions demonstrated a rather standard VLP pattern (Fig. 2b, right side).

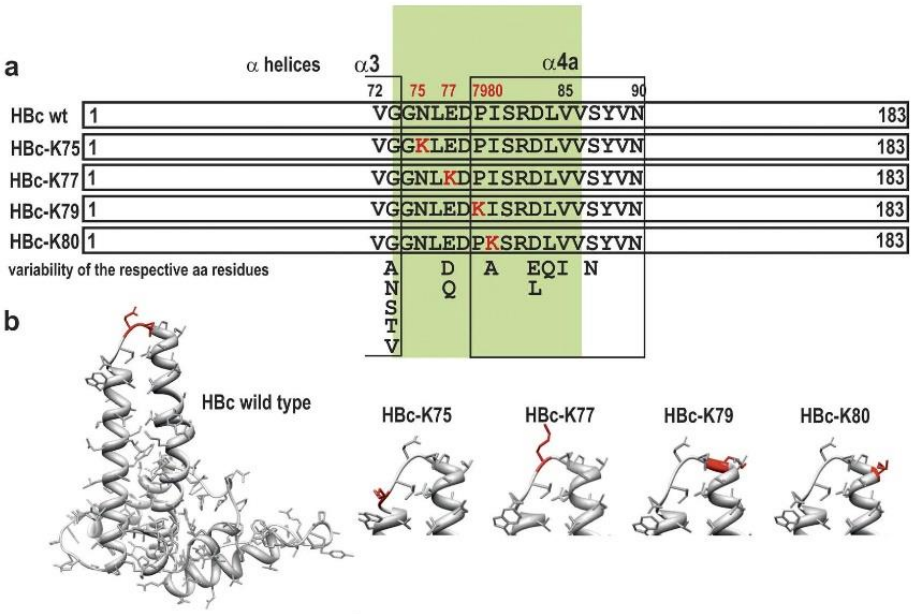

Figure 1. General structure of the initial wt HBc molecule from the HBV320 genome, genotype D1, subtype ayw2, GenBank accession number X02496[75] and four variants exposing lysine residues at the tips of the spikes. (**a**) Primary structure of the central part of the HBc molecule, with alternative naturally occurring aa residues[6,17]. (**b**) 3D maps for the initial HBc monomer with Glu77 and Asp78 marked red and for the tips of the spikes of four lysine-exposing HBc variants with inserted lysine residues marked red. The maps are based on the crystal structure of recombinant HBc VLPs produced in bacteria[9].

The B fractions of the HBc VLPs corresponded to the expected elution time from the column based on the VLP molecular mass and demonstrated UV spectra typical for proteins without any remarkable RNA contamination (see Supplementary Fig. S6 online). The B fraction prevailed over A fraction in bacteria- and yeast-produced wt HBc VLPs (Fig. 2a). However, four lysine-exposing HBc VLP variants demonstrated two different profiles characterised by the (i) prevailing A fraction and a clear disposition to aggregation in the case of HBc-K75 and HBc-K77 and (ii) prevailing B fraction and low level of aggregation in the case of HBc-K79 and HBc-K80. For this reason, only one representative chromatography pattern for each of the two groups, namely, HBc-K75 or HBc-K80, is shown in Fig. 2a. In contrast, Fig. 2b depicts two other representatives of the two lysine-exposing HBc VLP groups (HBc-K77 and HBc-K79). Yield of the B fraction in case of the bacteria-produced wt VLPs was 4.6 mg/g cells, which corresponded to 60% of material obtained after alkaline treatment and before fractionation. Approximately the same yield was observed for yeast-produced wt HBc VLPs. Regarding the lysine-exposing HBc VLPs, a higher yield of the B fraction was observed for HBc-K79 and HBc-K80 VLPs of approximately 2.8 mg/g cells, whereas the other two variants yielded only about 0.8 mg/g cells.

The empty HBc VLPs of B fractions demonstrated up to 100% size homogeneity by DLS analysis and high quality electron micrographs (Fig. 3). No significant DLS or EM differences were found by comparing the empty HBc VLPs with "natural" bacteria- or yeast-produced wt HBc VLPs before alkaline treatment (Fig. 3, rows b and d). DLS diameter measurements of both "natural" and alkaline-treated wt HBc VLPs from bacteria and yeast indicated interval approximately 31–33 nm in size (Fig. 3, rows a–d), whereas the lysine-exposing HBc variants appeared a bit larger, namely, 35–37 nm (Fig. 3, rows e-h).

As shown in Fig. 2a, the HBc VLPs from the intermediate-pooled chromatography fractions C and D demonstrated a lower level of aggregation than VLP products from fractions A by DLS analysis, and no evident signs of aggregation were shown by EM (for typical examples see Supplementary Fig. S7 online).

NAGE revealed the destruction of both traditionally purified ("natural") and empty HBc VLPs in acidic conditions (Fig. 4, row a). Starting from pH 6.5 until basic conditions at pH 12, "natural" and empty VLPs demonstrated standard EM characteristics (Fig. 4, row b). VLP mobility in NAGE was dependent on the surface charge of VLPs at the specific pH value. The mobility of initial RNA-filled and empty particles was similar at pH 7.5 (Fig. 4, row c). The CTD positive charge reached its maximum at pH 9.0, resulting in a total neutral charge of empty particles, which prevented the movement of empty HBc VLPs in NAGE (Fig. 4, row e). Remarkably, bacteria- and yeast-derived empty HBc VLPs

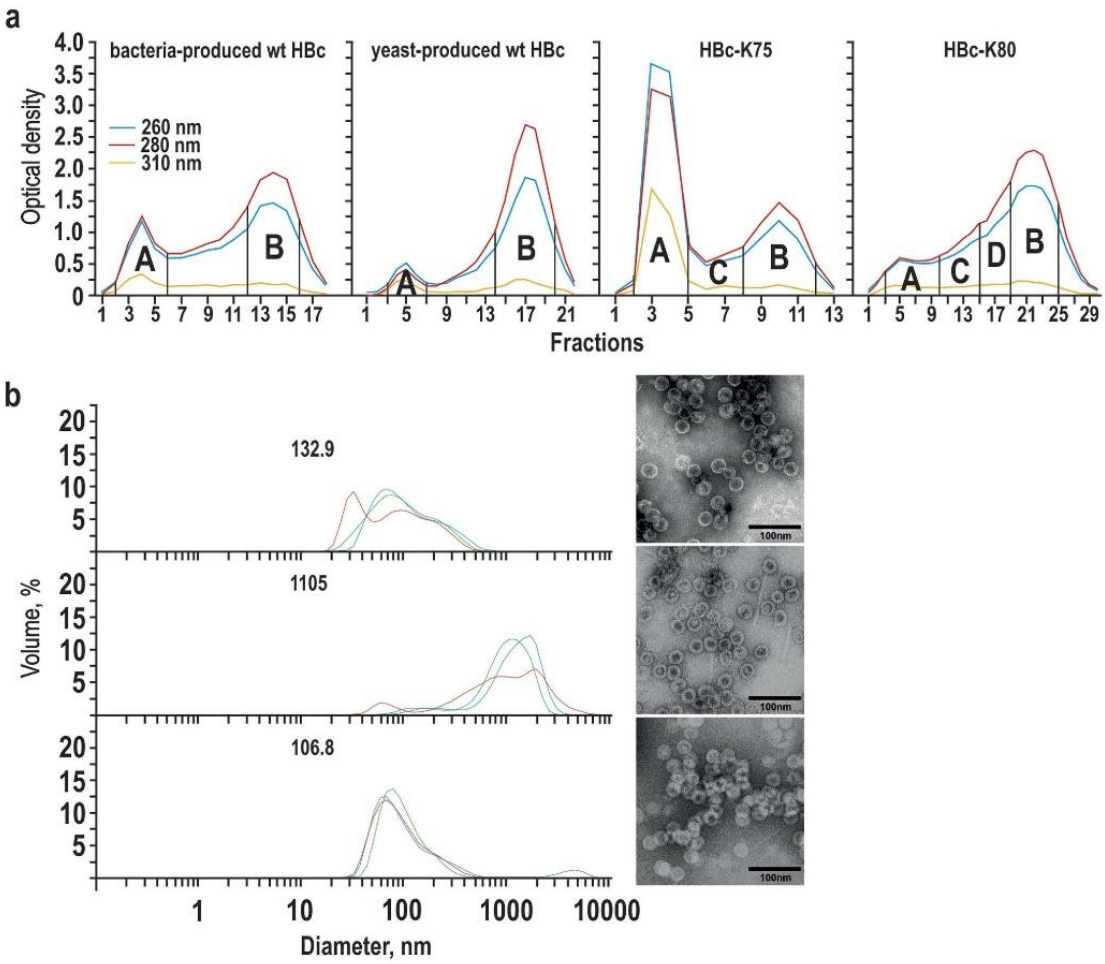

Figure 2. Separation of alkaline-treated HBc VLPs by Sepharose CL-4B column chromatography. (**a**) Chromatography of bacteria- and yeast-produced wt HBc VLPs as well as two representative lysine-exposing HBc VLP variants: HBc-K75 and HBc-K80. Pooled fractions are marked by capital letters. (**b**) DLS (left) and EM (right) characterisation of the fractions A of the alkaline-treated HBc VLP variants: bacteria-produced wt HBc (top), HBc-K77 (middle), HBc-K79 (bottom). Three independent DLS measurements are shown, mean particle diameters are indicated by numbers on the respective DLS graphs.

demonstrated different mobility at pH 8.3 (Fig. 4, row d), which may be explained by the presence of the exposed phosphate group at phosphorylated aa position Ser87 in the case of yeast-derived VLPs[13].

The lysine-exposing HBc variants moved slower than both wt HBc VLP variants because of the additional positive charge on the surface. Remarkably, the empty lysine-exposing VLPs preserved the same mobility characteristics in NAGE as their "natural" counterparts at pH 7.5. As an exception, both empty and "natural" HBc-K77 VLPs remained at the starting position in the NAGE at pH 7.5 and pH 8.3, which was most likely due to the neutralising effect of Glu78 on the neighbouring Lys77 residue (see Supplementary Fig. S2 online).

Antigenicity of HBc VLPs was characterized by (1) two standard commercial Siemens Enzygnost monoclonal kits: HBe/anti-HBe and HBc/anti-HBc, (2) in-house Ouchterlony's double radial immune diffusion test with (i) polyclonal rabbit antibodies or (ii) monoclonal C1-5 antibody recognizing 78-DPIxxD-83 epitope[39] as counter reagents. No differences in behaviour of empty and "natural" HBc VLP variants were found. All HBc VLP variants did not react in the Enzygnost HBe/anti-HBe test and confirmed therefore high self-assembled integrity of empty VLP preparations. In contrast to bacteria- and yeast-produced wt HBc, as well as HBc-K75 and HBc-K79 VLPs, the HBc-K77 and HBc-K80 VLPs were not detectable by the Enzygnost HBc/anti-HBc kit. All HBc VLP variants formed precipitation lines

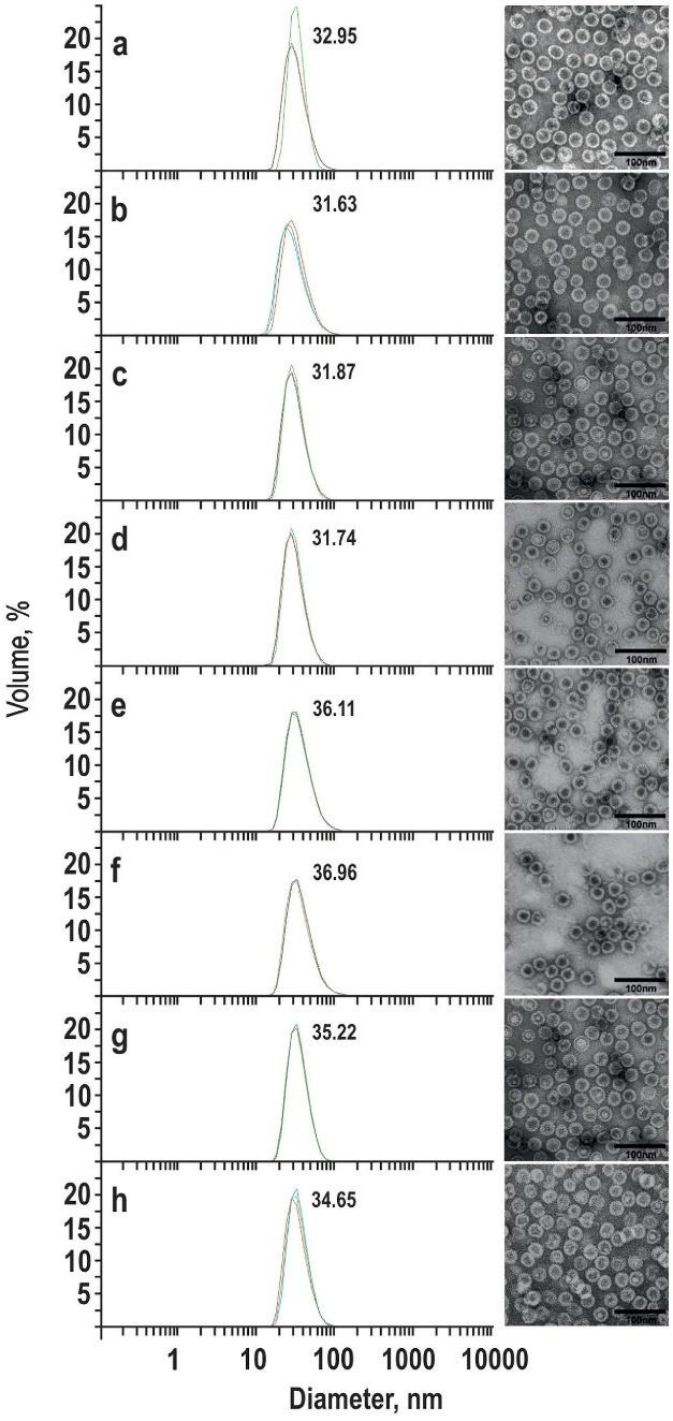

Figure 3. DLS (left) and EM (right) characterisation of the fractions B of the alkaline-treated HBc VLP variants. (**a**) Bacteria-produced wt HBc, (**c**) yeast-produced HBc, (**e**) HBc-K75, (**f**) HBc-K77, (**g**) HBc-K79, (h) HBc-K80. Bacteria- and yeast-produced wt HBc VLPs before alkaline treatment are shown for a comparison in (**b**) and (**d**), respectively. Three independent DLS measurements are shown, mean particle diameters are indicated by numbers on the DLS graphs.

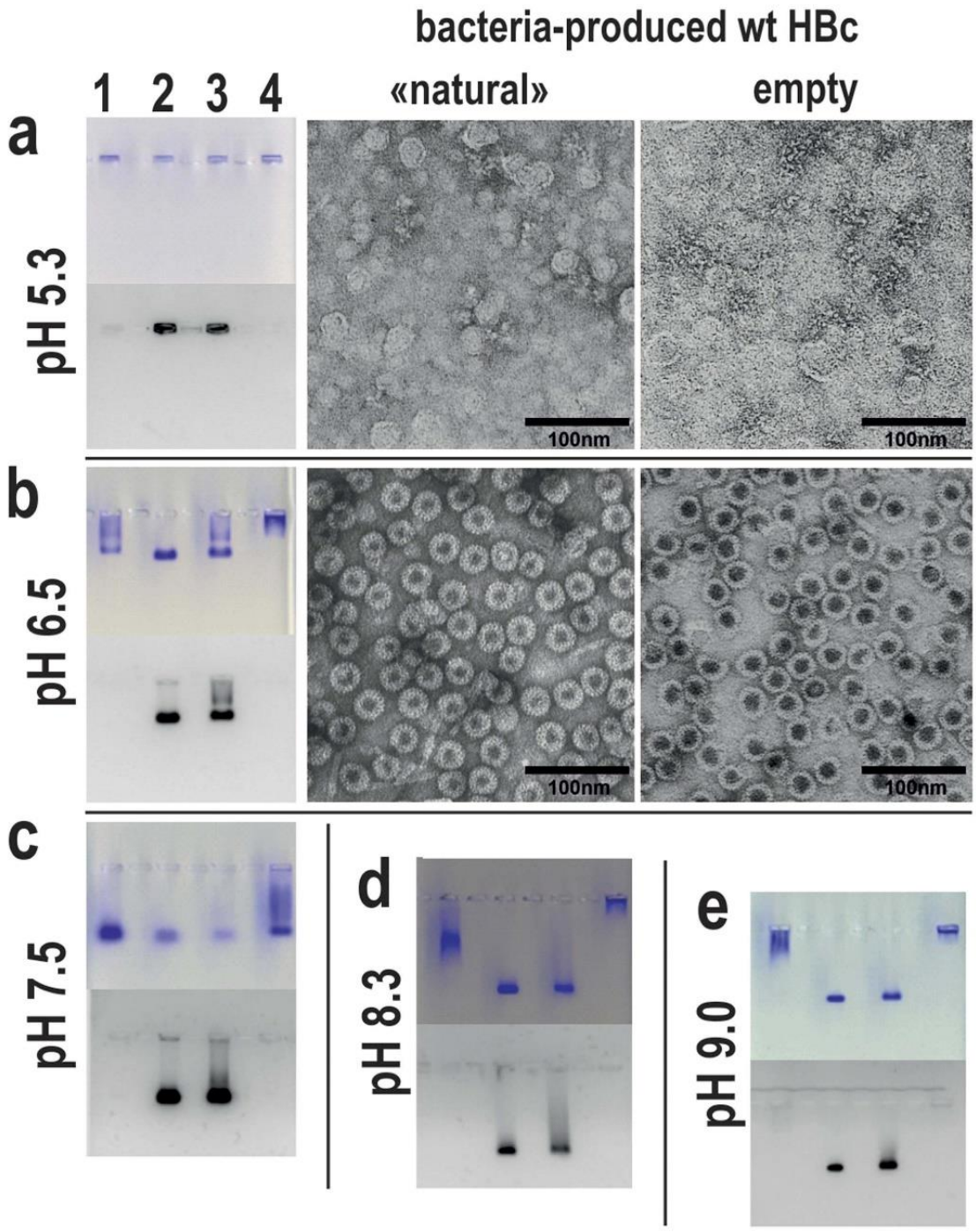

Figure 4. Comparison of "natural" and empty wt HBc VLPs by NAGE (left) and EM (right) at different pH values. Tracks correspond to the following wt HBc VLP preparations: yeast-produced empty (1) or "natural" (2), bacteria-produced "natural" (3) or empty (4). Gels are stained by Coomassie (upper part) and ethidium bromide (lower part).

in the Ouchterlony immune diffusion test using polyclonal rabbit anti-HBc antibodies, but not monoclonal C1-5 antibody, which was unable to precipitate HBc-K80 VLPs (see Supplementary Fig. S8 online).

Encapsidation of ribonucleic acid by empty HBc VLPs. Bacteria- and yeast-produced empty wt HBc VLPs and the four lysine-exposing VLP variants were loosened in 7 M urea. The electron micrographs of the urea-treated destroyed (Fig. 5a, micrograph 1) and fully restored particles: after removal of urea by dialysis without any additions (Fig. 5a, micrograph 2) or in the presence of added bacterial rRNA (Fig. 5a, micrograph 3) are shown for the bacteria-produced wt HBc VLPs. Further RNA encapsidation experiments showed that all studied HBc VLP variants packaged RNA immediately after direct contact of RNA and VLPs without the urea treatment step.

Preliminary quantification of RNA packaging was performed by titrating all of the studied VLPs using *E. coli* tRNA (see Supplementary Fig. S9 online for the packaging of bacteria- and yeast-produced wt HBc VLPs as examples) and rRNA (see Supplementary Fig. S10 online for the packaging of HBc-K75 as an example) with further NAGE analysis. The NAGE bands corresponding to the packaged VLPs are depicted by Coomassie and ethidium bromide staining and demonstrate higher mobility than their empty counterparts. The packaging capacity of empty bacteria-produced wt HBc VLPs was approximately two-fold higher than the same for the yeast-produced analogues. A part of the added tRNA appeared as unbound material in the case of yeast-produced wt HBc by 10-fold molar excess of tRNA; however, in the case of bacteria-produced wt HBc, the 25-fold molar tRNA excess was necessary to leave unbound tRNA (see Supplementary Fig. S9 online). The encapsidated RNA remained fixed to the VLPs after gel filtration (see Supplementary Fig. S9 online for the tRNA packaging as an example) and ammonium sulphate precipitation. Packaged HBc VLPs did not differ from "natural" or empty HBc VLPs by their DLS-measured diameters (see Supplementary Fig. S10 online for the HBc-K75-performed rRNA packaging as an example). Phenol extraction of the VLP-packaged RNA demonstrated strong tRNA (see Supplementary Fig. S9 online) and rRNA (see Supplementary Fig. S11 online) degradation as determined by PAGE and the BioAnalyzer, respectively.

A representative study of RNA incorporation into HBc VLPs by direct contact was performed for the encapsidation of well-characterised purified 1221 nt-long diphtheria toxin fragment A (DTA) mRNA (see Supplementary Fig. S12 and Supplementary Protocols online) as shown in Figs 5b–d. Figure 5b depicts a titration example of yeast-produced wt HBc VLPs with DTA mRNA that revealed optimal VLP/mRNA molar ratios of not more than one mRNA per one HBc particle. Figure 5c shows the stable retention of encapsidated mRNA within the VLPs during sucrose gradient centrifugation. The encapsidated DTA mRNA remained within particles during Sepharose CL-2B column chromatography and sedimentation with ammonium sulphate (see Supplementary Fig. S13 online). Empty bacteria-produced HBc VLPs bound more mRNA than yeast-produced empty VLPs. Specifically, in equal reaction mixtures, more mRNA remained unbound when incubated with empty yeast-produced HBc VLPs (see Supplementary Fig. S13 online).

The encapsidated RNA material differed markedly from the initial mRNA by length and demonstrated clear degradation features in formaldehyde agarose gel electrophoresis (FAGE) (Fig. 5d). Furthermore, fresh extra portions of unpackaged DTA mRNA that were added to mRNA-packaged HBc VLPs remained stable and did not demonstrate any signs of mRNA degradation (Fig. 5d). In contrast to empty particles incubated with DTA mRNA, naturally packaged HBc VLPs displayed no mRNA degradation (Fig. 6a). The percentage of the RNA material recovered from purified HBc VLPs and DTA mRNA complexes was approximately 13% and 19% for bacteria- and yeast-produced HBc VLPs, respectively. The percentage of the RNA material recovery was obtained by comparison of ethanol precipitated amount (after phenol/chloroform extraction) with theoretically calculated packaged amount. In comparison, the technical recovery of mRNA itself was approximately 50%. To estimate the consistency and fate of the packaged DTA mRNA, sequencing of the unpacked mRNA material was performed by massive parallel sequencing using the Ion Torrent PGM technique according to a protocol described in the Supplementary Methods section. DNA libraries were prepared for the exhaustive sequencing of VLP-packaged nucleic acid material. According to the sequencing data, more than 98% of the material before packaging was consistent with DTA mRNA (see Supplementary Table S1 online). Figure 6b presents a typical example of the length distribution of the nucleic acid extracted from bacteria- or yeast-produced wt HBc VLPs in comparison with DTA mRNA before packaging. Only approximately 1.5% of the unpacked material may be represented by full-length DTA mRNA (see inset in Fig. 6b). Just the same is shown in FAGE (Fig. 6a, lane 5) where the RNA material from the bacteria-produced wt HBc VLPs packaged with DTA mRNA was analysed. Most of the RNA material appeared as degraded and only a weak band of the full-length DTA mRNA fragment was observed. The profiles of respective DNA libraries that were created for the sequencing of extracted RNAs (see Supplementary Fig. S14 online) confirmed the mRNA degradation. Regarding HBc-K80 VLPs, analysis of the internal content showed that 86.77% of the sequences were DTA mRNA-derived, only 1.64% were pHBc183-derived and 11.59% were *E. coli*-derived (see Supplementary Fig. S15 and Table S1 online).

Encapsidation of deoxyribonucleic acid by empty HBc VLPs. Encapsidation of the following three representative DNA categories: (i) relatively short single-stranded oligodeoxynucleotides (CpG ODNs), (ii) full-length plasmids, and (iii) long double-stranded DNA fragments (for the full list of the

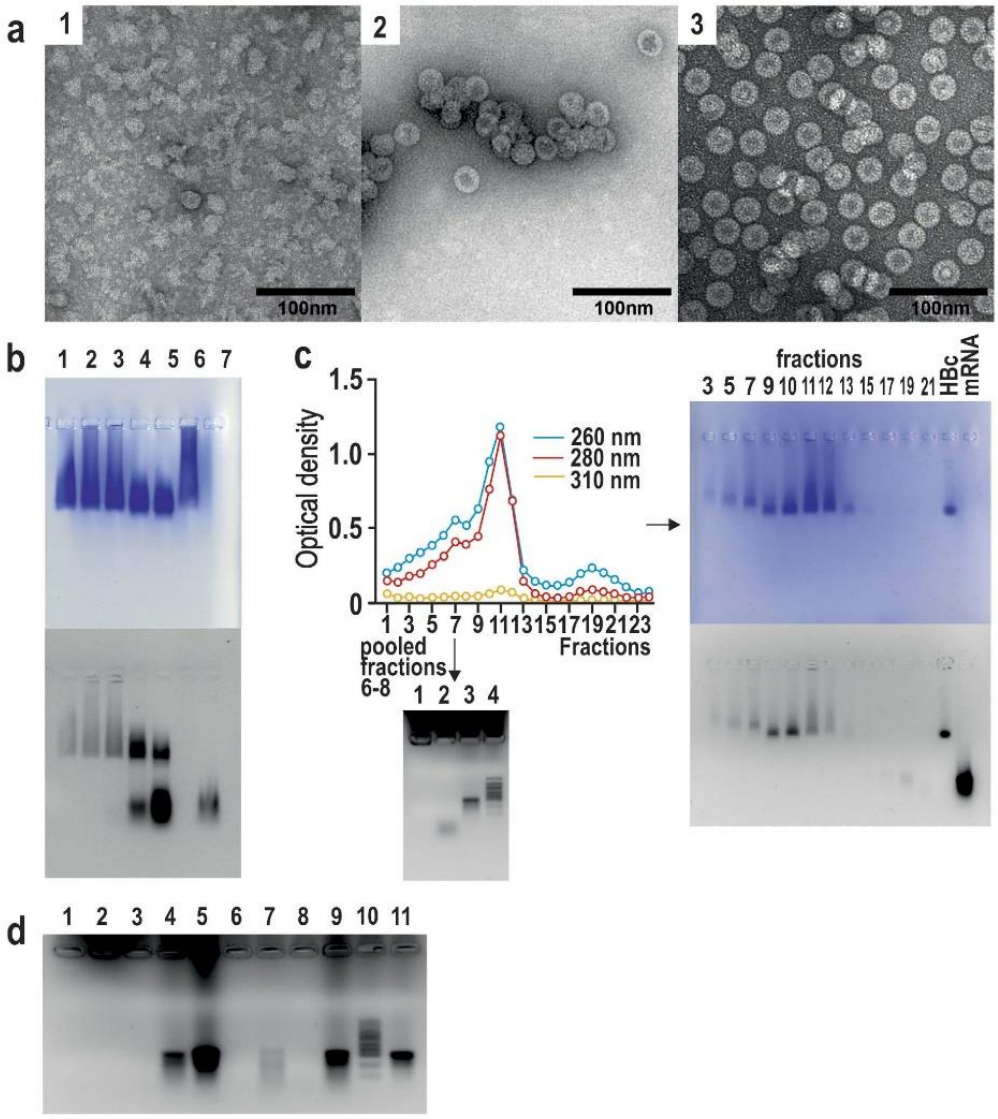

Figure 5. Restoration of empty bacteria-produced wt HBc VLPs after urea treatment or direct contact by RNA packaging. (**a**) Electron micrographs of HBc VLPs after 7 M urea treatment (1) and restoration of HBc VLPs without any additional RNA (2) or by *E. coli* ribosomal RNA predominance (8000 mononucleotide per one VLP) (3). (**b**) NAGE analysis by Coomassie (top) and ethidium bromide (bottom) staining of the DTA mRNA contact encapsidation by empty yeast-produced wt HBc VLPs at molar VLP/mRNA ratios 1:0.23 (1), 1:0.34 (2), 1:0.45 (3), 1:0.91 (4), 1:1.81 (5), and empty yeast wt HBc VLPs (6) and DTA mRNA (7) as controls. (**c**) Sucrose gradient centrifugation of DTA mRNA-packaged yeast-produced empty wt HBc VLPs with NAGE analysis of fractions (Coomassie (top) and ethidium bromide (bottom) staining) and formaldehyde agarose gel electrophoresis (FAGE) of pooled VLP fractions 6-8 before (1) and after (2) phenol treatment, DTA mRNA (3) and RNA ladder (4) as controls. (**d**) Fate of DTA mRNA within the packaged bacteria- and yeast-produced wt HBc as well as HBc-K75 VLPs by FAGE analysis. Phenol-treated samples of the bacteria- (1–4) and yeast- (6–9) produced empty wt HBc VLPs contacted with DTA mRNA at VLP versus mRNA molar ratio 1:0.85 (2 and 7), empty wt HBc VLPs saturated with DTA mRNA and purified by CsCl centrifugation (3 and 8), the same with the addition of 0.85 molar proportion of non-packaged DTA mRNA (4 and 9); empty wt HBc VLPs (1 and 6) and DTA mRNA (5), as well as phenol non-treated RNA ladder (10) and DTA mRNA (11) were taken as controls.

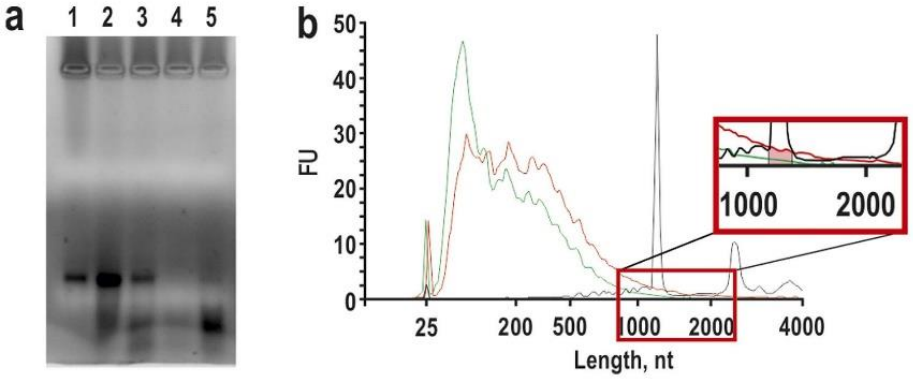

Figure 6. Length distribution of HBc VLP-encapsidated DTA mRNA with the BioAnalyzer 2100. (**a**) DTA mRNA after purification through the oligo-dT cellulose column before (1) and after (2) phenol/chloroform purification (lane (2) has two-fold more mRNA than lane (1)); extracted content from contact packaging experiments of DTA mRNA and bacteria-produced HBc VLPs (3) or empty bacteria-produced HBc VLPs (4) (in molar ratios 1:2); lane (5) shows extracted content from contact incubation of bacteria-produced HBc VLPs with DTA mRNA, that purified through a Sepharose CL-2B column chromatography where fraction containing non-aggregated VLPs and lacking free RNA were taken. (**b**) mRNA before packaging (black) and after extraction from bacteria- (red) or yeast- (green) produced wt HBc VLPs.

DNA structures used for the DNA encapsidation studies see Supplementary Table S2 online) by different empty HBc VLPs occurred with similar efficacy either via VLP restoration after 7 M urea treatment or via direct contact of empty VLPs with DNA samples.

First, VLP titration by short 20 nt single-stranded CpG ODNs (see Supplementary Fig. S16 online) or triplicate (63 nt) CpG ODNs (Fig. 7a) was performed. High ODN excess over HBc VLPs led to the optimal encapsidation of both ODN forms. Technical documentation of the ODN63 encapsidation process by bacteria- and yeast-produced wt HBc VLPs is presented in Table S3 (see Supplement online). Overall, empty bacteria-produced wt HBc VLPs demonstrated a higher capacity of packaging than the empty yeast-produced wt HBc VLPs. The complexes of HBc VLPs and ODNs retained their stability during NAGE and sucrose and CsCl density centrifugation (see Supplementary Fig. S17 online).

The second round of the encapsidation experiments included contacting of empty VLPs with long circular or linearised plasmids or plasmids restricted by rarely-cleaving restriction enzymes producing, for example, fragments of 7871 and 12268 bp (base pairs) in length. These encapsidations were performed in high excess of HBc VLPs (up to 50-fold molar excess over DNA) and resulted in the formation of complexes remaining in the start pockets of NAGE; such complexes were stable during CsCl density gradient centrifugation (see Fig. 8 and Supplementary Table S4 online) and size exclusion column chromatography (see Supplementary Fig. S18 online).

More details on the structure of the involved plasmids and the stability of the HBc VLP-DNA complexes are presented in the Supplement (see Supplementary Fig. S19 and Fig. S20 online). DLS measurements revealed marked VLP aggregation as demonstrated by the intensity analysis mode when compared with the volume mode (Fig. 8d). EM analysis demonstrated the presence of VLP chains (Fig. 8e) that may have been the result of VLP attachment to long DNA molecules. Plasmids and large DNA fragments in such complexes were protected by HBc VLPs against DNase cleavage (Fig. 8a,c).

The third round of the encapsidation experiments was performed with individual DNA fragments of different lengths at approximately equimolar ratios of VLPs to DNA. For example, titration performed with different amounts of VLPs by a relatively short DNA fragment of 601 bp showed that the fragment is packaged into individual particles and not to VLP chains (see Supplementary Fig. S16 online). Next, the maximal size of the packaged DNA fragment that after proper packaging was protected against DNase cleavage was established. Phenol elution of HBc VLP-packaged DNA after DNase treatment of HBc VLP-DNA complexes showed that DNA fragments of 1047 bp (see Supplementary Fig. S21 online) and 1289 bp (Figs 7b–d) were protected; however, 1811 bp (see Supplementary Fig. S21 online) and 1737 bp (Figs 7b–d) fragments were not protected against DNase cleavage. Therefore, the border of the HBc VLP encapsidation-allowed length of double-stranded DNA fragments is located between 1289 and 1737 bp. The quality of the HBc VLPs carrying a 1047 bp DNA fragment after DNase treatment was assessed by DLS measurements (see Supplementary Fig. S22 online). HBc VLPs carrying a 1289 bp DNA fragment after DNase treatment showed intact particles by EM (Fig. 7d).

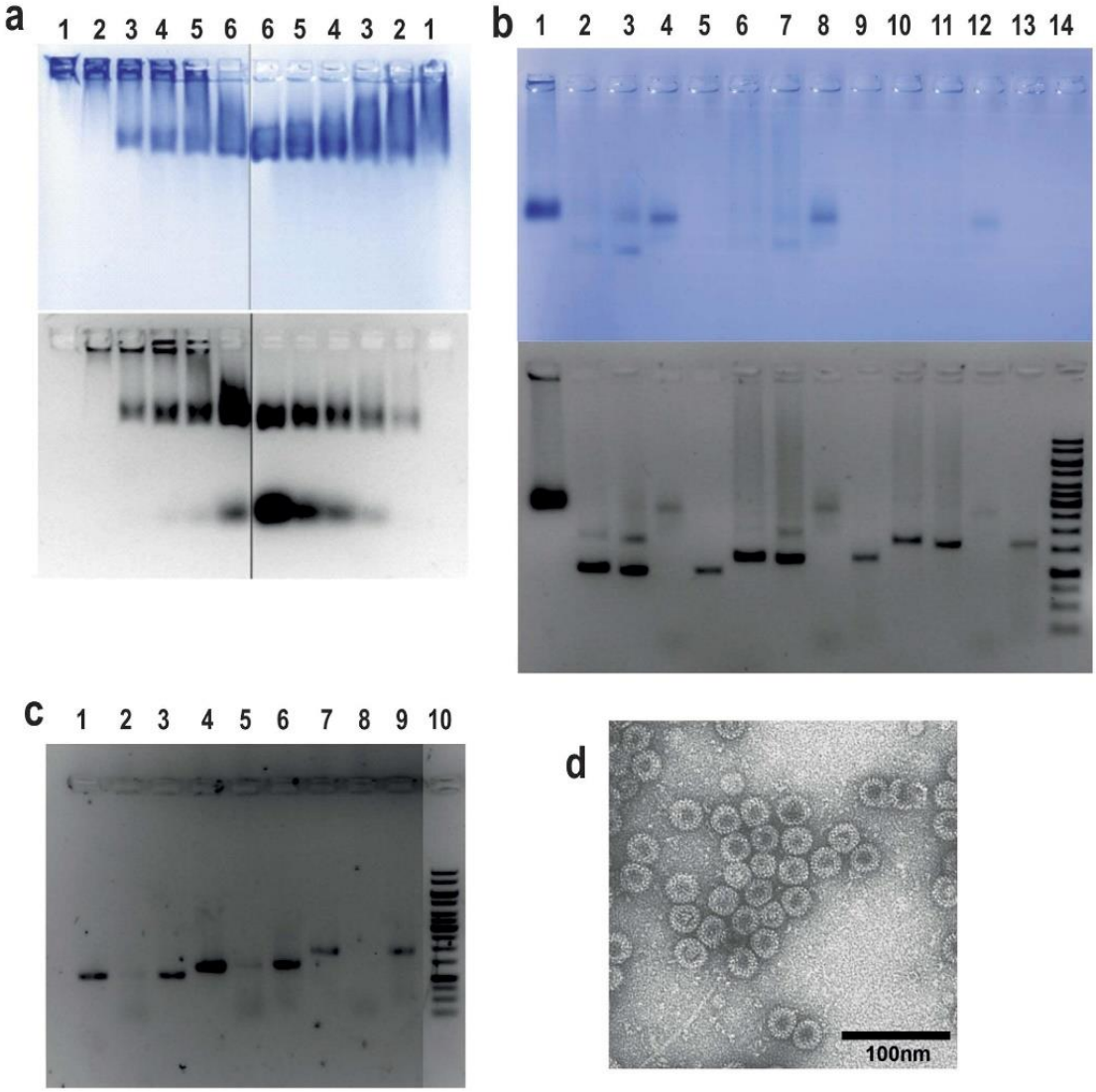

Figure 7. Packaging of bacteria- and yeast-produced wt HBc VLPs by a DNA fragment and two CpG ODNs. (**a**) Contact titration of bacteria-produced (left part) and yeast-produced (right part) wt HBc VLPs by ODN63 at appropriate VLP molar superiority over ODN: 10 (2), 20 (3), 30 (4), 40 (5), 50 (6) and the appropriate empty HBc VLPs as a control (1). (**b**) NAGE analysis of restoration of bacteria-produced wt HBc VLPs by DNA fragments of 1047, 1289, and 1737 bp in length. Coomassie- (top) and ethidium bromide- (bottom) stained gels of the restored encapsidated HBc VLPs (all purified by CsCl density gradient centrifugation) at the fragment to HBc VLP molar ratio 1:1.5 in the case of the fragments 1047 bp (2–5), 1289 bp (6–9), and 1737 (10–12) bp where samples (2,6,10) are in a restoration buffer, (3,7,11) are in DNase buffer, and (4,8,12) are samples in DNAse buffer and treated by DNase before phenol extraction; controls: 100 bp Plus DNA ladder (1), the respective DNA fragments (5,9,13), initial alkaline non-treated bacteria-produced wt HBc VLPs (14). (**c**) Ethidium bromide-stained NAGE of phenol-extracted content of the restored HBc VLPs carrying fragments 1047 (1–3), 1289 (4–6), and 1737 (7–9) bp where the encapsidated VLPs were not treated (1,4,7) or treated with DNase (2,5,8) before phenol extraction; controls: the respective DNA fragments (3,6,9), 1 kb ladder (10). (**d**) EM of bacteria-produced wt HBc VLPs restored with 1289 bp DNA fragment and treated with DNAse.

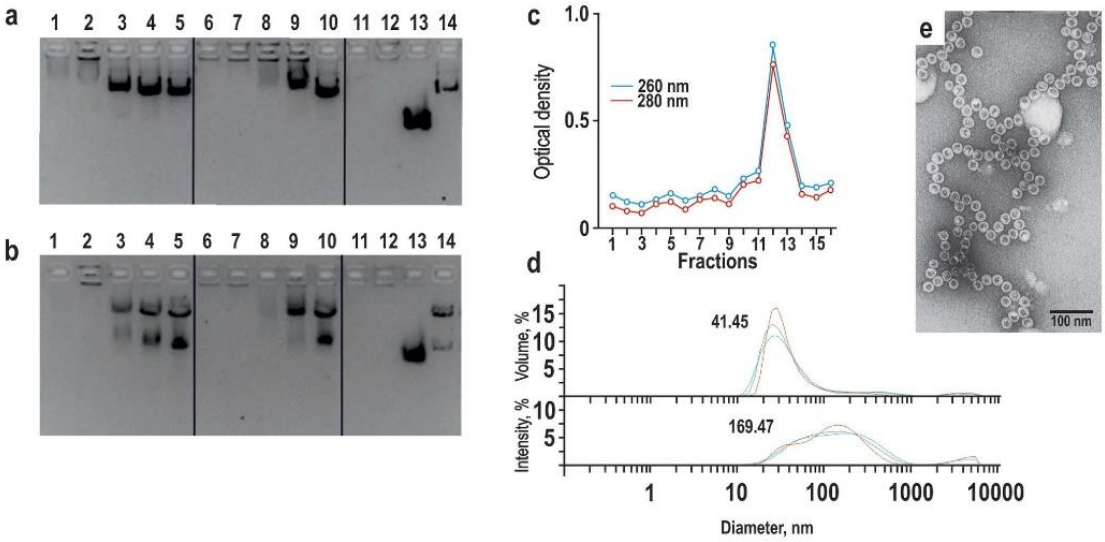

Figure 8. NAGE analysis of contact encapsidation of the pCEP-CXCR4-eGFP plasmid by empty bacteria- and yeast-produced HBc VLPs. (**a**) Titration of yeast-produced (1–5) and bacteria-produced (6–10) HBc VLPs (148 pmol) by varying pCEP-CXCR4-eGFP amounts: 52 pmol (1), 26 pmol (2), 13 pmol (3), 7 pmol (4), 3 pmol (5) with ratios indicated in Table S4 (see Supplementary online). Controls: empty yeast-produced HBc VLPs (11), empty bacteria-produced wt HBc VLPs (12), initial bacteria-produced alkali non-treated HBc VLPs (13), pCEP-CXCR4-eGFP plasmid (14). (**b**) Titration of yeast-produced (1–5) and bacteria-produced (6–10) HBc VLPs (74 pmol) by varying amounts of the plasmid pCEP-CXCR4-eGFP SalI fragments: 52 pmol (1), 26 pmol (2), 13 pmol (3), 7 pmol (4), 3 pmol (5) with the same ratios as indicated in Table S4 (see Supplementary online) for pCEP-CXCR4-eGFP plasmid. Controls: empty yeast-produced HBc VLPs (11), empty bacteria-produced wt HBc VLPs (12), initial bacteria-produced alkali non-treated HBc VLPs (13), pCEP-CXCR4-eGFP plasmid cleaved by SalI (14). (**c**) Yeast-produced wt HBc VLPs restored by pCEP-CXCR4-eGFP plasmid in 53-fold molar ratio of VLP versus plasmid CsCl density gradient centrifugation. (**d**) DLS of the complex of bacteria-produced empty HBc VLPs restored by 10-fold molar excess of VLPs over pCEP-CXCR4-eGFP plasmid after CsCl density gradient centrifugation, presented by volume (top) or intensity (bottom) measurements. (**e**) Electron micrograph of the complex formed by contact of empty yeast-produced wt HBc VLPs and pCEP-CXCR4-eGFP plasmid (ratio 53:1) after Sepharose CL-2B gel chromatography.

Discussion

HBc particles are complicated multifunctional nanodevices that perform numerous functions in strict order during HBV replication, such as successive dissociation/re-association[40] and phosphorylation/dephosphorylation[41–45]. These processes are necessary for nuclear targeting and entry, pregenomic mRNA encapsidation, dsDNA synthesis, nucleocapsid maturation, envelopment, and budding and release (for review see[1,46,47]).

Due to the highly efficient expression of HBc and its chimeric derivatives in *E. coli* (for review see[18–20]), HBc remains a widely used VLP carrier for the generation of putative vaccines over the past 28 years[48,49]. In addition to traditional vaccine applications, chimeric HBc VLPs have been suggested as candidate tools for specific cell targeting[50]. In addition to classical methods to expose foreign aa stretches to HBc spikes, various advanced approaches, such as SplitCore[51,52], nano-glue[53], and metalloporphyrin complexes on hexahistidine tags, have been recently elaborated[54].

HBc applications are connected with its ability to recognise HBV nucleic acids, in which HBc phosphorylation is necessary and sufficient for pregenomic RNA encapsidation[55] and HBc dephosphorylation enables genomic dsDNA synthesis[56] and triggers maturation (i.e., envelopment and secretion)[44,57]. Mature DNA-containing HBc particles demonstrate significant differences in structure versus immature RNA-containing particles[58]. DNA appears as a poor substrate for encapsidation; therefore, dsDNA-filled HBc particles are spring-loaded[59]. Moreover, a significant portion of the CTD is exposed at the surface of the immature RNA-containing HBc particles, whereas the CTD is mostly confined within mature DNA-containing HBc particles[26].

Recombinant HBc particles purified from *E. coli* cells contain heterologous RNA in amounts comparable with the pregenomic HBV mRNA content[35,59,60]. In accordance with our results, yeast-produced

HBc VLPs reveal packaging of approximately 3000–3200 nt. The bacteria-produced HBc VLPs demonstrate a higher level of packaging by at least 300 nt, which appears to correlate with at least 240 phosphogroups on the inner HBc VLP surface as a result of HBc protein phosphorylation in yeast[13].

Traditional attempts to prepare full-length HBc particles for *in vitro* packaging by desired molecules are based on the following two approaches: (i) non-dissociating osmotic shock[61] and (ii) full HBc dissociation after micrococcal nuclease[34] or guanidine chloride[35] treatment. Interestingly, incorporated RNA can be removed by a nuclease, which is covalently added to the HBc protein and displayed on the inner surface of HBc VLPs[62]. Regarding practical packaging of functionally important material, only successful encapsidation of short ISS CpG ODNs has been previously achieved[31,32,63,64].

Here, we propose a technological solution that combines both epitope exposure and nucleic acid packaging approaches, which promotes versatile HBc VLP applications in vaccinology and gene therapy. First, surface-exposed lysine residues that are applicable for chemical coupling of foreign peptides or oligonucleotides were introduced on the protruding HBc spikes. Natural HBc molecules harbour only two lysine residues at positions 7 and 96 that are positioned on the external VLP surface at the base of the HBc spikes. Therefore, the CTD positive charge is ensured by the arginine, while the lysine residues play a specific role in HBc ubiquitination[65]. Although lysine never appears at the selected positions in naturally mutated HBc variants[6,17], the incorporation of lysine residues at the fully conserved positions 75 and 79 and minimally variable positions 77 and 80 (Fig. 1) does not prevent self-assembly. Second, we performed exhaustive purification and standardisation conditions of bacteria- and yeast-produced HBc VLPs by full deprivation of contaminating encapsidated RNAs during simple, rapid, and highly efficacious alkaline treatment at pH 12. This method also efficiently purified four HBc variants carrying lysine residues on the tips of the HBc spikes. Recently, efficiency of the alkaline treatment was demonstrated for purification of RNA phage PP7 VLPs carrying human papillomavirus epitopes[66].

The obtained empty particles encapsidated both RNA and DNA by the following two alternate approaches: (i) the restoration of HBc VLPs after 7 M urea treatment and (ii) direct contact of nucleic acids with empty HBc VLPs. Notably, the encapsidation of bacterial rRNA and specific DTA mRNA was accompanied by the cleavage of the packaged RNA, and the excessive unpackaged RNA remained stable. This phenomenon suggests that HBc, itself, may possess ribonucleolytic activity that prevents the encapsidation of unspecific RNAs *in vivo*. Nucleoproteins, structural analogues of the HBc protein, possess exoribonuclease activity in the case of Lassa and Tacaribe viruses belonging to arenaviruses[67,68] and endodeoxyribonuclease activity in the case of Crimean-Congo haemorrhagic fever virus belonging to bunyaviruses[69].

The HBc VLPs may protect the long double-stranded DNAs that exceed the length of the HBV genome from DNase attack by forming VLP chains that cover the DNA. This protection is mediated by a strong excess of HBc VLPs compared with the DNA. When the VLP to DNA ratio is approximately equimolar, HBc VLPs package DNA fragments of approximately 1200 bp in length. The most efficient packaging was achieved for single-stranded CpG ODNs during the strong ODN excess compared with HBc VLPs.

Comparing bacteria- and yeast-produced HBc particles, no significant difference was observed in their ability to reassemble and package desired RNAs or DNAs. Both HBc particle products are technologically equal in semi-preparative propagation and purification trials. However, the encapsidation capacity of the bacteria-produced HBc VLPs is always higher (Fig. 7a) than that of the yeast-produced HBc VLPs, which is in full accordance with the above-mentioned differences in the initial RNA content of both purified particles and is connected with the phosphorylated status of yeast-produced HBc VLPs[13].

Unusually high packaging capacity of HBc particles can be explained by their extended inner space due to the absence of bulky HBV-related proteins, such as the viral polymerase. Highly efficient and technologically sound packaging ranks the HBc carrier with other VLP candidates used for nucleic acid packaging, such as polyoma and papilloma viruses, RNA phages, and cowpea chlorotic mottle virus (for references see[20]).

Strong advantages of utilising the HBc carrier consist of the capacity to employ the proposed packaging technology in combination with traditional approaches to construct chimeric HBc VLPs as vaccines and/or cell targeting tools because HBc protein is one of the most studied VLP models (for review, see[18–20]). Furthermore, HBc particles possess a highly specific nuclear targeting ability, which may allow for the highly specific delivery of packaged DNA to the cell nucleus (for review, see[1]). Finally, initial HBc VLPs, without any added ligands, are naturally targeted to B lymphocytes because the latter function as antigen-presenting cells (APCs) both in murine[70] and human[71,72] B cells. Employing B cells as APCs for HBc protein explains its enhanced immunogenicity in mice and humans and the contribution of the HBc antigen in the induction and/or maintenance of chronic HBV infection[70].

In summary, the proposed versatile approach is beneficial for vaccine production by exposing foreign epitopes through the chemical coupling of the integrated lysine residues, by the efficient packaging of CpG ODNs and by the potential immunostimulation of ribonucleic acids. Furthermore, this method also promises gene therapy applications by exposing cell targeting peptides and/or oligonucleotides and by the efficient packaging of relatively long DNA fragments.

Methods

Bacterial strains. *Escherichia coli* strain RR1 [F^-_ r_B^- m_B^- *leuB6 proA2 thi-1 araC14 lacY1 galK2 xyl-5 mtl-1 rpsL20* (Str^r) *glnV44*_Δ(*mcrC-mrr*)] was used for cloning purposes. *E. coli* strain K802

($F^- r_K^- m_K^+$ *e14 McrA metB1lac Y1 [or lacI-Y6] galK2 galT22 glnV44 mcrB*) was used for the transformation of the plasmids expressing recombinant HBc proteins.

Plasmid construction for HBc VLP expression. The lysine-exposing variants of HBc protein were constructed by standard mutagenesis procedures using the pHBc183 plasmid expressing HBc gene with codons optimised for synthesis in *E. coli*[60]. Four mutant plasmids were constructed: pHBc-K75 with primers pINC-312 (5′-GCTACCTGGGTGGGTGGTAAATTGGAAGATCCAATATC-3′) and pINC-313 (5′-GATATTGGATCTTCCAATTTACCACCCACCCAGGTAGC-3′); pHBc-K77 with primers pINC-314 (5′-GCTACCTGGGTGGGTGGTAATTTGAAGGATCCAATATC-3′) and pINC-315 (5′-GATATTG GATCCTTCAAATTACCACCCACCCAGGTAGC-3′); pHBc-79K with primers pINC-572 (5′-GGTAA TTTGGAAGATAAAATATCCAGGGACCTAGT-3′) and pINC-573 (5′-ACTAGGTCCCTGGATATTTT ATCTTCCAAATTACC-3′); and pHBc-80K with primers pINC-574 (5′-GGTAATTTGGAAGATCCAA AATCCAGGGACCTAGTAGT-3′) and pINC-575 (5′-ACTACTAGGTCCCTGGATTTTGGATCTTC CAAATTACC-3′).

HBc VLP production. Regarding *E. coli*, after cell transformation with the appropriate plasmids, 5 ml of LB liquid medium supplemented with 20 μg/ml ampicillin was inoculated with a single colony and incubated at 37 °C for 16–24 h without shaking. The prepared inoculum was diluted 50-fold with 2xTY medium containing 20 μg/ml ampicillin and supplemented with 2 g glucose, 3.47 g KH_2PO_4, 18.8 g K_2HPO_4 per litre and incubated at 37 °C overnight on a shaker (200 rpm). The cells were harvested by centrifugation. Regarding *P. pastoris*, HBc VLP expression and purification were performed according to the protocol described in[13].

Deprivation of HBc particles from encapsidated RNA by alkaline treatment. To prepare the HBc VLPs for alkaline treatment, the purified particles were solubilised in 7 M urea, placed onto a Sephacryl S300 column (1.4 × 55 cm) and chromatographed by elution with 0.1 M Na_2CO_3, 2 mM DTT solution at a velocity of 2 ml/h (30 min/1 ml fraction). Pure fractions (see Supplementary Fig. S1 online) were transferred to a dialysis tubing cellulose membrane (Sigma Aldrich) and dialysed intensively against 100 ml of an "alkaline" solution (0.1 M Na_2HPO_4 / Na_3PO_4, 0.65 M NaCl, pH 12 (NaOH)) at 37 °C for 18 h. Then, the "alkaline" solution was exchanged for a restoration buffer (0.1 M Na_2HPO_4, 0.65 M NaCl, pH 7.8 (H_3PO_4)), and the material was dialysed at room temperature for 1 h and then placed at 4 °C for 3–4 h. The content of the tube was precipitated with ammonium sulphate (till 50% saturation), and the sedimented VLPs were dissolved in working buffer (20 mM Tris-HCl, 5 mM EDTA, 0.65 M NaCl, pH 7.8) and fractionated on a Sepharose CL-4B (Sigma Aldrich) column. Specifically, yeast-produced wt HBc and HBc-K80 VLPs were placed onto a larger column (1.4 × 70 cm) at a velocity 2 ml/h (90 min/3 ml fraction), and the bacteria-produced wt HBc and HBc-K75 VLPs were placed onto a smaller column (1 × 40 cm) at a velocity 2 ml/h (60 min/2 ml fraction).

Detection of protein and nucleic acids. All optical density measurements were performed using WPA BioWave S2100 (Biochrom Ltd., UK), SmartSpec™ Plus (BioRad) and Nanodrop ND-1000 (Thermo Scientific, USA) spectrophotometers. The amount of protein (in the presence of nucleic acids) was estimated according to[73]. To calculate that one optical absorbance unit of empty VLPs corresponds to 0.71 mg of HBc protein, the Vector NTI 10.0.1 (Invitrogen) software package was used.

VLP analysis. The VLP preparations were analysed with respect to the presence of protein and nucleic acids using native agarose gel electrophoresis (NAGE). For NAGE, 0.7% TopVision LE GQ Agarose (Fermentas) in TAE buffer (40 mM Tris, 20 mM acetic acid, 1 mM EDTA) supplemented with 1 μg/ml ethidium bromide was used with subsequent Coomassie Blue R-250 (60 μg/ml of Coomassie Blue R-250 in 10% acetic acid) staining of the gels. The following buffers were used to create the different pH conditions: 0.1 M sodium acetate/acetic acid at pH 5.3; 0.1 M K_2PO_4/NaOH at pH 6.5 and pH 7.5; TAE buffer at pH 8.3; and 0.025 M $Na_2B_4O_7 \times 10H_2O$/HCl at pH 9.0 (according[74]).

Protein samples were analysed on 15% SDS-PAGE gels in a Tris-glycine-SDS system with subsequent Coomassie or silver staining according to standard procedures (LKB Laboratory Manual).

RNA analysis was performed using formaldehyde agarose gel electrophoresis (FAGE) and also on a 2100 Bioanalyser (Agilent Technologies) with the RNA Analysis Kit. To determine the RNA size and to enable comparisons between the different RNA samples, internal markers were used.

Electron microscopy and dynamic light scattering analysis. For electron microscopy, VLPs in suspension were adsorbed to carbon-formvar coated copper grids and negatively stained with a 1% uranyl acetate aqueous solution. The grids were examined with a JEM-1230 electron microscope (Jeol Ltd., Tokyo, Japan) at 100 kV.

The size of the particles was detected by dynamic light scattering (DLS) in a Zetasizer Nano ZS (Malvern Instruments Ltd, UK) instrument. Histograms based on the intensity and volume parameters were drawn and statistics were calculated from data files using the software provided with apparatus.

VLP packaging. Contact packaging was conducted by mixing empty HBc particles with nucleic acid material in working buffer (PBS is also suitable) and placing the mixture at ambient temperature for 10–15 min. The reconstruction reaction for plasmids and long DNA fragment packaging in empty HBc VLPs was conducted by dialysing the desired mixture against 7 M urea + 1 M NaCl at 4 °C for one hour. Next, dialysis against the restoration buffer was performed for one hour and then a fresh portion of restoration buffer was added and dialysed overnight.

CsCl density gradient. The empty core and DNA plasmid or DNA fragment complexes were purified on a preformed CsCl gradient. The gradient consisted of two 6 ml layers in a 12 ml polyallomer tube. The bottom layer was taken from ready solution (44 g CsCl + 60 ml working buffer), and the upper layer consisted of protein to purify, 2.2 g of CsCl and working buffer. After centrifugation in a Beckman Coulter Optima L-100XP ultracentrifuge (rotor SW32 Ti) at 20 500 rpm for 13 h at 4 °C, the tube was pierced, and 0.5 ml fractions were collected. After OD measurements and fraction NAGE, the fractions were dialysed, concentrated in a dialysis tube using dry Sephadex G-100 (GE Healthcare Life Sciences) or directly used for further experiments.

Sucrose density gradient. RNA or DNA complexes with VLPs were loaded onto a pre-formed 5–36% sucrose gradient in Polyallomer 14 × 95 mm (12 ml) tubes (following sucrose concentrations (w/v) of the layers: 36% - 1 ml; 30% - 1 ml; 25% - 2 ml; 20% - 2.7 ml; 15% - 2 ml; 10% - 2 ml; 5% - 1 ml) for centrifugation in a Beckman Coulter Optima L-100XP ultracentrifuge (rotor SW32 Ti) at 20,500 rpm for 13 h at 4 °C. Next, 0.5-ml fractions were collected from the pierced bottom of the tube.

References

1. Kann, M. & Gerlich, W. H. Replication of hepatitis B virus in *Molecular Medicine of Viral Hepatitis* (eds T. J. Harrison & A. J. Zuckerman), 63–87 (John Wiley & Sons, 1997).
2. Gerlich, W. H., Goldmann, U., Muller, R., Stibbe, W. & Wolff, W. Specificity and localization of the hepatitis B virus-associated protein kinase. *J Virol* **42,** 761–766 (1982).
3. Zhou, S. & Standring, D. N. Hepatitis B virus capsid particles are assembled from core-protein dimer precursors. *Proc Natl Acad Sci USA* **89,** 10046–10050 (1992).
4. Cohen, B. J. & Richmond, J. E. Electron microscopy of hepatitis B core antigen synthesized in *E. coli*. *Nature* **296,** 677–679 (1982).
5. Packianathan, C., Katen, S. P., Dann, C. E., 3rd & Zlotnick, A. Conformational changes in the hepatitis B virus core protein are consistent with a role for allostery in virus assembly. *J Virol* **84,** 1607–1615 doi: 10.1128/JVI.02033-09 (2010).
6. Pumpens, P. & Grens, E. HBV core particles as a carrier for B cell/T cell epitopes. *Intervirology* **44,** 98–114 doi: 50037 (2001).
7. Crowther, R. A. *et al.* Three-dimensional structure of hepatitis B virus core particles determined by electron cryomicroscopy. *Cell* **77,** 943–950 (1994).
8. Roseman, A. M. *et al.* Structures of hepatitis B virus cores presenting a model epitope and their complexes with antibodies. *J Mol Biol* **423,** 63–78 doi: 10.1016/j.jmb.2012.06.032 (2012).
9. Wynne, S. A., Crowther, R. A. & Leslie, A. G. The crystal structure of the human hepatitis B virus capsid. *Mol Cell* **3,** 771–780 (1999).
10. Kniskern, P. J. *et al.* Unusually high-level expression of a foreign gene (hepatitis B virus core antigen) in *Saccharomyces cerevisiae*. *Gene* **46,** 135–141 (1986).
11. Miyanohara, A. *et al.* Expression of hepatitis B virus core antigen gene in *Saccharomyces cerevisiae*: synthesis of two polypeptides translated from different initiation codons. *J Virol* **59,** 176–180 (1986).
12. Rolland, D. *et al.* Purification of recombinant HBc antigen expressed in *Escherichia coli* and *Pichia pastoris*: comparison of size-exclusion chromatography and ultracentrifugation. *J Chromatogr B Biomed Sci Appl* **753,** 51–65 (2001).
13. Freivalds, J. *et al.* Highly efficient production of phosphorylated hepatitis B core particles in yeast *Pichia pastoris*. *Protein Expr Purif* **75,** 218–224 doi: 10.1016/j.pep.2010.09.010 (2011).
14. Birnbaum, F. & Nassal, M. Hepatitis B virus nucleocapsid assembly: primary structure requirements in the core protein. *J Virol* **64,** 3319–3330 (1990).
15. Seifer, M. & Standring, D. N. A protease-sensitive hinge linking the two domains of the hepatitis B virus core protein is exposed on the viral capsid surface. *J Virol* **68,** 5548–5555 (1994).
16. Watts, N. R. *et al.* The morphogenic linker peptide of HBV capsid protein forms a mobile array on the interior surface. *EMBO J* **21,** 876–884 doi: 10.1093/emboj/21.5.876 (2002).
17. Chain, B. M. & Myers, R. Variability and conservation in hepatitis B virus core protein. *BMC Microbiol* **5,** 33 doi: 10.1186/1471-2180-5-33 (2005).
18. Pumpens, P. *et al.* Construction of novel vaccines on the basis of the virus-like particles: Hepatitis B virus proteins as vaccine carriers in *Medicinal* Protein Engineering (ed. Y. Khudyakov), 205–248 (CRC Press, Taylor & Francis Group, 2008).
19. Whitacre, D. C., Lee, B. O. & Milich, D. R. Use of hepadnavirus core proteins as vaccine platforms. *Expert Rev Vaccines* **8,** 1565–1573 doi: 10.1586/erv.09.121 (2009).
20. Pushko, P., Pumpens, P. & Grens, E. Development of virus-like particle technology from small highly symmetric to large complex virus-like particle structures. *Intervirology* **56,** 141–165 doi: 10.1159/000346773 (2013).
21. Nassal, M. The arginine-rich domain of the hepatitis B virus core protein is required for pregenome encapsidation and productive viral positive-strand DNA synthesis but not for virus assembly. *J Virol* **66,** 4107–4116 (1992).
22. Hatton, T., Zhou, S. & Standring, D. N. RNA- and DNA-binding activities in hepatitis B virus capsid protein: a model for their roles in viral replication. *J Virol* **66,** 5232–5241 (1992).
23. Machida, A. *et al.* Antigenic sites on the arginine-rich carboxyl-terminal domain of the capsid protein of hepatitis B virus distinct from hepatitis B core or e antigen. *Mol Immunol* **26,** 413–421 (1989).
24. Bundule, M. A. *et al.* [C-terminal polyarginine tract of hepatitis B core antigen is located on the outer capsid surface]. *Dokl Akad Nauk SSSR* **312,** 993–996 (1990).
25. Vanlandschoot, P., Van Houtte, F., Serruys, B. & Leroux-Roels, G. The arginine-rich carboxy-terminal domain of the hepatitis B virus core protein mediates attachment of nucleocapsids to cell-surface-expressed heparan sulfate. *J Gen Virol* **86,** 75–84 doi: 10.1099/vir.0.80580-0 (2005).
26. Meng, D., Hjelm, R. P., Hu, J. & Wu, J. A theoretical model for the dynamic structure of hepatitis B nucleocapsid. *Biophys J* **101,** 2476–2484 doi: 10.1016/j.bpj.2011.10.002 (2011).

27. Borisova, G. P. *et al.* Genetically engineered mutants of the core antigen of the human hepatitis B virus preserving the ability for native self-assembly. *Dokl Akad Nauk SSSR* **298,** 1474–1478 (1988).
28. Gallina, A. *et al.* A recombinant hepatitis B core antigen polypeptide with the protamine-like domain deleted self-assembles into capsid particles but fails to bind nucleic acids. *J Virol* **63,** 4645–4652 (1989).
29. Dhason, M. S., Wang, J. C., Hagan, M. F. & Zlotnick, A. Differential assembly of Hepatitis B Virus core protein on single- and double-stranded nucleic acid suggest the dsDNA-filled core is spring-loaded. *Virology* **430** 20–29 doi: 10.1016/j.virol.2012.04.012 (2012).
30. Shlomai, A., Lubelsky, Y., Har-Noy, O. & Shaul, Y. The "Trojan horse" model-delivery of anti-HBV small interfering RNAs by a recombinant HBV vector. *Biochem Biophys Res Commun* **390,** 619–623 doi: 10.1016/j.bbrc.2009.10.016 (2009).
31. Storni, T. *et al.* Nonmethylated CG motifs packaged into virus-like particles induce protective cytotoxic T cell responses in the absence of systemic side effects. *J Immunol* **172,** 1777–1785 (2004).
32. Kazaks, A., Balmaks, R., Voronkova, T., Ose, V. & Pumpens, P. Melanoma vaccine candidates from chimeric hepatitis B core virus-like particles carrying a tumor-associated MAGE-3 epitope. *Biotechnol J* **3,** 1429–1436 doi: 10.1002/biot.200800160 (2008).
33. Cooper, A. & Shaul, Y. Recombinant viral capsids as an efficient vehicle of oligonucleotide delivery into cells. *Biochem Biophys Res Commun* **327,** 1094–1099 doi: 10.1016/j.bbrc.2004.12.118 (2005).
34. Newman, M., Chua, P. K., Tang, F. M., Su, P. Y. & Shih, C. Testing an electrostatic interaction hypothesis of hepatitis B virus capsid stability by using an *in vitro* capsid disassembly/reassembly system. *J Virol* **83,** 10616–10626 doi: 10.1128/JVI.00749-09 (2009).
35. Porterfield, J. Z. *et al.* Full-length hepatitis B virus core protein packages viral and heterologous RNA with similarly high levels of cooperativity. *J Virol* **84,** 7174–7184 doi: 10.1128/JVI.00586-10 (2010).
36. Renhofa, R., Dishlers, A., Ose-Klinklava, V., Ozols, J. & Pumpens, P., inventors. Latvian Biomedical Research and Study Centre, assignee. Packaging of magnetic nanoparticles into HBV core protein-formed capsids. Latvia patent. LV 14304 B. 20 May 2011.
37. Renhofa, R. *et al.* inventors. Latvian Biomedical Research and Study Centre, assignee. Modificēti HBV *core* nanokonteineri kā universāla platforma bioloģiskā materiāla eksponēšanai. Latvia patent application. P-14-06. 13 Jan 2014.
38. Renhofa, R. *et al.* inventors. Latvian Biomedical Research and Study Centre, assignee. Paņēmiens izvēlēta materiāla piešūšanai HBV core proteīna veidotajām nanodaļiņām. Latvia patent application. P-14-05. 13 Jan 2014.
39. Pushko, P. *et al.* Identification of hepatitis B virus core protein regions exposed or internalized at the surface of HBcAg particles by scanning with monoclonal antibodies. *Virology* **202,** 912–920 doi: 10.1006/viro.1994.1413 (1994).
40. Rabe, B. *et al.* Nuclear entry of hepatitis B virus capsids involves disintegration to protein dimers followed by nuclear reassociation to capsids. *PLoS Pathog* **5,** e1000563 doi: 10.1371/journal.ppat.1000563 (2009).
41. Machida, A. *et al.* Phosphorylation in the carboxyl-terminal domain of the capsid protein of hepatitis B virus: evaluation with a monoclonal antibody. *J Virol* **65,** 6024–6030 (1991).
42. Lan, Y. T., Li, J., Liao, W. & Ou, J. Roles of the three major phosphorylation sites of hepatitis B virus core protein in viral replication. *Virology* **259,** 342–348 doi: 10.1006/viro.1999.9798 (1999).
43. Le Pogam, S., Chua, P. K., Newman, M. & Shih, C. Exposure of RNA templates and encapsidation of spliced viral RNA are influenced by the arginine-rich domain of human hepatitis B virus core antigen (HBcAg 165-173). *J Virol* **79,** 1871–1887 doi: 10.1128/JVI.79.3.1871-1887.2005 (2005).
44. Perlman, D. H., Berg, E. A., O'Connor, P. B., Costello, C. E. & Hu, J. Reverse transcription-associated dephosphorylation of hepadnavirus nucleocapsids. *Proc Natl Acad Sci USA* **102,** 9020–9025 doi: 10.1073/pnas.0502138102 (2005).
45. Lewellyn, E. B. & Loeb, D. D. Serine phosphoacceptor sites within the core protein of hepatitis B virus contribute to genome replication pleiotropically. *PLoS One* **6,** e17202 doi: 10.1371/journal.pone.0017202 (2011).
46. Moses, S. E., Lim, Z. & Zuckerman, M. A. Hepatitis B virus infection: pathogenesis, reactivation and management in hematopoietic stem cell transplant recipients. *Expert Rev Anti Infect Ther* **9,** 891–899 doi: 10.1586/eri.11.105 (2011).
47. Schadler, S. & Hildt, E. HBV life cycle: entry and morphogenesis. *Viruses* **1,** 185–209 doi: 10.3390/v1020185 (2009).
48. Clarke, B. E. *et al.* Improved immunogenicity of a peptide epitope after fusion to hepatitis B core protein. *Nature* **330,** 381–384 doi: 10.1038/330381a0 (1987).
49. Borisova, G. *et al.* Recombinant capsid structures for exposure of protein antigenic epitopes. *Mol Gen. (Life Sci Adv)* **6,** 169–174 (1987).
50. Ranka, R. *et al.* Fibronectin-binding nanoparticles for intracellular targeting addressed by B. burgdorferi BBK32 protein fragments. *Nanomedicine* **9,** 65–73 doi: 10.1016/j.nano.2012.05.003 (2013).
51. Walker, A., Skamel, C. & Nassal, M. SplitCore: an exceptionally versatile viral nanoparticle for native whole protein display regardless of 3D structure. *Sci Rep* **1,** 5 doi: 10.1038/srep00005 (2011).
52. Lange, M. *et al.* Hepatitis C virus hypervariable region 1 variants presented on hepatitis B virus capsid-like particles induce cross-neutralizing antibodies. *PLoS One* **9,** e102235 doi: 10.1371/journal.pone.0102235 (2014).
53. Lee, K. W., Tey, B. T., Ho, K. L., Tejo, B. A. & Tan, W. S. Nanoglue: an alternative way to display cell-internalizing peptide at the spikes of hepatitis B virus core nanoparticles for cell-targeting delivery. *Mol Pharm* **9,** 2415–2423 doi: 10.1021/mp200389t (2012).
54. Prasuhn, D. E., Jr. *et al.* Polyvalent display of heme on hepatitis B virus capsid protein through coordination to hexahistidine tags. *Chem Biol* **15,** 513–519 doi: 10.1016/j.chembiol.2008.03.018 (2008).
55. Gazina, E. V., Fielding, J. E., Lin, B. & Anderson, D. A. Core protein phosphorylation modulates pregenomic RNA encapsidation to different extents in human and duck hepatitis B viruses. *J Virol* **74,** 4721–4728 (2000).
56. Basagoudanavar, S. H., Perlman, D. H. & Hu, J. Regulation of hepadnavirus reverse transcription by dynamic nucleocapsid phosphorylation. *J Virol* **81,** 1641–1649 doi: 10.1128/JVI.01671-06 (2007).
57. Mabit, H. & Schaller, H. Intracellular hepadnavirus nucleocapsids are selected for secretion by envelope protein-independent membrane binding. *J Virol* **74,** 11472–11478 (2000).
58. Roseman, A. M., Berriman, J. A., Wynne, S. A., Butler, P. J. & Crowther, R. A. A structural model for maturation of the hepatitis B virus core. *Proc Natl Acad Sci USA* **102,** 15821–15826 doi: 10.1073/pnas.0504874102 (2005).
59. Zlotnick, A. *et al.* Localization of the C terminus of the assembly domain of hepatitis B virus capsid protein: implications for morphogenesis and organization of encapsidated RNA. *Proc Natl Acad Sci USA* **94,** 9556–9561 (1997).
60. Sominskaya, I. *et al.* A VLP library of C-terminally truncated Hepatitis B core proteins: correlation of RNA encapsidation with a Th1/Th2 switch in the immune responses of mice. *PLoS One* **8,** e75938 doi: 10.1371/journal.pone.0075938 (2013).
61. Kann, M. & Gerlich, W. H. Effect of core protein phosphorylation by protein kinase C on encapsidation of RNA within core particles of hepatitis B virus. *J Virol* **68,** 7993–8000 (1994).
62. Beterams, G., Bottcher, B. & Nassal, M. Packaging of up to 240 subunits of a 17 kDa nuclease into the interior of recombinant hepatitis B virus capsids. *FEBS Lett* **481,** 169–176 (2000).
63. Song, S. *et al.* Augmented induction of CD8+ cytotoxic T-cell response and antitumor effect by DCs pulsed with virus-like particles packaging with CpG. *Cancer Lett* **256,** 90–100 doi: 10.1016/j.canlet.2007.06.004 (2007).
64. Song, S. *et al.* Significant anti-tumour activity of adoptively transferred T cells elicited by intratumoral dendritic cell vaccine injection through enhancing the ratio of CD8(+) T cell/regulatory T cells in tumour. *Clin Exp Immunol* **162,** 75–83 doi: 10.1111/j.1365-2249.2010.04226.x (2010).

65. Braun, S. *et al.* Proteasomal degradation of core protein variants from chronic hepatitis B patients. *J Med Virol* **79,** 1312–1321 doi: 10.1002/jmv.20939 (2007).
66. Tumban, E., Peabody, J., Peabody, D. S. & Chackerian, B. A universal virus-like particle-based vaccine for human papillomavirus: longevity of protection and role of endogenous and exogenous adjuvants. *Vaccine* **31,** 4647–4654 doi: 10.1016/j.vaccine.2013.07.052 (2013).
67. Hastie, K. M., Kimberlin, C. R., Zandonatti, M. A., MacRae, I. J. & Saphire, E. O. Structure of the Lassa virus nucleoprotein reveals a dsRNA-specific 3' to 5' exonuclease activity essential for immune suppression. *Proc Natl Acad Sci USA* **108,** 2396–2401 doi: 10.1073/pnas.1016404108 (2011).
68. Jiang, X. *et al.* Structures of arenaviral nucleoproteins with triphosphate dsRNA reveal a unique mechanism of immune suppression. *J Biol Chem* **288,** 16949–16959 doi: 10.1074/jbc.M112.420521 (2013).
69. Guo, Y. *et al.* Crimean-Congo hemorrhagic fever virus nucleoprotein reveals endonuclease activity in bunyaviruses. *Proc Natl Acad Sci USA* **109,** 5046–5051 doi: 10.1073/pnas.1200808109 (2012).
70. Milich, D. R. *et al.* Role of B cells in antigen presentation of the hepatitis B core. *Proc Natl Acad Sci USA* **94,** 14648–14653 (1997).
71. Lazdina, U. *et al.* Molecular basis for the interaction of the hepatitis B virus core antigen with the surface immunoglobulin receptor on naive B cells. *J Virol* **75,** 6367–6374 doi: 10.1128/JVI.75.14.6367-6374.2001 (2001).
72. Cao, T. *et al.* Hepatitis B virus core antigen binds and activates naive human B cells *in vivo*: studies with a human PBL-NOD/SCID mouse model. *J Virol* **75,** 6359–6366 doi: 10.1128/JVI.75.14.6359-6366.2001 (2001).
73. Ehresmann, B., Imbault, P. & Weil, J. H. Spectrophotometric determination of protein concentration in cell extracts containing tRNA's and rRNA's. *Anal Biochem* **54,** 454–463 (1973).
74. Lloyd, D. D. *Delloyd's Lab Tech resources reagents and Solutions*, <http://delloyd.50megs.com/moreinfo/buffers2.html>, (2014) (Date of access: 28/01/2015).
75. Bichko, V., Pushko, P., Dreilina, D., Pumpen, P. & Gren, E. Subtype ayw variant of hepatitis B virus. DNA primary structure analysis. *FEBS Lett* **185,** 208–212 (1985).

Acknowledgments

We thank Mrs. Inara Akopjana for performing the *E. coli* transformations and preparing the bacteria for HBc VLP purification, Mr. Ivars Silamikelis for the NGS data analysis, and Dr. Frida Arsha and Dr. Valentina Sondore for valuable support. This work was supported by a European Regional Development Foundation grant 2DP/2.1.1.1.0/10/APIA/VIAA/052.

Author Contributions

A.S., G.K. and R.R. performed experiments, analysed data, and prepared the initial versions of the manuscript and figures. V.O. performed the E.M. JB analysed the samples using DLS. I.C. constructed the pT7CFE1-Chis-DTA plasmid and plasmids expressing the HBc mutants. IR analysed the RNA using the 2100 Bioanalyser and NGS. A.K. purified yeast-produced wt HBc VLPs. P.P. contributed to the preparation and editing of the final versions of the manuscript and figures. All authors reviewed the manuscript.

Additional Information

Supplementary information accompanies this paper at http://www.nature.com/srep

Competing financial interests: The authors declare no competing financial interests.

How to cite this article: Strods, A. *et al.* Preparation by alkaline treatment and detailed characterisation of empty hepatitis B virus core particles for vaccine and gene therapy applications. *Sci. Rep.* **5**, 11639; doi: 10.1038/srep11639 (2015).

Conclusion

Strong alkaline treatment can be applicable for HBc VLPs without impairing capsid structure, but at the same time being sufficient for wiping out the inner content of the particle. Empty particles are capable to package short nucleic acid fragments either RNA or DNA by simple contact, however long DNA fragment packaging can be achieved only after restoration of particles by using urea treatment. Fixed length DNA fragment was able to be packed in one particle if its length was 1289 bp, but not if it was 1737 bp. After packaging, DNA was protected from DNAse ifluence, whereas RNA after packaging and extraction appeared to be strongly degraded. All lysine bearing point-mutant HBc-75K, HBc-77K, HBc-79K and HBc-80K formed VLPs were capable to withstand alkali treatment and to package nucleic material. Lysine residues on the spike tips can be used for chemically provided attachments, therefore allowing addressing of particles.

Thesis

- Single-point mutations N75K, E77K, P79K and I80K in HBV core protein allow formation of particles morphologically indistinguishable from natural recombinat capsids.
- Alkali treatment based technology can be used for depletion of HBV core VLPs inner content and obtain empty particles for bacterial, yeast and all four point-mutants HBc-75K, HBc-77K, HBc-79K and HBc-80K.
- Empty HBc VLPs can package nucleic material either by direct contact incubation or through restoration in urea and refolding.
- Empty HBc VLPs package, but remarkably degrade RNA material.
- DNA material packaged in empty HBc VLPs is protected from DNAse I cleavage.
- HBc VLP maximum packaging length for discrete double-stranded DNA fragments is between 1289 bp and 1737 bp.

Main theses of defence

- Yeast-produced bacteriophage GA coat protein derived VLPs are capable to form mosaic particles, including HIV-Tat (48-60) sequence and immunologically competent region of WNV domain III.
- Two-promoter system based on plasmid pESC-URA was used for *in vivo* packaging of IL-2 and GFP mRNA into GA coat protein particles; the packaging specifity was remarkably improved by supplementing MS2 operator sequence to GFP mRNA and using GA VLP mutants that mimicks MS2 operator binding site, however particles still contained its own coat protein mRNA.
- Mosaic particles containing phage AP205 coat protein and protein C-terminally fused with 111 amino acids long WNV envelope protein E domain III sequence can be obtained in *E.coli* expression system.
- Bacteriophage AP205 WNV DIII sequence containing mosaic VLPs elicit WNV specific antibody response after immunisation in mice.
- Single-point mutations N75K, E77K, P79K and I80K in HBV core protein allow formation of particles morphologically indistinguishable from natural recombinat capsids.
- Alkali treatment based technology can be used for depletion of HBV core VLPs inner content and obtain empty particles for bacterial, yeast and all four point-mutants HBc-75K, HBc-77K, HBc-79K and HBc-80K.
- Empty HBc VLPs can package nucleic material either by direct contact incubation or through restoration in urea and refolding.
- Empty HBc VLPs package, but remarkably degrade RNA material.
- DNA material packaged in empty HBc VLPs is protected from DNAse I cleavage.
- HBc VLP maximum packaging length for discrete double-stranded DNA fragments is between 1289 bp and 1737 bp.

List of original publications

1. Strods, A., Argule, D., Cielens, I., Jackeviča, L., and Renhofa, R. (2013). Expression of GA Coat Protein-Derived Mosaic Virus-Like Particles in Saccharomyces cerevisiae and Packaging in vivo of mRNAs into Particles. Proc. Latv. Acad. Sci. Sect. B Nat. Exact Appl. Sci. 66, 234–241.

2. Cielens, I., Jackevica, L., Strods, A., Kazaks, A., Ose, V., Bogans, J., Pumpens, P., and Renhofa, R. (2014). Mosaic RNA phage VLPs carrying domain III of the West Nile virus E protein. Mol. Biotechnol. *56,* 459–469.

3. Strods, A., Ose, V., Bogans, J., Cielens, I., Kalnins, G., Radovica, I., Kazaks, A., Pumpens, P., and Renhofa, R. (2015). Preparation by alkaline treatment and detailed characterisation of empty hepatitis B virus core particles for vaccine and gene therapy applications. Sci. Rep., *5,* 11639.

Approbation of research

1. Strods, A., Papule., U., Renhofa, R., Kazāks, A., and Skrastiņa, D. Hepatitis B virus core particles as a platform for vaccine development. Modern Vaccines Adjuvants & Delivery Systems 2015 (MVADS 2015), Leiden (Netherlands), May 18-20, 2015.

2. Strods, A., Maļinovskis, U., Kalniņš, G., Renhofa, R. Plazmīdu un DNS fragmentu veidotie kompleksi ar HBc nanodaļiņām. The 73rd Scientific Conference of the University of Latvia, Rīga, January 30, 2015.

3. Renhofa, R., Cielēns, I., Strods, A., Kalniņš, G., Priede, D., Ose-Klinklāva, V., and Pumpēns, P. (2014) Modificēti HBV core nanokonteineri kā universāla platforma bioloģiskā materiāla eksponēšanai, Latvia patent application. P-14-06.

4. Renhofa, R., Ozols, J., Cielēns, I., and Strods, A. (2009). Antibiotikas doksorubicīna iepakošana bakteriofāga GA apvalka proteīna veidotajās nanodaļiņās – kapsīdās. Latvia patent. LV 13979 B.

Acknowledgements

This research was supported by the European Social Foundation (ESF) project Nr. 2013/0002/1DP/1.1.1.2.0/13/APIA/VIAA/005, by a European Regional Development Foundation grant 2DP/2.1.1.1.0/10/APIA/VIAA/052 and European Social Foundation (ESF) project Nr. 2009/0138/1DP/1.1.2.1.2/09/IPIA/VIAA/004.

I would like to thank to all co-authors, especially Prof. Paul Pumpens. Also the biggest thanks to Dr. Regina Renhofa for leading my work.

Literature references

Bachmann, M., Tissot, A., Pumpens, P., Cielens, I., and Renhofa, R. (2012). Molecular Antigen Arrays Using a Virus Like Particle Derived from the Ap205 Coat Protein.

Bachmann, M.F., Tissot, A., Jennings, G., Renhofa, R., Pumpens, P., and Cielens, I. (2008). Virus-Like Particles Comprising a Fusion Protein of the Coat Protein of Ap205 and an Antigenic Polypeptide.

Bachmann, M.F., Tissot, A., Pumpens, P., Cielens, I., and Renhofa, R. (2010). Molecular Antigen Arrays.

Banerjee, D., Liu, A.P., Voss, N.R., Schmid, S.L., and Finn, M.G. (2010). Multivalent display and receptor-mediated endocytosis of transferrin on virus-like particles. Chembiochem Eur. J. Chem. Biol. *11*, 1273–1279.

Beterams, G., Böttcher, B., and Nassal, M. (2000). Packaging of up to 240 subunits of a 17 kDa nuclease into the interior of recombinant hepatitis B virus capsids. FEBS Lett. *481*, 169–176.

Birnbaum, F., and Nassal, M. (1990). Hepatitis B virus nucleocapsid assembly: primary structure requirements in the core protein. J. Virol. *64*, 3319–3330.

Blokhina, E.A., Kuprianov, V.V., Stepanova, L.A., Tsybalova, L.M., Kiselev, O.I., Ravin, N.V., and Skryabin, K.G. (2013). A molecular assembly system for presentation of antigens on the surface of HBc virus-like particles. Virology *435*, 293–300.

Borisova, G., Borschukova Wanst, O., Mezule, G., Skrastina, D., Petrovskis, I., Dislers, A., Pumpens, P., and Grens, E. (1996). Spatial structure and insertion capacity of immunodominant region of hepatitis B core antigen. Intervirology *39*, 16–22.

Borisova, G., Borschukova, O., Skrastina, D., Mezule, G., Dišlers, A., Petrovskis, I., Ose-Klinklāva, V., Gusars, I., Pumpēns, P., and Grēns, E. (1997). Display vectors. I. Hepatitis B core particle as a display moiety. Proc. Latvian Acad. Sci. *51*, 1–7.

Borisova, G., Borschukova, O., Skrastina, D., Dislers, A., Ose, V., Pumpens, P., and Grens, E. (1999). Behavior of a short preS1 epitope on the surface of hepatitis B core particles. Biol. Chem. *380*, 315–324.

Borisova, G.P., Berzins, I., Pushko, P.M., Pumpen, P., Gren, E.J., Tsibinogin, V.V., Loseva, V., Ose, V., Ulrich, R., and Siakkou, H. (1989). Recombinant core particles of hepatitis B virus exposing foreign antigenic determinants on their surface. FEBS Lett. *259*, 121–124.

Brandenburg, B., Stockl, L., Gutzeit, C., Roos, M., Lupberger, J., Schwartlander, R., Gelderblom, H., Sauer, I.M., Hofschneider, P.H., and Hildt, E. (2005). A novel system for efficient gene transfer into primary human hepatocytes via cell-permeable hepatitis B virus-like particle. Hepatol. Baltim. Md *42*, 1300–1309.

Broos, K., Vanlandschoot, P., Maras, M., Robbens, J., Leroux-Roels, G., and Guisez, Y. (2007). Expression, purification and characterization of full-length RNA-free hepatitis B core particles. Protein Expr. Purif. *54*, 30–37.

Brown, A.L., Francis, M.J., Hastings, G.Z., Parry, N.R., Barnett, P.V., Rowlands, D.J., and Clarke, B.E. (1991). Foreign epitopes in immunodominant regions of hepatitis B core particles are highly immunogenic and conformationally restricted. Vaccine *9*, 595–601.

Brown, W.L., Mastico, R.A., Wu, M., Heal, K.G., Adams, C.J., Murray, J.B., Simpson, J.C., Lord, J.M., Taylor-Robinson, A.W., and Stockley, P.G. (2002). RNA bacteriophage capsid-mediated drug delivery and epitope presentation. Intervirology *45*, 371–380.

Brunn, A. von, Brand, M., Reichhuber, C., Morys-Wortmann, C., Deinhardt, F., and Schödel, F. (1993). Principal neutralizing domain of HIV-1 is highly immunogenic when expressed on the surface of hepatitis B core particles. Vaccine *11*, 817–824.

Chen, X., Li, M., Le, X., Ma, W., and Zhou, B. (2004). Recombinant hepatitis B core antigen carrying preS1 epitopes induce immune response against chronic HBV infection. Vaccine *22*, 439–446.

Chou, M.-I., Hsieh, Y.-F., Wang, M., Chang, J.T., Chang, D., Zouali, M., and Tsay, G.J. (2010). In vitro and in vivo targeted delivery of IL-10 interfering RNA by JC virus-like particles. J. Biomed. Sci. *17*, 51.

Chu, J.J.H., Rajamanonmani, R., Li, J., Bhuvanakantham, R., Lescar, J., and Ng, M.-L. (2005). Inhibition of West Nile virus entry by using a recombinant domain III from the envelope glycoprotein. J. Gen. Virol. *86*, 405–412.

Chubb, J.R., Trcek, T., Shenoy, S.M., and Singer, R.H. (2006). Transcriptional Pulsing of a Developmental Gene. Curr. Biol. *16*, 1018–1025.

Cielens, I., Jackevica, L., Strods, A., Kazaks, A., Ose, V., Bogans, J., Pumpens, P., and Renhofa, R. (2014). Mosaic RNA phage VLPs carrying domain III of the West Nile virus E protein. Mol. Biotechnol. *56*, 459–469.

Clark, J.R., and March, J.B. (2004). Bacteriophage-mediated nucleic acid immunisation. FEMS Immunol. Med. Microbiol. *40*, 21–26.

Clark, J.R., Bartley, K., Jepson, C.D., Craik, V., and March, J.B. (2011). Comparison of a bacteriophage-delivered DNA vaccine and a commercially available recombinant protein vaccine against hepatitis B. FEMS Immunol. Med. Microbiol. *61*, 197–204.

Cohen, B.J., and Richmond, J.E. (1982). Electron microscopy of hepatitis B core antigen synthesized in E. coli. Nature *296*, 677–679.

Cooper, A., and Shaul, Y. (2005). Recombinant viral capsids as an efficient vehicle of oligonucleotide delivery into cells. Biochem. Biophys. Res. Commun. *327*, 1094–1099.

Cooper, A., and Shaul, Y. (2006). Clathrin-mediated endocytosis and lysosomal cleavage of hepatitis B virus capsid-like core particles. J. Biol. Chem. *281*, 16563–16569.

Crowther, R.A., Kiselev, N.A., Böttcher, B., Berriman, J.A., Borisova, G.P., Ose, V., and Pumpens, P. (1994). Three-dimensional structure of hepatitis B virus core particles determined by electron cryomicroscopy. Cell *77*, 943–950.

Daniels, T.R., Bernabeu, E., Rodríguez, J.A., Patel, S., Kozman, M., Chiappetta, D.A., Holler, E., Ljubimova, J.Y., Helguera, G., and Penichet, M.L. (2012). The transferrin receptor

and the targeted delivery of therapeutic agents against cancer. Biochim. Biophys. Acta *1820*, 291–317.

Dhanasooraj, D., Kumar, R.A., and Mundayoor, S. (2013). Vaccine delivery system for tuberculosis based on nano-sized hepatitis B virus core protein particles. Int. J. Nanomedicine *8*, 835–843.

Diamond, M.S., Pierson, T.C., and Fremont, D.H. (2008). The Structural Immunology of Antibody Protection against West Nile Virus. Immunol. Rev. *225*, 212–225.

Ding, F.-X., Wang, F., Lu, Y.-M., Li, K., Wang, K.-H., He, X.-W., and Sun, S.-H. (2009). Multiepitope peptide-loaded virus-like particles as a vaccine against hepatitis B virus-related hepatocellular carcinoma. Hepatol. Baltim. Md *49*, 1492–1502.

Ehresmann, B., Imbault, P., and Weil, J.H. (1973). Spectrophotometric determination of protein concentration in cell extracts containing tRNA's and rRNA's. Anal. Biochem. *54*, 454–463.

Fiers, W. (1979). Structure and Function of RNA Bacteriophages. In Comprehensive Virology Volume 13: Structure and Assembly, H. Fraenkel-Conrat, and R.R. Wagner, eds. (Springer US), pp. 69–204.

Fiers, W., Contreras, R., Duerinck, F., Haegeman, G., Iserentant, D., Merregaert, J., Min Jou, W., Molemans, F., Raeymaekers, A., Van den Berghe, A., et al. (1976). Complete nucleotide sequence of bacteriophage MS2 RNA: primary and secondary structure of the replicase gene. Nature *260*, 500–507.

Freivalds, J., Rūmnieks, J., Ose, V., Renhofa, R., and Kazāks, A. (2008). High-level expression and purification of bacteriophage GA virus-like particles from yeast Saccharomyces cerevisiae and Pichia pastoris. Acta Univ Latv *745*, 75–85.

Freivalds, J., Dislers, A., Ose, V., Pumpens, P., Tars, K., and Kazaks, A. (2011). Highly efficient production of phosphorylated hepatitis B core particles in yeast Pichia pastoris. Protein Expr. Purif. *75*, 218–224.

Freivalds, J., Kotelovica, S., Voronkova, T., Ose, V., Tars, K., and Kazaks, A. (2014). Yeast-expressed bacteriophage-like particles for the packaging of nanomaterials. Mol. Biotechnol. *56*, 102–110.

Gallina, A., Bonelli, F., Zentilin, L., Rindi, G., Muttini, M., and Milanesi, G. (1989). A recombinant hepatitis B core antigen polypeptide with the protamine-like domain deleted self-assembles into capsid particles but fails to bind nucleic acids. J. Virol. *63*, 4645–4652.

Garcea, R.L., and Gissmann, L. (2004). Virus-like particles as vaccines and vessels for the delivery of small molecules. Curr. Opin. Biotechnol. *15*, 513–517.

Georgens, C., Weyermann, J., and Zimmer, A. (2005). Recombinant virus like particles as drug delivery system. Curr. Pharm. Biotechnol. *6*, 49–55.

Gerin, J.L., Holland, P.V., and Purcell, R.H. (1971). Australia antigen: large-scale purification from human serum and biochemical studies of its proteins. J. Virol. *7*, 569–576.

Gleiter, S., and Lilie, H. (2003). Cell-type specific targeting and gene expression using a variant of polyoma VP1 virus-like particles. Biol. Chem. *384*, 247–255.

Gott, J.M., Wilhelm, L.J., and Uhlenbeck, O.C. (1991). RNA binding properties of the coat protein from bacteriophage GA. Nucleic Acids Res. *19*, 6499–6503.

Gregory, A.E., Titball, R., and Williamson, D. (2013). Vaccine delivery using nanoparticles. Front. Cell. Infect. Microbiol. *3*, 13.

Grene, E., Mezule, G., Borisova, G., Pumpens, P., Bentwich, Z., and Arnon, R. (1997). Relationship between antigenicity and immunogenicity of chimeric hepatitis B virus core particles carrying HIV type 1 epitopes. AIDS Res. Hum. Retroviruses *13*, 41–51.

Guo, Y., Wang, W., Ji, W., Deng, M., Sun, Y., Zhou, H., Yang, C., Deng, F., Wang, H., Hu, Z., et al. (2012). Crimean-Congo hemorrhagic fever virus nucleoprotein reveals endonuclease activity in bunyaviruses. Proc. Natl. Acad. Sci. U. S. A. *109*, 5046–5051.

Hastie, K.M., Kimberlin, C.R., Zandonatti, M.A., MacRae, I.J., and Saphire, E.O. (2011). Structure of the Lassa virus nucleoprotein reveals a dsRNA-specific 3′ to 5′ exonuclease activity essential for immune suppression. Proc. Natl. Acad. Sci. U. S. A. *108*, 2396–2401.

Hitzeman, R.A., Chen, C.Y., Hagie, F.E., Patzer, E.J., Liu, C.C., Estell, D.A., Miller, J.V., Yaffe, A., Kleid, D.G., Levinson, A.D., et al. (1983). Expression of hepatitis B virus surface antigen in yeast. Nucleic Acids Res. *11*, 2745–2763.

Hofstetter, H., Monstein, H.J., and Weissmann, C. (1974). The readthrough protein A1 is essential for the formation of viable Q beta particles. Biochim. Biophys. Acta *374*, 238–251.

Hohn, T. (1969). Studies on a Possible Precursor in the Self Assembly of the Bacteriophage fr. Eur. J. Biochem. *8*, 552–556.

Hoofnagle, J., Gerety, R., and Barker, L. (1973). Antibody to hepatitis-B-virus core in man. The Lancet *302*, 869–873.

Hooker, J.M., Kovacs, E.W., and Francis, M.B. (2004). Interior surface modification of bacteriophage MS2. J. Am. Chem. Soc. *126*, 3718–3719.

Huang, X., Stein, B.D., Cheng, H., Malyutin, A., Tsvetkova, I.B., Baxter, D.V., Remmes, N.B., Verchot, J., Kao, C., Bronstein, L.M., et al. (2011). Magnetic Virus-like Nanoparticles in N. benthamiana Plants: a New Paradigm for Environmental and Agronomic Biotechnological Research. ACS Nano *5*, 4037–4045.

Inokuchi, Y., Takahashi, R., Hirose, T., Inayama, S., Jacobson, A.B., and Hirashima, A. (1986). The complete nucleotide sequence of the group II RNA coliphage GA. J. Biochem. (Tokyo) *99*, 1169–1180.

Ishikawa, T., Yamanaka, A., and Konishi, E. (2014). A review of successful flavivirus vaccines and the problems with those flaviviruses for which vaccines are not yet available. Vaccine *32*, 1326–1337.

Jegerlehner, A., Schmitz, N., Storni, T., and Bachmann, M.F. (2004). Influenza A vaccine based on the extracellular domain of M2: weak protection mediated via antibody-dependent NK cell activity. J. Immunol. Baltim. Md 1950 *172*, 5598–5605.

Jiang, X., Huang, Q., Wang, W., Dong, H., Ly, H., Liang, Y., and Dong, C. (2013). Structures of Arenaviral Nucleoproteins with Triphosphate dsRNA Reveal a Unique Mechanism of Immune Suppression. J. Biol. Chem. *288*, 16949–16959.

Kaczmarczyk, S.J., Sitaraman, K., Young, H.A., Hughes, S.H., and Chatterjee, D.K. (2011). Protein delivery using engineered virus-like particles. Proc. Natl. Acad. Sci. U. S. A. *108*, 16998–17003.

Kanai, R., Kar, K., Anthony, K., Gould, L.H., Ledizet, M., Fikrig, E., Marasco, W.A., Koski, R.A., and Modis, Y. (2006). Crystal Structure of West Nile Virus Envelope Glycoprotein Reveals Viral Surface Epitopes. J. Virol. *80*, 11000–11008.

Kann, M., and Gerlich, W.H. (1994). Effect of core protein phosphorylation by protein kinase C on encapsidation of RNA within core particles of hepatitis B virus. J. Virol. *68*, 7993–8000.

Kann, M., Sodeik, B., Vlachou, A., Gerlich, W.H., and Helenius, A. (1999). Phosphorylation-dependent Binding of Hepatitis B Virus Core Particles to the Nuclear Pore Complex. J. Cell Biol. *145*, 45–55.

Kazaks, A., Borisova, G., Cvetkova, S., Kovalevska, L., Ose, V., Sominskaya, I., Pumpens, P., Skrastina, D., and Dislers, A. (2004). Mosaic hepatitis B virus core particles presenting the complete preS sequence of the viral envelope on their surface. J. Gen. Virol. *85*, 2665–2670.

Kazaks, A., Balmaks, R., Voronkova, T., Ose, V., and Pumpens, P. (2008). Melanoma vaccine candidates from chimeric hepatitis B core virus-like particles carrying a tumor-associated MAGE-3 epitope. Biotechnol. J. *3*, 1429–1436.

Keryer-Bibens, C., Barreau, C., and Osborne, H.B. (2008). Tethering of proteins to RNAs by bacteriophage proteins. Biol. Cell Auspices Eur. Cell Biol. Organ. *100*, 125–138.

Klovins, J., Overbeek, G.P., van den Worm, S.H.E., Ackermann, H.-W., and van Duin, J. (2002). Nucleotide sequence of a ssRNA phage from Acinetobacter: kinship to coliphages. J. Gen. Virol. *83*, 1523–1533.

Koletzki, D., Zankl, A., Gelderblom, H.R., Meisel, H., Dislers, A., Borisova, G., Pumpens, P., Krüger, D.H., and Ulrich, R. (1997). Mosaic hepatitis B virus core particles allow insertion of extended foreign protein segments. J. Gen. Virol. *78 (Pt 8)*, 2049–2053.

Koletzki, D., Biel, S.S., Meisel, H., Nugel, E., Gelderblom, H.R., Krüger, D.H., and Ulrich, R. (1999). HBV core particles allow the insertion and surface exposure of the entire potentially protective region of Puumala hantavirus nucleocapsid protein. Biol. Chem. *380*, 325–333.

Koletzki, D., Lundkvist, A., Sjölander, K.B., Gelderblom, H.R., Niedrig, M., Meisel, H., Krüger, D.H., and Ulrich, R. (2000). Puumala (PUU) hantavirus strain differences and insertion positions in the hepatitis B virus core antigen influence B-cell immunogenicity and protective potential of core-derived particles. Virology *276*, 364–375.

Kratz, P.A., Böttcher, B., and Nassal, M. (1999). Native display of complete foreign protein domains on the surface of hepatitis B virus capsids. Proc. Natl. Acad. Sci. U. S. A. *96*, 1915–1920.

Krieg, A.M. (2012). CpG still rocks! Update on an accidental drug. Nucleic Acid Ther. *22*, 77–89.

Kushnir, N., Streatfield, S.J., and Yusibov, V. (2012). Virus-like particles as a highly efficient vaccine platform: diversity of targets and production systems and advances in clinical development. Vaccine *31*, 58–83.

Lange, M., Fiedler, M., Bankwitz, D., Osburn, W., Viazov, S., Brovko, O., Zekri, A.-R., Khudyakov, Y., Nassal, M., Pumpens, P., et al. (2014). Hepatitis C Virus Hypervariable Region 1 Variants Presented on Hepatitis B Virus Capsid-Like Particles Induce Cross-Neutralizing Antibodies. PLoS ONE *9*.

Lee, K.W., and Tan, W.S. (2008). Recombinant hepatitis B virus core particles: association, dissociation and encapsidation of green fluorescent protein. J. Virol. Methods *151*, 172–180.

Legendre, D., and Fastrez, J. (2005). Production in Saccharomycescerevisiae of MS2 virus-like particles packaging functional heterologous mRNAs. J. Biotechnol. *117*, 183–194.

Lim, F., and Peabody, D.S. (1994). Mutations that increase the affinity of a translational repressor for RNA. Nucleic Acids Res. *22*, 3748–3752.

Lim, F., Spingola, M., and Peabody, D.S. (1994). Altering the RNA binding specificity of a translational repressor. J. Biol. Chem. *269*, 9006–9010.

Lindsey, N.P., Erin Staples, J., Lehman, J.A., and Fischer, M. (2010). Surveillance for human west Nile virus disease-United States, 1999-2008. Morb. Mortal. Wkly. Rep. *59*, 1–17.

Liu, J., Liu, B., Cao, Z., Inoue, S., Morita, K., Tian, K., Zhu, Q., and Gao, G.F. (2008). Characterization and application of monoclonal antibodies specific to West Nile virus envelope protein. J. Virol. Methods *154*, 20–26.

Livingston, B.D., Crimi, C., Fikes, J., Chesnut, R.W., Sidney, J., and Sette, A. (1999). Immunization with the HBV core 18-27 epitope elicits CTL responses in humans expressing different HLA-A2 supertype molecules. Hum. Immunol. *60*, 1013–1017.

Makeeva, I.V., Kalinina, T.I., Khudiakov, I.E., Samoshin, V.V., Smirnova, E.A., Semiletov, I.A., Pavliuchenkova, R.P., Kadoshnikov, I.P., and Smirnov, V.D. (1995). [Heterologous epitopes in the central part of the hepatitis B virus core protein]. Mol. Biol. (Mosk.) *29*, 211–224.

Mamo, T., and Poland, G.A. (2012). Nanovaccinology: The next generation of vaccines meets 21st century materials science and engineering. Vaccine *30*, 6609–6611.

Maurer, P., Jennings, G.T., Willers, J., Rohner, F., Lindman, Y., Roubicek, K., Renner, W.A., Müller, P., and Bachmann, M.F. (2005). A therapeutic vaccine for nicotine dependence: preclinical efficacy, and Phase I safety and immunogenicity. Eur. J. Immunol. *35*, 2031–2040.

Monie, A., Hung, C.-F., Roden, R., and Wu, T.-C. (2008). Cervarix^{TM}: a vaccine for the prevention of HPV 16, 18-associated cervical cancer. Biol. Targets Ther. *2*, 107–113.

Murphy, A.F. (1980). 8 - Togavirus Morphology and Morphogenesis. In The Togaviruses, R.W. Schlesinger, ed. (Academic Press), pp. 241–316.

Murray, K., and Shiau, A.L. (1999). The core antigen of hepatitis B virus as a carrier for immunogenic peptides. Biol. Chem. *380*, 277–283.

Nassal, M. (1992a). Conserved cysteines of the hepatitis B virus core protein are not required for assembly of replication-competent core particles nor for their envelopment. Virology *190*, 499–505.

Nassal, M. (1992b). The arginine-rich domain of the hepatitis B virus core protein is required for pregenome encapsidation and productive viral positive-strand DNA synthesis but not for virus assembly. J. Virol. *66*, 4107–4116.

Nassal, M., Rieger, A., and Steinau, O. (1992). Topological analysis of the hepatitis B virus core particle by cysteine-cysteine cross-linking. J. Mol. Biol. *225*, 1013–1025.

Neirynck, S., Deroo, T., Saelens, X., Vanlandschoot, P., Jou, W.M., and Fiers, W. (1999). A universal influenza A vaccine based on the extracellular domain of the M2 protein. Nat. Med. *5*, 1157–1163.

Nekrasova, O.V., Boĭchenko, V.E., Boldyreva, E.F., Borisova, G.P., Pumpen, P., Perevozchikova, N.A., and Korobko, V.G. (1997). [Bacterial synthesis of immunogenic epitopes of foot-and-mouth disease virus fused either to human necrosis factor or to hepatitis B core antigen]. Bioorg. Khim. *23*, 118–126.

Nelson, S., Jost, C.A., Xu, Q., Ess, J., Martin, J.E., Oliphant, T., Whitehead, S.S., Durbin, A.P., Graham, B.S., Diamond, M.S., et al. (2008). Maturation of West Nile Virus Modulates Sensitivity to Antibody-Mediated Neutralization. PLoS Pathog. *4*.

Newman, M., Suk, F.-M., Cajimat, M., Chua, P.K., and Shih, C. (2003). Stability and Morphology Comparisons of Self-Assembled Virus-Like Particles from Wild-Type and Mutant Human Hepatitis B Virus Capsid Proteins. J. Virol. *77*, 12950–12960.

Newman, M., Chua, P.K., Tang, F.-M., Su, P.-Y., and Shih, C. (2009). Testing an Electrostatic Interaction Hypothesis of Hepatitis B Virus Capsid Stability by Using an In Vitro Capsid Disassembly/Reassembly System. J. Virol. *83*, 10616–10626.

Ni, C.Z., White, C.A., Mitchell, R.S., Wickersham, J., Kodandapani, R., Peabody, D.S., and Ely, K.R. (1996). Crystal structure of the coat protein from the GA bacteriophage: model of the unassembled dimer. Protein Sci. Publ. Protein Soc. *5*, 2485–2493.

Nybakken, G.E., Nelson, C.A., Chen, B.R., Diamond, M.S., and Fremont, D.H. (2006). Crystal Structure of the West Nile Virus Envelope Glycoprotein. J. Virol. *80*, 11467–11474.

Pastori, C., Tudor, D., Diomede, L., Drillet, A.S., Jegerlehner, A., Röhn, T.A., Bomsel, M., and Lopalco, L. (2012). Virus like particle based strategy to elicit HIV-protective antibodies to the alpha-helic regions of gp41. Virology *431*, 1–11.

Patel, K.G., and Swartz, J.R. (2011). Surface functionalization of virus-like particles by direct conjugation using azide-alkyne click chemistry. Bioconjug. Chem. *22*, 376–387.

Paul Pumpens (2008). Construction of Novel Vaccines on the Basis of Virus-Like Particles. In Medicinal Protein Engineering, (CRC Press),.

Pei, X., Zhang, J., and Liu, J. (2014). Clinical applications of nucleic acid aptamers in cancer. Mol. Clin. Oncol. *2*, 341–348.

Peyret, H., Gehin, A., Thuenemann, E.C., Blond, D., Turabi, A. El, Beales, L., Clarke, D., Gilbert, R.J.C., Fry, E.E., Stuart, D.I., et al. (2015). Tandem fusion of hepatitis B core

antigen allows assembly of virus-like particles in bacteria and plants with enhanced capacity to accommodate foreign proteins. PloS One *10*, e0120751.

Pickett, G.G., and Peabody, D.S. (1993). Encapsidation of heterologous RNAs by bacteriophage MS2 coat protein. Nucleic Acids Res. *21*, 4621–4626.

Pijlman, G.P. (2015). Enveloped virus-like particles as vaccines against pathogenic arboviruses. Biotechnol. J. *0*.

Pokorski, J.K., and Steinmetz, N.F. (2011). The Art of Engineering Viral Nanoparticles. Mol. Pharm. *8*, 29–43.

Porterfield, J.Z., and Zlotnick, A. (2010). A simple and general method for determining the protein and nucleic acid content of viruses by UV absorbance. Virology *407*, 281–288.

Porterfield, J.Z., Dhason, M.S., Loeb, D.D., Nassal, M., Stray, S.J., and Zlotnick, A. (2010). Full-length hepatitis B virus core protein packages viral and heterologous RNA with similarly high levels of cooperativity. J. Virol. *84*, 7174–7184.

Pumpens, P., and Grens, E. (2001). HBV core particles as a carrier for B cell/T cell epitopes. Intervirology *44*, 98–114.

Pumpens, P., and Grens, E. (2002). Artificial Genes for Chimeric Virus-Like Particles. In Artificial DNA: Methods and Application, (Florida: CRC Press), pp. 250–327.

Pumpens, P., Borisova, G.P., Crowther, R.A., and Grens, E. (1995). Hepatitis B virus core particles as epitope carriers. Intervirology *38*, 63–74.

Pushko, P., Pumpens, P., and Grens, E. (2013). Development of virus-like particle technology from small highly symmetric to large complex virus-like particle structures. Intervirology *56*, 141–165.

Ranka, R., Petrovskis, I., Sominskaya, I., Bogans, J., Bruvere, R., Akopjana, I., Ose, V., Timofejeva, I., Brangulis, K., Pumpens, P., et al. (2013). Fibronectin-binding nanoparticles for intracellular targeting addressed by B. burgdorferi BBK32 protein fragments. Nanomedicine Nanotechnol. Biol. Med. *9*, 65–73.

Ray, P., and White, R.R. (2010). Aptamers for Targeted Drug Delivery. Pharmaceuticals *3*, 1761–1778.

Renhofa, R., Cielēns, I., Strods, A., Kalniņš, G., Priede, D., Ose-Klinklāva, V., and Pumpēns, P. (2014). Modificēti HBV core nanokonteineri kā universāla platforma bioloģiskā materiāla eksponēšanai.

Roldão, A., Mellado, M.C.M., Castilho, L.R., Carrondo, M.J., and Alves, P.M. (2010). Virus-like particles in vaccine development. Expert Rev. Vaccines *9*, 1149–1176.

Roose, K., De Baets, S., Schepens, B., and Saelens, X. (2013). Hepatitis B core-based virus-like particles to present heterologous epitopes. Expert Rev. Vaccines *12*, 183–198.

Rūmnieks, J., Freivalds, J., Cielēns, I., and Renhofa, R. (2008). Specificity of packaging mRNAs in bacteriophage GA virus-like particles in yeast Saccharomyces cerevisiae. Acta Univ Latv *745*, 145–154.

Scaglioni, P.P., Melegari, M., and Wands, J.R. (1997). Posttranscriptional regulation of hepatitis B virus replication by the precore protein. J. Virol. *71*, 345–353.

Schödel, F., Milich, D.R., and Will, H. (1990). Hepatitis B virus nucleocapsid/pre-S2 fusion proteins expressed in attenuated Salmonella for oral vaccination. J. Immunol. Baltim. Md 1950 *145*, 4317–4321.

Schödel, F., Moriarty, A.M., Peterson, D.L., Zheng, J.A., Hughes, J.L., Will, H., Leturcq, D.J., McGee, J.S., and Milich, D.R. (1992). The position of heterologous epitopes inserted in hepatitis B virus core particles determines their immunogenicity. J. Virol. *66*, 106–114.

Schwarz, K., Meijerink, E., Speiser, D.E., Tissot, A.C., Cielens, I., Renhof, R., Dishlers, A., Pumpens, P., and Bachmann, M.F. (2005). Efficient homologous prime-boost strategies for T cell vaccination based on virus-like particles. Eur. J. Immunol. *35*, 816–821.

Skrastina, D., Petrovskis, I., Petraityte, R., Sominskaya, I., Ose, V., Liekniņa, I., Bogans, J., Sasnauskas, K., and Pumpens, P. (2013). Chimeric Derivatives of Hepatitis B Virus Core Particles Carrying Major Epitopes of the Rubella Virus E1 Glycoprotein. Clin. Vaccine Immunol. CVI *20*, 1719–1728.

Sominskaya, I., Skrastina, D., Petrovskis, I., Dishlers, A., Berza, I., Mihailova, M., Jansons, J., Akopjana, I., Stahovska, I., Dreilina, D., et al. (2013). A VLP library of C-terminally truncated Hepatitis B core proteins: correlation of RNA encapsidation with a Th1/Th2 switch in the immune responses of mice. PloS One *8*, e75938.

Spohn, G., Jennings, G.T., Martina, B.E., Keller, I., Beck, M., Pumpens, P., Osterhaus, A.D., and Bachmann, M.F. (2010). A VLP-based vaccine targeting domain III of the West Nile virus E protein protects from lethal infection in mice. Virol. J. *7*, 146.

Storni, T., Ruedl, C., Schwarz, K., Schwendener, R.A., Renner, W.A., and Bachmann, M.F. (2004). Nonmethylated CG motifs packaged into virus-like particles induce protective cytotoxic T cell responses in the absence of systemic side effects. J. Immunol. Baltim. Md 1950 *172*, 1777–1785.

Strods, A., Argule, D., Cielens, I., Jackeviča, L., and Renhofa, R. (2013). Expression of GA Coat Protein-Derived Mosaic Virus-Like Particles in Saccharomyces cerevisiae and Packaging in vivo of mRNAs into Particles. Proc. Latv. Acad. Sci. Sect. B Nat. Exact Appl. Sci. *66*, 234–241.

Strods, A., Ose, V., Bogans, J., Cielens, I., Kalnins, G., Radovica, I., Kazaks, A., Pumpens, P., and Renhofa, R. (2015a). Preparation by alkaline treatment and detailed characterisation of empty hepatitis B virus core particles for vaccine and gene therapy applications. Sci. Rep. *5*, 11639.

Strods, A., Papule, U., Renhofa, R., Kazāks, A., and Skrastina, D. (2015b). Hepatitis B virus core particles as a platform for vaccine development. In Modern Vaccines Adjuvants & Delivery Systems 2015 (MVADS 2015), (Leiden, Netherlands),.

Sun, J., DuFort, C., Daniel, M.-C., Murali, A., Chen, C., Gopinath, K., Stein, B., De, M., Rotello, V.M., Holzenburg, A., et al. (2007). Core-controlled polymorphism in virus-like particles. Proc. Natl. Acad. Sci. U. S. A. *104*, 1354–1359.

Sun, S., Li, W., Sun, Y., Pan, Y., and Li, J. (2011). A new RNA vaccine platform based on MS2 virus-like particles produced in Saccharomyces cerevisiae. Biochem. Biophys. Res. Commun. *407*, 124–128.

Tarar, M.R., Emery, V.C., and Harrison, T.J. (1996). Expression of a human cytomegalovirus gp58 antigenic domain fused to the hepatitis B virus nucleocapsid protein. FEMS Immunol. Med. Microbiol. *16*, 183–192.

Tars, K., Bundule, M., Fridborg, K., and Liljas, L. (1997). The crystal structure of bacteriophage GA and a comparison of bacteriophages belonging to the major groups of Escherichia coli leviviruses. J. Mol. Biol. *271*, 759–773.

Tissot, A.C., Renhofa, R., Schmitz, N., Cielens, I., Meijerink, E., Ose, V., Jennings, G.T., Saudan, P., Pumpens, P., and Bachmann, M.F. (2010). Versatile Virus-Like Particle Carrier for Epitope Based Vaccines. PLoS ONE *5*.

Tumban, E., Peabody, J., Peabody, D.S., and Chackerian, B. (2013). A Universal Virus-Like Particle-based Vaccine for Human Papillomavirus: Longevity of Protection and Role of Endogenous and Exogenous Adjuvants. Vaccine *31*, 4647–4654.

Tyler, M., Tumban, E., Peabody, D.S., and Chackerian, B. (2014). The use of hybrid virus-like particles to enhance the immunogenicity of a broadly protective HPV vaccine. Biotechnol. Bioeng. *111*, 2398–2406.

Ulrich, R., Koletzki, D., Lachmann, S., Lundkvist, Å., Zankl, A., Kazaks, A., Kurth, A., Gelderblom, H.R., Borisova, G., Meisel, H., et al. (1999). New chimaeric hepatitis B virus core particles carrying hantavirus (serotype Puumala) epitopes: immunogenicity and protection against virus challenge. J. Biotechnol. *73*, 141–153.

Valenzuela, P., Medina, A., Rutter, W.J., Ammerer, G., and Hall, B.D. (1982). Synthesis and assembly of hepatitis B virus surface antigen particles in yeast. Nature *298*, 347–350.

Vanlandschoot, P., Van Houtte, F., Serruys, B., and Leroux-Roels, G. (2005). The arginine-rich carboxy-terminal domain of the hepatitis B virus core protein mediates attachment of nucleocapsids to cell-surface-expressed heparan sulfate. J. Gen. Virol. *86*, 75–84.

Vivès, E., Brodin, P., and Lebleu, B. (1997). A truncated HIV-1 Tat protein basic domain rapidly translocates through the plasma membrane and accumulates in the cell nucleus. J. Biol. Chem. *272*, 16010–16017.

Walker, A., Skamel, C., and Nassal, M. (2011). SplitCore: An exceptionally versatile viral nanoparticle for native whole protein display regardless of 3D structure. Sci. Rep. *1*.

Wei, B., Wei, Y., Zhang, K., Wang, J., Xu, R., Zhan, S., Lin, G., Wang, W., Liu, M., Wang, L., et al. (2009). Development of an antisense RNA delivery system using conjugates of the MS2 bacteriophage capsids and HIV-1 TAT cell-penetrating peptide. Biomed. Pharmacother. Bioméd. Pharmacothérapie *63*, 313–318.

Wingfield, P.T., Stahl, S.J., Williams, R.W., and Steven, A.C. (1995). Hepatitis core antigen produced in Escherichia coli: subunit composition, conformational analysis, and in vitro capsid assembly. Biochemistry (Mosc.) *34*, 4919–4932.

van den Worm, S.H.E., Koning, R.I., Warmenhoven, H.J., Koerten, H.K., and van Duin, J. (2006). Cryo electron microscopy reconstructions of the Leviviridae unveil the densest icosahedral RNA packing possible. J. Mol. Biol. *363*, 858–865.

Wu, M., Brown, W.L., and Stockley, P.G. (1995). Cell-Specific Delivery of Bacteriophage-Encapsidated Ricin A Chain. Bioconjug. Chem. *6*, 587–595.

Wynne, S.A., Crowther, R.A., and Leslie, A.G. (1999). The crystal structure of the human hepatitis B virus capsid. Mol. Cell *3*, 771–780.

Yang, H.-J., Chen, M., Cheng, T., He, S.-Z., Li, S.-W., Guan, B.-Q., Zhu, Z.-H., Gu, Y., Zhang, J., and Xia, N.-S. (2005). Expression and immunoactivity of chimeric particulate antigens of receptor binding site-core antigen of hepatitis B virus. World J. Gastroenterol. WJG *11*, 492–497.

Yon, J., Rud, E., Corcoran, T., Kent, K., Rowlands, D., and Clarke, B. (1992). Stimulation of specific immune responses to simian immunodeficiency virus using chimeric hepatitis B core antigen particles. J. Gen. Virol. *73 (Pt 10)*, 2569–2575.

Yoo, L., Park, J.-S., Kwon, K.C., Kim, S.-E., Jin, X., Kim, H., and Lee, J. (2012). Fluorescent viral nanoparticles with stable in vitro and in vivo activity. Biomaterials *33*, 6194–6200.

Yoshikawa, A., Tanaka, T., Hoshi, Y., Kato, N., Tachibana, K., Iizuka, H., Machida, A., Okamoto, H., Yamasaki, M., and Miyakawa, Y. (1993). Chimeric hepatitis B virus core particles with parts or copies of the hepatitis C virus core protein. J. Virol. *67*, 6064–6070.

Yu, X., Jin, L., Jih, J., Shih, C., and Zhou, Z.H. (2013). 3.5Å cryoEM structure of hepatitis B virus core assembled from full-length core protein. PloS One *8*, e69729.

Zeltins, A. (2013). Construction and characterization of virus-like particles: a review. Mol. Biotechnol. *53*, 92–107.

Zhao, Y., and Zhan, M. (2002). The coexpression of the preS1 (1-42) and the core (1-144) antigen of HBV in E. coli. Chin. Med. Sci. J. Chung-Kuo Hsüeh Ko Hsüeh Tsa Chih Chin. Acad. Med. Sci. *17*, 68–72.

Zhao, L., Seth, A., Wibowo, N., Zhao, C.-X., Mitter, N., Yu, C., and Middelberg, A.P.J. (2014). Nanoparticle vaccines. Vaccine *32*, 327–337.

Zhao, Q., Li, S., Yu, H., Xia, N., and Modis, Y. (2013). Virus-like particle-based human vaccines: quality assessment based on structural and functional properties. Trends Biotechnol. *31*, 654–663.

Zheng, J., Schödel, F., and Peterson, D.L. (1992). The structure of hepadnaviral core antigens. Identification of free thiols and determination of the disulfide bonding pattern. J. Biol. Chem. *267*, 9422–9429.

Zlotnick, A., Cheng, N., Conway, J.F., Booy, F.P., Steven, A.C., Stahl, S.J., and Wingfield, P.T. (1996). Dimorphism of hepatitis B virus capsids is strongly influenced by the C-terminus of the capsid protein. Biochemistry (Mosc.) *35*, 7412–7421.

Appendix

***In vivo* packaging of yeast-produced bacteriophage GA derived virus-like particles**

Dagnija Ārgule[1], Indulis Cielēns[1], Regīna Renhofa[1], Arnis Strods[1,2,*]

[1] Latvian Biomedical Research and Study Centre, Ratsupites 1 k-1, Riga LV-1067, Latvia

[2] Latvian Institute of Organic Synthesis, Aizkraukles 21, Riga LV-1006, Latvia

* Corresponding author

Abstract

Bacteriophage GA coat protein formed self-assembly competent virus like particles (VLPs) have been expressed previously in bacteria and yeast cells. On the base of our previous experiments in yeast vector pESC-URA / *S.cerevisiae* system containing two opposite oriented promoters, new constructions were created with point-mutations in coat protein to mimic phage MS2-like RNA binding characteristics. Simultaneously MS2 operator sequence was added to mRNA desired for packaging. After introduction of single-point mutations (S87N, K55N, R43K) and double-point mutations (S87N + K55N and S87N + R43K) coat protein ability to form VLPs was retained except that yield from cells was decreased. Exchange of the 87th Ser to Asn in coat protein sequence together in combination with bacteriophage MS2 translational operator provided specific packaging of the gene of interest (GFP). Although non-specific nucleic acid sequences were packaged, the remarkable specificity for packaging of the gene of interest using above mentioned approach can be achieved.

Key words: VLPs, GA, MS2, operator

Introduction

Recent work is a further development of our previous investigations in the production of recombinant bacteriophage GA coat protein formed nanoparticles with *in vivo* packaged mRNAs. It was found that high-yield production of GA coat protein formed virus like particles (GA CP VLPs) occurred by expression of appropriate coding gene in yeast *Pichia pastoris* (Freivalds et al., 2008), whereas gene constructs based on vector pESC-URA from Stratagene in *Saccharomyces cerevisiae* gave much lower production of VLPs, which allowed to produce mosaic particles (Rūmnieks et al., 2008) and to pack mRNAs into particles during growth (Rūmnieks et al., 2008; Strods et al., 2013).

It is well-known that the coat proteins of single-strand RNA bacteriophages are bifunctional. They form the icosahedral shells for protection of viral nucleic acids, and also shutting off viral replicase synthesis by binding to specific RNA hairpin that contains the replicase ribosome binding site. This hairpin structure is placed just downstream coat protein coding sequence, before the next- replicase coding sequence. The MS2 genome was the first genome to be completely sequenced by Walter Fiers and his team in 1976 (Fiers et al., 1976). The above mentioned hairpin or stem-loop structure designated as a translational operator (Bernardi & Spahr, 1972) is also bifunctional. It is involved not only in the effective repressing of the synthesis of replicase, but also believed to be a packaging signal that initiates the assembly of the capsid and ensures recognition and selective encapsidation of the phage RNA.

Recombinant VLPs derived from bacteriophage coat proteins retains the ability for packaging of RNA (unspecific, host source). Nevertheless, translational operator sequences are involved into the target RNA sequences to improve specificity of packaging.

RNA binding properties of the coat protein from bacteriophage GA was investigated by Dr. Uhlenbeck with co-workers (Gott et al., 1991). Filter binding assays *in vitro* showed that despite 46 of 129 amino acid differences between GA (serological group II) and R17 (serological group I) coat proteins, the binding sites are fairly similar and GA coat protein binds RNA with „considerable specificity".

We have described previously that the operator had rather small effect on the specificity of capsid contents for recombinant capsids which are produced with and without GA-operator sequences in mRNAs (Strods et al., 2013). Therefore, many successful examples of use of MS2 operator have been elaborated (Legendre & Fastrez, 2005; Pasloske et al., 1998; Pickett & Peabody, 1993; Wei et al., 2008).

Altering RNA binding specificities of translational repressors and coat protein mutants that influence this binding were studied by Dr Peabody's group (Lim et al., 1994; Lim & Peabody, 1994). The first strategy of this study involves investigation of the affinity of the coat protein variants for RNA *in vitro*, and the second one includes measurements of translational repression *in vivo*. Taken together, the introduction of specific GA-like substitutions into MS2 coat protein sequence have been performed, which resulted in one case six amino acid substitutions (positions 43, 55, 59, 83, 87, 89) that markedly influenced the RNA binding sites of MS2 and GA coat proteins (Lim et al., 1994). In the next series the role of two additional substitutions (positions 29 and 66) and deletion of FG-loop was established (Lim & Peabody, 1994). Three of the most important mutations K43R, N55K and R83K were called by authors as „super-repressor mutations", because they bound both operator RNAs more tightly than wild type protein (Lim et al., 1994). The main determinant of the difference in GA and MS2 specificity seems to be the N87S substitution (Lim et al., 1994). Other codon-directed mutagenesis experiments confirmed earlier results showing that the identity of Asn-87 was for specific binding of MS2 RNA and for discrimination of Qb RNA binding (Spingola & Peabody, 1997). Intensively were studied also crystal structures of complexes between recombinant MS2 capsids with mutations and RNA operator sequences (Helgstrand et al., 2002; Horn et al., 2004; Johansson et al., 1998; Valegård et al., 1997). The conversion of Asn-87 to Ala improved the ability of purine-RNAs (GA operator type) to bind MS2 coat protein, but binding to pyrimidine-RNAs (MS2 operator type) remained still to be more tight (Johansson et al., 1998). The authors also appointed the possible role of some other amino acids in the complex formation and particularly of Ser-52, Asn-55 and Lys-57. Lys-57 is present in all types of coat protein and therefore might not to be responsible for specificity of interaction. Instead of Ser-52 in GA is Gly, instead of Asn-55 in GA is Lys (Tars et al., 1997). It is assumed, that in spite of large differences in binding affinities, the structures of the variant complexes are very similar to the wild-type operator complexes, and the interaction of wild-type MS2 operator with native MS2 coat protein seems to be if not the strongest one, but at least more functionally specific. Two new techniques based on wild-type MS2 protein-MS2 operator interaction have been developed recently. Those are MS2 tagging (Chubb et al., 2006) and tethering (Keryer-Bibens et al., 2008) techniques. MS2 tagging and tethering are based upon the high-specific interaction of the MS2 bacteriophage coat protein with the stem-loop structure of the MS2 operator sequence. The mRNA packaging into VLPs in eukaryotes during growth process has one very distinguishing advantage – it goes through 3'-end- processing, which includes posttranslational cleavage of mRNA precursor with followed the 3'-end processing and polyadenilation (Colgan & Manley, 1997; Dheur et al., 2005; Keller & Minvielle-Sebastia, 1997; Zhao et al., 1999), becoming functionally matured. Most eukaryotic mRNAs, with a very few exceptions, acquire a poly (A) tracts at their 3'-ends. Entity of the poly(A) tail in translation processes is the main importance

for mRNA function (Preiss & Hentze, 1999). Poly(A) tail behaves as a stabilizing factor and in the absence or removal of its, mRNA is rapidly decapped and degraded. If we have plans to package functionally active mRNAs into virus like particles for delivery and „work" in a certain kind of eukaryotic cells, we must pack functionally active mRNAs, and the direct packaging *in vivo* during VLP growth solves this problem. It is known that in yeast poly(A) tails are with average length of about 70 adenosine residues, whereas in other (higher) mammals such tails are synthesized to an average length up to 250 adenosine residues (Dheur et al., 2005).

For us was very important to combine our rather good results in production of GA CP VLPs with more specific packaging of desired mRNAs *in vivo*. Therefore, our goal was directly opposite to the Peabody's work (Lim et al., 1994) – to introduce into GA coat protein such amino acids what would make them like MS2 coat protein (mimic them as MS2) for strong and specific interaction with MS2 operator sequence joined to packaged GFP mRNA. Single substitutions as well as combinations of these mutations in pairs (Table 1) were chosen. Simultaneously with this main task to improve packaging we must to find out under which promoter GAL1 or GAL10 it might get higher yield of VLPs and, basically, to fix the first cases for expression in yeast of the capsid formation facts from mutated GA coat protein.

Several tasks were envisaged for this study. First of all to test the GA capsid formation by expression in yeast of GA coat protein with three single amino acid mutations (amino acids 43, 55, 87) and with two double mutations (amino acids 43+87 or 55+87). Mutations for the introduction into GA coat protein sequence were chosen basing on the analysis of literature data (Gott et al., 1991; Lim et al., 1994; Lim & Peabody, 1994; Ni et al., 1996). It was also planned to compare the yield of VLPs dependency on construct – under which promoter was placed GA CP sequence. The next question for us was to analyse the amount of packaged RNA dependently upon obstacle mentioned above. And finally the last but not the least was to ascertain wherever the introduction of MS2 operator sequence into packaged GFP mRNA raised specificity of packaging also resulting in the best quality particles for further investigation. This final task was solved in the case of prognostic the more important mutation of 87th amino acid serine to asparagine.

Materials and methods

Plasmid constructions

All constructions were based on plasmid pESC-URA (Agilent Technologies) for protein expression in yeast. This plasmid contains two promoters (GAL1 and GAL10) for expression of GA coat protein – unmodified and modified – and for synthesis of mRNA. New constructions are based on plasmids pIC921 and pIC984 (Strods et al., 2013) by introducing single amino acid change following standard site-directed mutagenesis protocol. PCR reaction mixture consisted from 2x PCR Master Mix (Thermo Scientific), pair of degenerate primers and template DNA as described in manufacturer's protocol, and summarised in the Table 2 – constructions pIC994, pIC995, pIC989, pIC991, pIC996, pIC997 are based on either pIC921 or pIC984 and constructions pIC904, pIC906, pIC905, pIC907 are based either on pIC994 or pIC995. In case of construction pIC1076, firstly, vector was obtained by digestion of plasmid pIC995 with restriction endonucleases EcoRI and NotI and, secondly, GFP sequence containing fragment from plasmid pIC921 was cloned out by using primers pINC-525 (5'-TCG AAT TCC ATG GTG AGC AAG GGC GAG GA-3') and pINC-526 (5'-AAG CGG CCG CGA CAT GGG TAA TCC TCA TGT TTT GCT TAC TTG TAC AGC TCG TCC ATG CC-3') and digested with abovementioned restriction endonucleases, and, thirdly, vector and fragment were ligated together. All constructs were produced through transformation in *E.coli* competent cells

and purification with GeneJET Plasmid Miniprep Kit (Thermo Scientific), followed by sequence verification using sequencing method.

Expression of constructions

Yeast *Saccharomyces cerevisiae* (S. cerevisiae) strain YPH499 (ura3-*52 lys2-801^{amber} ade2-101^{ochre} trp1-Δ63 his3-Δ200 leu2-Δ1*, haplotype a) was transformed with all plasmid constructs according to the standard lithium acetate/polyethylene glycol procedure using Sigma-Aldrich Yeast Transformation Kit according to the protocol described by Gietz et al. (Gietz et al., 1992). Transformants were selected and grown in uracil-free synthetic dextrose minimal medium (SDU-) for maximum protein expression as described previously by Strods et al. (Strods et al., 2013).

Purification of VLPs

Yeast cells were suspended in working buffer (20mM Tris-HCl, 5 mM EDTA, 0.65 M NaCl, pH7.8, supplemented with 0.03 mM PMSF) and subjected through French press (three strokes, 20 000 psi), after which cell lysate was stirred with equal volume of glass beads (30 sec stirring and 1 min rest on ice, repeated 15 times) and sonicated at 22 kHz (14 sec sonicate and 1 min rest on ice, repeated 15 times). Cell lysate was centrifuged (30 min at 12 000 rpm), debris was additionally washed with working buffer and volume of joined supernatants was reduced by dialysis against solution consisting from mixture of working buffer and glycerol (1:1 by volume). Afterwards, VLPs were subsequently purified through Sepharose CL-4B gelfiltration column (2 x 63 cm), eluting them with working buffer (at flow rate 2 ml per hour). As a next step was purification through DEAE Sephadex A-50 column (1 x 5 cm) – samples were subjected on column, then flow-through and additional washing with 3 ml of TEN buffer (20mM Tris-HCl, 5 mM EDTA, 0.15 M NaCl, pH7.8) were combined in dialysis tube and concentrated using dry Sephadex G-100 powder (GE Healthcare).

Products were purified by sucrose density gradient centrifugation, using preformed stepwise sucrose gradient from 36% till 5% sucrose concentration in working buffer (total volume of each tube - 12 ml, centrifugation was performed at 25000 rpm for 13h in Beckman Coulter Optima L-100XP ultracentrifuge (rotor SW32 Ti)). After piercing the bottom of the tube, fractions were collected (1 ml each) and those containing VLPs were joined together, dialysed against working buffer and, if necessary, concentrated using dry Sephadex G-100 powder.

VLPs preparations from constructions IC991, IC989, IC995 and IC996 were subjected onto the two equal layer CsCl gradient, where the bottom 6 millilitre was from ready solution (44 g CsCl + 60 ml working buffer), and the upper 6 millilitre consisted of VLPs solution, 2.2 g of CsCl and working buffer. Ultracentrifugation and fractionation were performed similarly as with sucrose gradient, with only the exception that 20500 rpm for 13h regime was used.

Extraction of VLPs inner content

To the solution of VLPs the mixture of equal amounts of phenol and chloroform (1:1) was added, thoroughly vortexed and centrifuged (8000 rpm for 5 min). Upper (aqueous) phase was subtracted, washed triple with diethyl ether and nucleic acids were precipitated by adding ethanol. After centrifugation (13000 rpm for 15 min), the debris was washed with 70% ethanol and dissolved in DEPC-water. RNA quantity measurements were carried out using ND-1000 spectrophotometer (NanoDrop).

Purification of poly-A tail containing RNA

In order to measure mRNA content in whole RNA extract from VLPs, affinity chromatography using oligo(dT)-cellulose (Sigma-Aldrich) column was used. Oligo(dT) cellulose was

incubated with RNA in binding buffer (10mM Tris-HCl, 1mM EDTA, 400mM NaCl, 0.1% SDS) at 65°C 10 min, followed by washing with binding buffer, washing buffer (10 mM Tris-HCl, 1 mM EDTA, 100 mM NaCl, 0.1% SDS) and finally eluted with elution buffer (10 mM Tris-HCl, 1 mM EDTA, 0.1% SDS). mRNA containing elution fractions were combined and total amount of RNA was determined using optical density measurements.

Reverse transcription qPCR

Reverse transcription real-time PCR (RT-qPCR) was done in two steps. Firstly, cDNA with random hexamer or oligo(dT) primers were synthesized from equal amount of each sample by using First Strand cDNA Synthesis Kit (Thermo Scientific) according manufacturer's recommendations, using from VLPs extracted total RNA as a template. Secondly, qPCR reaction mixture for each sample was prepared in duplicates as follows – 6 µl Power SYBR Green PCR Master Mix (Life Technologies), 2 µl H_2O, 2 µl primer mix (2pmol/µl), 2 µl cDNA (diluted two-fold). qPCR reaction was done on ViiA™ 7 Real-Time PCR System (Life Technologies) according pre-set protocol for SYBR Green qPCR reaction. Ct values were used to calculate $2^{deltaCt}$ to represent the amount of PCR product.

Results

Synthesis and purification of virus-like particles

For all constructions from pIC904 till pIC1067 (listed in Table 1) were used plasmids pIC921 and pIC984, based on commercial plasmid pESC-URA (Stratagene) and contained bacteriophage GA coat protein sequence with optimized codons that was described previously (Strods et al., 2013). In synthesis process (described in Methods and Table 2) totally were generated 11 constructions which included single-point mutations S87N, K55N, R43K and double-point mutations S87N + K55N and S87N + R43K. In Figure 1 is shown construction of main interest – IC1067 – based on IC984 and containing bacteriophage MS2 operator sequence added to the 3' end of the GFP gene in order to provide more specific packaging of GFP gene through binding of operator's stem-loop structure (Figure 2) with modified bacteriophage GA coat protein. After transformation and protein expression in yeast *S. cerevisiae* all of the above mentioned constructions (with exception of construction IC997) produced virus-like particles.

A typical example of purification process is shown in the case of IC984 VLPs (Figure 3), where fractions after cell lysate gelfiltration on Sepharose CL-4B column were measured in spectrophotometer (Figure 3A) and analysed on agarose gel electrophoresis (Figure 3B). Presence of nucleic acid seen in fractions with VLPs (agarose gel) promoted us to introduce purification on DEAE ion-exchange column. Due to the overall positive charge of GA VLPs, they were eluted from column as unbound material free from nucleic acid contamination. As a last step, additional purification using sucrose density gradient ultracentrifugation was done (Figure 3C). Similarly were purified IC989 VLPs, using other Sephadex CL-4B column (Figure 4A), Coomassie stained PAGE (Figure 4B) and Western blot (Figure 4C) analysis methods were used to reveal fractions that contain coat protein. In similar manner VLPs from all constructions were obtained, then the yield was calculated and summarized in the Table 3. The presence of VLPs was confirmed via electron microscopy, showing two variants as an example (Figure 6).

As it can be seen in the Table 3, the best yield after VLPs purification is observed in case of constructions where no modification in coat protein are inserted, respectively, in constructions IC921 and IC984, and these data roughly correspond to the yield of the VLPs, formed from GA coat protein, expressed from native coat protein sequence (Freivalds et al., 2008). At the same

time the yield was lower than in the case of construction A65 [3] that can be probably explained with additional stress for the yeast cells to transcribe and synthesize both coat protein and GFP gene. Comparing gene placements under promoters, the yield of the VLPs differed almost twice in favour for the coat protein placed under GAL1 promoter (i.e., construction IC984).

All other constructions bearing point-mutations in coat protein amino acid sequences show noticeably lower yields of VLPs per gram of cells. Yields of VLPs according to the placement of the coat protein under GAL1 or GAL10 promoter were different and showed no obvious regularity. Also no coherences between VLPs yields and different mutations – either single or double amino acid exchanges – were found, suggesting that our mutations introduced in different places of the coat protein sequence did not significantly interfere the protein production or particle assembly process. Exception in this series showed only one construction – IC1067, with mutation (S87→N) in coat protein and MS2 operator sequence added to the GFP sequence. Appropriate construction without MS2 operator sequence (IC995) showed almost four times less yield of VLPs, indicating important role of MS2 operator in process of particle formation.

Analysis of VLPs inner content

Comparing VLPs yield and RNA yield from purified VLPs (Table 3), direct correlation can be seen, possibly suggesting important role of RNA packaging ability and assembly of VLPs. Lowest RNA packaging capacity can be seen in construction IC904 and IC906 bearing S87→N and K55→N double-mutation, but otherwise – no prevalence of RNA packaging level in comparison with the location of the coat protein under GAL1 or GAL10 promoter.

Constructions that each possess different point-mutation were compared in CsCl density gradient (Figure 5), and also this method revealed divergent properties of those VLPs. VLPs with mutations S87N (IC995) and R43K (IC996) showed similar densities, but mutation K55N (constructions IC991 and IC989) bearing VLPs showed markedly lower density of VLPs in CsCl density gradient. These disparities in VLPs densities can explain also different yield and inner filling of the VLPs.

No prevalence of mRNA packaging in the case of construction IC1067 was observed. Despite the varieties of the mRNA content in different constructions, its average amount roughly corresponds to the relative amount of mRNA from total RNA found in yeast cells (Table 3).

Total RNA from two constructions – constructions IC984 containing GFP gene and construction IC1067 containing GFP gene supplemented with MS2 operator – were used as a template for quantitative PCR. cDNA from total RNA pool and mRNA pool were obtained using random hexamer and oligo(dT) primers, respectively. Despite the fact that extracted RNA does not contain any reference genes, we assumed that real time PCR data are comparable due to the fact that initial RNA was taken in equal amounts between both samples (Figure 8). Real time PCR analysis with GFP primer set revealed the presence of GFP gene in both VLPs, however when GFP gene was prolonged with MS2 operator sequence (IC1067), the packaging level in S87N coat protein mutant VLPs was at least one and a half higher (Figure 8, random hexamer cDNA with GFP primers). Analysing packaging level of the GFP specific mRNA, we can see difference even more – at least three times (Figure 8, oligo(dT) cDNA with GFP primers). Using MS2 operator specific primer set, the prolongation of GFP mRNA sequence with MS2 operator sequence was confirmed (Figure 8, MS2 operator primers).

Discussion

Exploration of above mentioned construction are meant to cover different things – possibility to form VLPs, the yield of VLPs and its dependency from coat protein placement under one of the two promoters, the RNA filling level and also the specificity of its packaging. Formation of VLPs were observed in all except one construction therefore it was possible to investigate other abovementioned statements. Our previous observations in the case of VLPs with unmodified coat protein showed overall better VLPs yield in comparison with mutant constructions. While in all mutation containing constructions yields of the VLPs were lower independently from promoters. Our idea of duplicate constructs with opposite orientation of genes (regarding placement under GAL1 or GAL10 promoter) was to find best combination for increasing of VLPs production and for ensuring specific packaging. Minor variations of VLPs yield in mutant constructs were observed, but no clear preference in favour to coat protein alignment under one of the promoters was discerned. The same was observed when total RNA was extracted and also mRNA purified, suggesting that gene placement under promoter influence VLPs yield and inner content, but it is not the only factor and for the optimal results different construction strategies should be used. When comparing VLPs yield and total RNA amount among all constructions, direct correlation can be seen allowing for us to hypothesize that wholesome nucleic acid filling is necessary for optimal self-assembly of the capsids.

Observed higher yield of VLPs due to the coat protein placement under GAL1 promoter in S87N mutant encouraged us to add MS2 operator exactly to this construction. As a result was created construction of our interest - IC1067, which was examined in more details. Introduction of the point mutation S87→N in GA coat protein resulted in more specific interaction with the MS2 operator sequence, especially in the comparison with the GA operator interaction with GA coat protein (Rūmnieks et al., 2008). Packaging of the mRNA of interest (in our case – from GFP gene supplemented with MS2 operator) was also higher, proving our hypothesis that specific attachment of the MS2 operator sequence to the modified coat protein can provide specific packaging of RNA. These results are in the accordance with Lim's et al. (Lim et al., 1994), that the main determinant for the specificity of MS2 operator binding is S87N substitution in coat protein. More specific packaging of RNA is also strong enough to partially compensate negative effects of amino acid exchange in coat protein, therefore rising overall VLPs production level. Nevertheless that the positive tendency for specific packaging is realised, VLPs still contains a broad spectra of internal filling. Sample analysis with coat protein specific primers showed that full specificity of GFP packaging was not achieved and VLPs contained significant amount of coat protein gene mRNA (Figure 8). Some previous packaging experiments on the basis of the GA operator indicated the same tendency, that even some specificity of the gene of interest was achieved, full exclusion of unnecessary amino acid sequences could not be done (Rūmnieks et al., 2008). Mimicking of GA virus like particles toward MS2 like particles gave relatively more specific packaging of the sequence of interest – it was found that GFP mRNA with MS2 operator (Figure 8, oligo(dT) cDNA with GFP primers) was packaged approximately three times better than without operator.

Tables

Table 1. Constructions for expression of GA CP and/or GFP in yeasts.

Introduced mutation(s)	Construct Nr	Construct	
		GAL1	**GAL10**
	921	GFP	GA CP
	984	GA CP	GFP
S87→N	***994***	GFP	GA CP (S87→N)
	995	GA CP (S87→N)	GFP
	1067	GA CP (S87→N)	GFP + MS2op
K55→N	***989***	GFP	GA CP (K55→N)
	991	GA CP (K55→N)	GFP
R43→K	***996***	GFP	GA CP (R43→K)
	997	GA CP (R43→K)	GFP
S87→N; K55→N	***904***	GFP	GA CP (S87→N; K55→N)
	906	GA CP (S87→N; K55→N)	GFP
S87→N; R43→K	***905***	GFP	GA CP (S87→N; R43→K)
	907	GA CP (S87→N; R43→K)	GFP

Table 2. Summary of constructions made with site-directed mutagenesis method.

Construct	primers	template DNA
pIC994	pINC-439 (5'-TGG AAG GCA TAT GCT AAT ATT GAT TTG AC-3') and pINC-440 (5'-GTC AAA TCA ATA TTA GCA TAT GCC TTC CA-3')	pIC921
pIC995	pINC-439 and pINC-440	pIC984
pIC989	pINC-437 (5'-GCT TCT GGT GCT GAT AAT AGA AAA TAT AC-3) and pINC-438 (5'-GTA TAT TTT CTA TTA TCA GCA CCA GAA GC-3)	pIC921
pIC991	pINC-437 and pINC-438	pIC984
pIC996	pINC-451 (5'-CAA GCA TAT AAA GTT ACT GCT TC-3') and pINC-452 (5'-GAA GCA GTA ACT TTA TAT GCT TG-3')	pIC921
pIC997	pINC-451 and pINC-452	pIC984
pIC904	pINC-437 and pINC-438	pIC994
pIC906	pINC-437 and pINC-438	pIC995
pIC905	pINC-451 and pINC-452	pIC994
pIC907	pINC-451 and pINC-452	pIC995

Table 3. Yield of purified VLPs per g of cells and yield of total RNA and mRNA extracted from purified VLPs.

	Nr	Construction		yield, mg VLPs per gram cells	µg of RNA from 1 mg of VLPs		*% of mRNA from total RNA*
		GAL1	GAL10		total RNA	mRNA	
	IC921	***GFP***	***GA CP***	***0.872***	104.2	8.6	8.3%
	IC984	***GA CP***	***GFP***	***1.525***	168.6	29.8	17.7%
S87→N	**IC994**	***GFP***	***GA CP (S87→N)***	***0.184***	32.4	2.4	7.4%
	IC995	***GA CP (S87→N)***	***GFP***	***0.271***	42.0	4.2	10.0%
	IC1067	***GA CP (S87→N)***	***GFP + MS2op***	***0.943***	104.4	14.0	13.4%
K55→N	**IC989**	***GFP***	***GA CP (K55→N)***	***0.312***	56.2	12.6	22.4%
	IC991	***GA CP (K55→N)***	***GFP***	***0.183***	38.2	2.4	6.3%
R43→K	**IC996**	***GFP***	***GA CP (R43→K)***	***0.110***	30.4	2.2	7.2%
	IC997	***GA CP (R43→K)***	***GFP***	-	165.2	0.0	-
S87→N; K55→N	**IC904**	***GFP***	***GA CP (S87→N; K55→N)***	***0.163***	16.2	2.0	12.3%
	IC906	***GA CP (S87→N; K55→N)***	***GFP***	***0.240***	12.4	2.6	21.0%
S87→N; R43→K	**IC905**	***GFP***	***GA CP (S87→N; R43→K)***	***0.250***	24.2	2.2	9.1%
	IC907	***GA CP (S87→N; R43→K)***	***GFP***	***0.233***	52.0	2.6	5.0%

Figures

Figure 1 Plasmid map for construction 1067 (created with Vector NTI software package (Invitrogen)).

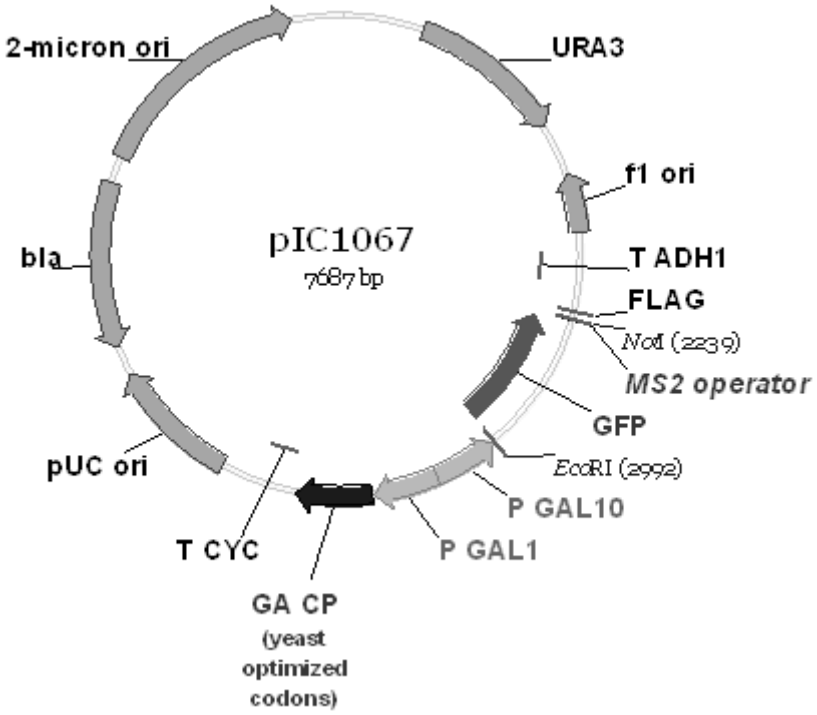

Figure 2 Secondary structure of MS2 RNA operator stem-loop, compared with GA RNA operator stem-loop (according Lim et al. 1994 (Lim et al., 1994)).

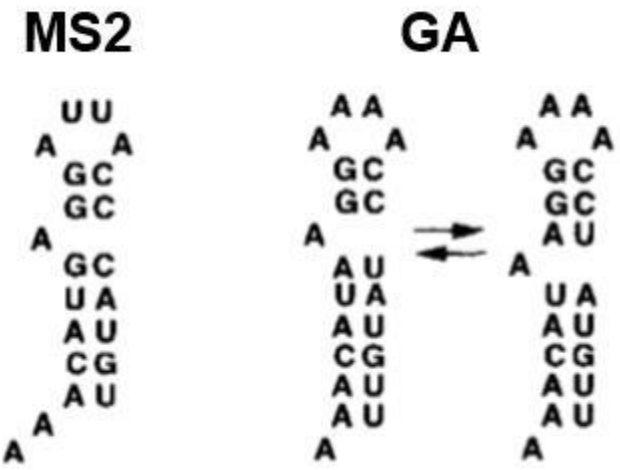

Figure 3 Purification steps of IC984 VLPs: optical density (**A**) and native agarose gel electrophoresis (**B**) profile after column chromatography on Sephadex CL-4B; (**C**) optical density profile of sucrose gradient (fraction size 0.5 ml). Brackets show collected fractions, in agarose gel electrophoresis red ellipse and blue ellipse show VLPs and nucleic acids, respectively.

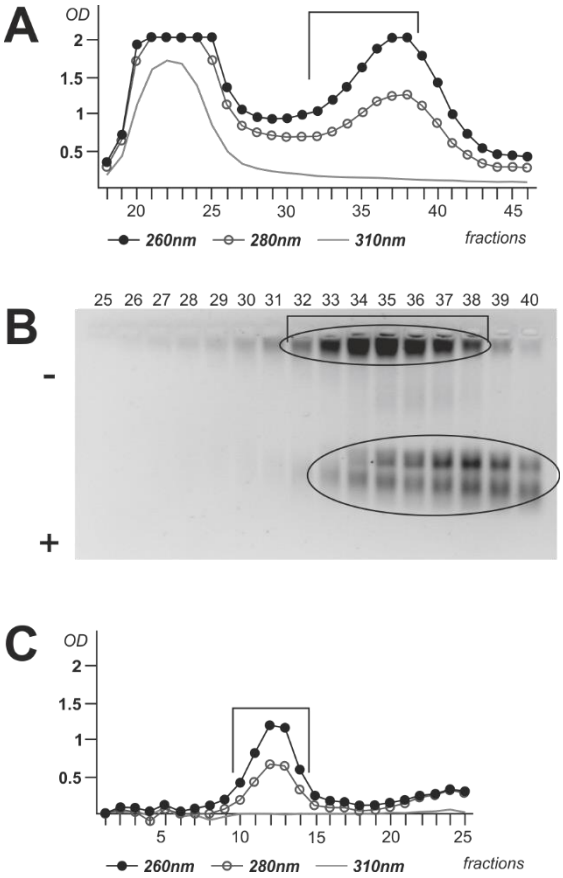

Figure 4 Purification steps of IC989 VLPs: optical density (**A**), native agarose gel electrophoresis (**B**) and Western blot (**C**) profile after column chromatography on Sepharose CL-4B. Red arrow points to the coat protein monomer.

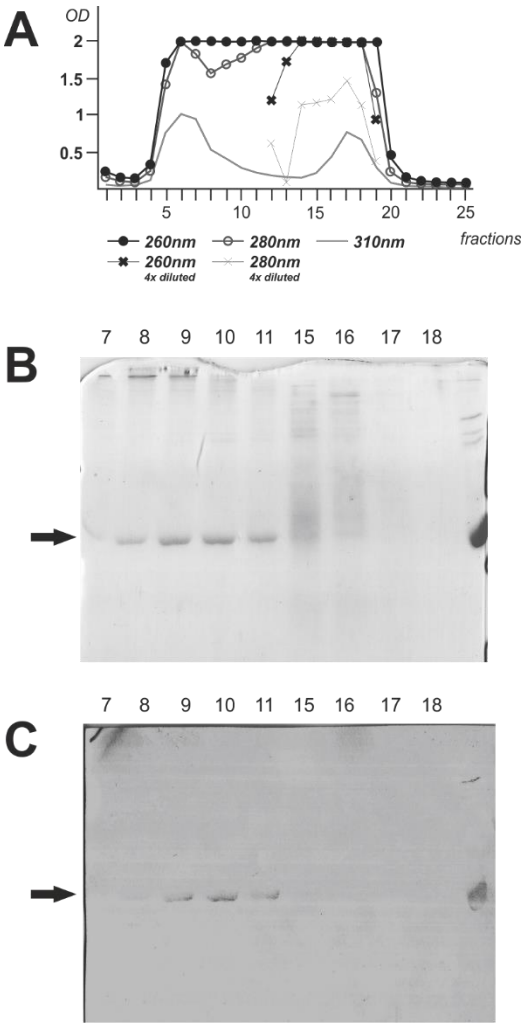

Figure 5 Optical density profiles of sucrose density gradients for IC991 (**A**), IC995 (**B**), IC996 (**C**) and IC989 (**D**) VLPs. Brackets show collected fractions.

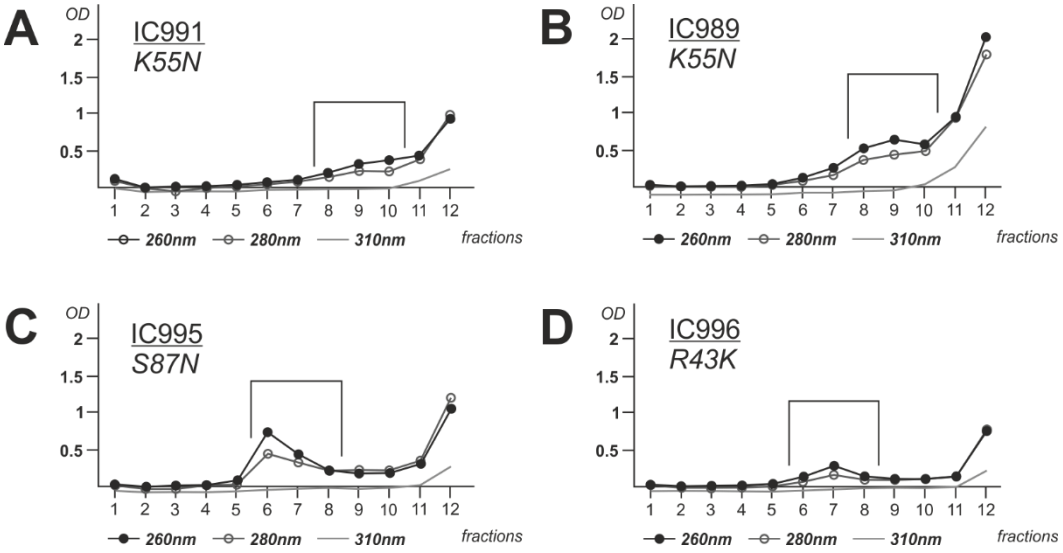

Figure 6 Electron microscopy images with purified IC995 (**A**) and IC996 (**B**) VLPs.

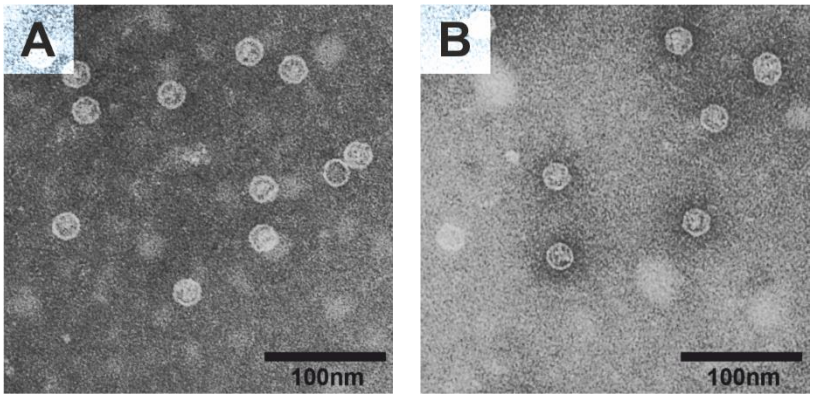

Figure 7 Oligo(dT) cellulose affinity chromatography of the RNA, extracted from construction IC984 and analysed in a denaturing 1% FA agarose gel. Samples are as follows: M - RiboRuler High Range RNA Ladder; 1. – total extracted RNA from VLPs; 2. – washing buffer fraction from oligo(dT) column; 3. – eluted mRNA from oligo(dT) column.

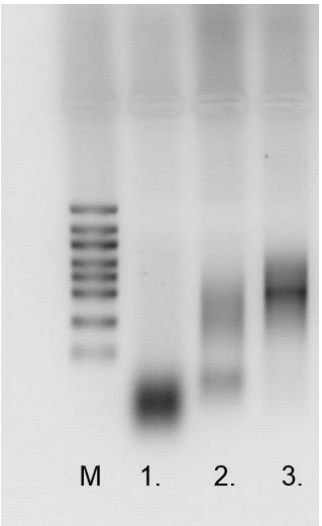

Figure 8 Real-time qPCR, using appropriate (gene specific) primers and cDNA amplified with random hexamer or oligo(dT) primers from extracted VLPs RNA as a template. Graphs are showing $2^{deltaCt}$ values.

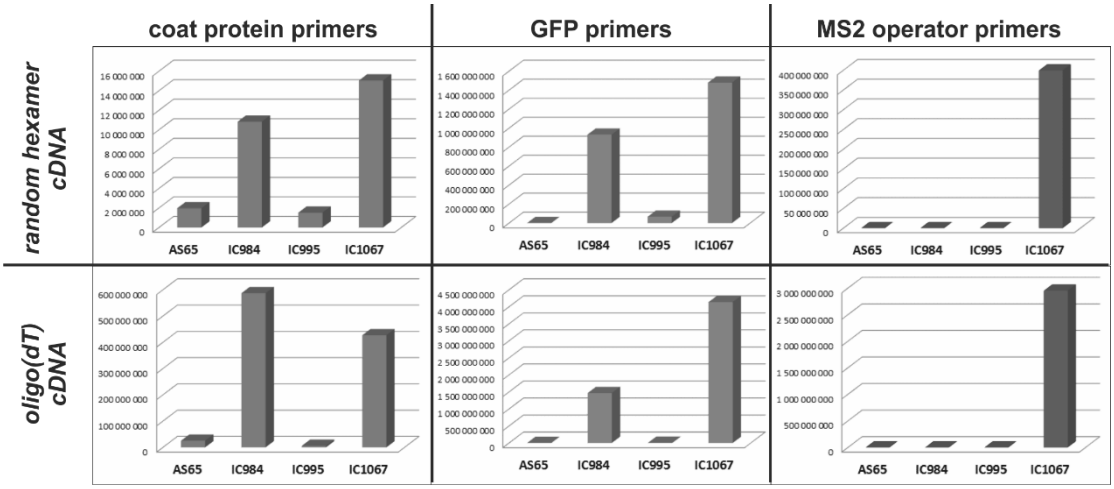

Acknowledgements

We thank Dr. Velta Ose for electron microscopy.

This research was supported by the European Social Foundation (ESF), Project Nr. 2013/0002/1DP/1.1.1.2.0/13/APIA/VIAA/005.

Literature

Bernardi, A., & Spahr, P.-F. (1972). Nucleotide Sequence at the Binding Site for Coat Protein on RNA of Bacteriophage R17. *Proceedings of the National Academy of Sciences of the United States of America*, 69(10), 3033–3037.

Chubb, J. R., Trcek, T., Shenoy, S. M., & Singer, R. H. (2006). Transcriptional Pulsing of a Developmental Gene. *Current Biology*, 16(10), 1018–1025. DOI: 10.1016/j.cub.2006.03.092

Colgan, D. F., & Manley, J. L. (1997). Mechanism and regulation of mRNA polyadenylation. *Genes & Development*, 11(21), 2755–2766. DOI: 10.1101/gad.11.21.2755

Dheur, S., Nykamp, K. R., Viphakone, N., Swanson, M. S., & Minvielle-Sebastia, L. (2005). Yeast mRNA Poly(A) tail length control can be reconstituted in vitro in the absence of Pab1p-dependent Poly(A) nuclease activity. *The Journal of Biological Chemistry*, 280(26), 24532–24538. DOI: 10.1074/jbc.M504720200

Fiers, W., Contreras, R., Duerinck, F., Haegeman, G., Iserentant, D., Merregaert, J., … Ysebaert, M. (1976). Complete nucleotide sequence of bacteriophage MS2 RNA: primary and secondary structure of the replicase gene. *Nature*, 260(5551), 500–507. DOI: 10.1038/260500a0

Freivalds, J., Rūmnieks, J., Ose, V., Renhofa, R., & Kazāks, A. (2008). High-level expression and purification of bacteriophage GA virus-like particles from yeast Saccharomyces cerevisiae and Pichia pastoris. *Acta Univ. Latv.*, 745, 75–85.

Gietz, D., St Jean, A., Woods, R. A., & Schiestl, R. H. (1992). Improved method for high efficiency transformation of intact yeast cells. *Nucleic Acids Research*, 20(6), 1425.

Gott, J. M., Wilhelm, L. J., & Uhlenbeck, O. C. (1991). RNA binding properties of the coat protein from bacteriophage GA. *Nucleic Acids Research*, 19(23), 6499–6503.

Helgstrand, C., Grahn, E., Moss, T., Stonehouse, N. J., Tars, K., Stockley, P. G., & Liljas, L. (2002). Investigating the structural basis of purine specificity in the structures of MS2 coat protein RNA translational operator hairpins. *Nucleic Acids Research*, 30(12), 2678–2685.

Horn, W. T., Convery, M. A., Stonehouse, N. J., Adams, C. J., Liljas, L., Phillips, S. E. V., & Stockley, P. G. (2004). The crystal structure of a high affinity RNA stem-loop complexed with the bacteriophage MS2 capsid: further challenges in the modeling of ligand-RNA interactions. *RNA (New York, N.Y.)*, 10(11), 1776–1782. DOI: 10.1261/rna.7710304

Johansson, H. E., Dertinger, D., LeCuyer, K. A., Behlen, L. S., Greef, C. H., & Uhlenbeck, O. C. (1998). A thermodynamic analysis of the sequence-specific binding of RNA by bacteriophage MS2 coat protein. *Proceedings of the National Academy of Sciences of the United States of America*, 95(16), 9244–9249.

Keller, W., & Minvielle-Sebastia, L. (1997). A comparison of mammalian and yeast pre-

mRNA 3'-end processing. *Current Opinion in Cell Biology*, 9(3), 329–336.

Keryer-Bibens, C., Barreau, C., & Osborne, H. B. (2008). Tethering of proteins to RNAs by bacteriophage proteins. *Biology of the Cell / Under the Auspices of the European Cell Biology Organization*, 100(2), 125–138. DOI: 10.1042/BC20070067

Legendre, D., & Fastrez, J. (2005). Production in Saccharomyces cerevisiae of MS2 virus-like particles packaging functional heterologous mRNAs. *Journal of Biotechnology*, 117(2), 183–194. DOI: 10.1016/j.jbiotec.2005.01.010

Lim, F., & Peabody, D. S. (1994). Mutations that increase the affinity of a translational repressor for RNA. *Nucleic Acids Research*, 22(18), 3748–3752.

Lim, F., Spingola, M., & Peabody, D. S. (1994). Altering the RNA binding specificity of a translational repressor. *The Journal of Biological Chemistry*, 269(12), 9006–9010.

Ni, C. Z., White, C. A., Mitchell, R. S., Wickersham, J., Kodandapani, R., Peabody, D. S., & Ely, K. R. (1996). Crystal structure of the coat protein from the GA bacteriophage: model of the unassembled dimer. *Protein Science: A Publication of the Protein Society*, 5(12), 2485–2493. DOI: 10.1002/pro.5560051211

Pasloske, B. L., Walkerpeach, C. R., Obermoeller, R. D., Winkler, M., & DuBois, D. B. (1998). Armored RNA technology for production of ribonuclease-resistant viral RNA controls and standards. *Journal of Clinical Microbiology*, 36(12), 3590–3594.

Pickett, G. G., & Peabody, D. S. (1993). Encapsidation of heterologous RNAs by bacteriophage MS2 coat protein. *Nucleic Acids Research*, 21(19), 4621–4626.

Preiss, T., & Hentze, M. W. (1999). From factors to mechanisms: translation and translational control in eukaryotes. *Current Opinion in Genetics & Development*, 9(5), 515–521.

Rūmnieks, J., Freivalds, J., Cielēns, I., & Renhofa, R. (2008). Specificity of packaging mRNAs in bacteriophage GA virus-like particles in yeast Saccharomyces cerevisiae. *Acta Univ. Latv.*, 745, 145–154.

Spingola, M., & Peabody, D. S. (1997). MS2 coat protein mutants which bind Qβ RNA. *Nucleic Acids Research*, 25(14), 2808–2815. DOI: 10.1093/nar/25.14.2808

Strods, A., Argule, D., Cielens, I., Jackeviča, L., & Renhofa, R. (2013). Expression of GA Coat Protein-Derived Mosaic Virus-Like Particles in Saccharomyces cerevisiae and Packaging in vivo of mRNAs into Particles. *Proceedings of the Latvian Academy of Sciences. Section B. Natural, Exact, and Applied Sciences*, 66(6), 234–241. DOI: 10.2478/v10046-012-0015-y

Tars, K., Bundule, M., Fridborg, K., & Liljas, L. (1997). The crystal structure of bacteriophage GA and a comparison of bacteriophages belonging to the major groups of Escherichia coli leviviruses. *Journal of Molecular Biology*, 271(5), 759–773. DOI: 10.1006/jmbi.1997.1214

Valegård, K., Murray, J. B., Stonehouse, N. J., van den Worm, S., Stockley, P. G., & Liljas, L. (1997). The three-dimensional structures of two complexes between recombinant MS2 capsids and RNA operator fragments reveal sequence-specific protein-RNA interactions. *Journal of Molecular Biology*, 270(5), 724–738. DOI: 10.1006/jmbi.1997.1144

Wei, Y., Yang, C., Wei, B., Huang, J., Wang, L., Meng, S., … Li, J. (2008). RNase-resistant virus-like particles containing long chimeric RNA sequences produced by two-plasmid

coexpression system. *Journal of Clinical Microbiology*, 46(5), 1734–1740. DOI: 10.1128/JCM.02248-07

Zhao, J., Hyman, L., & Moore, C. (1999). Formation of mRNA 3′ Ends in Eukaryotes: Mechanism, Regulation, and Interrelationships with Other Steps in mRNA Synthesis. *Microbiology and Molecular Biology Reviews*, 63(2), 405–445.

In vivo **iepakošana raugos producētās no bakteriofāga GA atvasinātās vīrusiem-līdzīgās daļiņās**

Bakteriofāga GA apvalka proteīna veidotās pašsavākties spējīgās vīrusiem-līdzīgās daļiņas (VLD) ir ekspresētas baktērijās un raugos. Uz iepriekšējo eksperimentu bāzes divus pretēji vērstus promoterus saturošā rauga vektora pESC-URA / *S.cerevisiae* sistēmā tika izveidotas jaunas konstrukcijas ar punktveida mutācijām apvalka proteīna gēnā, lai iegūtu MS2 fāgam līdzīgu RNS saistību. Vienlaicīgi pie iepakojamā mRNS tika pievienota MS2 operatora sekvence. Pēc punktveida (S87N, K55N, R43K) un dubultmutācijām (S87N + K55N and S87N + R43K) apvalka proteīns saglabāja spēju veidot VLD, lai arī ar mazāku iznākumu no šūnām. Serīna nomaiņa uz asparagīnu 87. apvalka proteīna sekvences pozīcijā kombinācijā ar bakteriofāga MS2 translācijas operatoru nodrošināja interesējošā gēna (GFP) specifisku iepakošanos. Lai arī tika iepakotas nespecifiskas nukleīnskābju sekvences, ievērojama interesējošā gēna specifiska iepakošanās var tikt panākta izmantojot iepriekšminēto pieeju.